

DEVELOPMENT OF BIOINTEGRATED ELECTROSPUN  
NANOFIBERS FOR ENVIRONMENTAL APPLICATIONS

A DISSERTATION SUBMITTED TO  
THE GRADUATE SCHOOL OF ENGINEERING AND SCIENCE  
OF BILKENT UNIVERSITY  
IN PARTIAL FULFILLMENT OF THE REQUIREMENTS FOR  
THE DEGREE OF  
DOCTOR OF PHILOSOPHY  
IN  
MATERIALS SCIENCE AND NANOTECHNOLOGY

By  
Ömer Faruk Sarioğlu  
August 2016

DEVELOPMENT OF BIOINTEGRATED ELECTROSPUN NANOFIBERS  
FOR ENVIRONMENTAL APPLICATIONS

By Ömer Faruk Sarioğlu

August 2016

We certify that we have read this dissertation and that in our opinion it is fully adequate, in scope and in quality, as a dissertation for the degree of Doctor of Philosophy.

---

Tamer Uyar (Advisor)

---

Mahinur Akkaya

---

Mehmet Mutlu

---

Hasan Tarık Baytekin

---

Urartu Özgür Şafak Şeker

Approved for the Graduate School of Engineering and Science

---

Levent Onural

Director of the Graduate School

# **ABSTRACT**

## **DEVELOPMENT OF BIOINTEGRATED ELECTROSPUN NANOFIBERS FOR ENVIRONMENTAL APPLICATIONS**

Ömer Faruk Sarioğlu

Ph.D. in Materials Science and Nanotechnology

Advisor: Tamer Uyar

August 2016

Electrospinning is an easy and economical production technique to produce nanofiber/nanofibrous webs from different polymers, polymer mixtures, inorganic materials, supramolecular structures and composite materials. These nanofibers have unique physical/chemical properties due to their large surface areas and highly nanoporous structures. Since these nanofibers have superior properties, various functions and can be modified by physical/chemical methods, they have a great potential to be applied in membrane/filter applications.

Bioremediation is a commonly used technique for removal of water contaminants, and different kinds of bacteria have been used for bioremediation of water systems. Use of biointegrated hybrid materials is an alternative approach for bioremediation, and this may provide higher efficiency, ease of application and reusability. As a carrier system, electrospun nanofibers are suitable materials for integration of bacteria, since electrospinning can allow production of nano/micro scale composites with tunable physical/chemical properties.

In this thesis, it was aimed to integrate bacteria that have bioremediation capability with electrospun nanofibers by using immobilization/encapsulation

techniques and test the potential of these biocomposites for treatment of contaminated water systems. The integration of bacteria that can remediate ammonium, heavy metal, textile dye and surfactant with electrospun nanofibers was achieved by two different approaches. In the first approach, bacterial cells were physically immobilized on cellulose acetate (CA), polysulfone (PSU), polystyrene (PS), polycaprolactone (PCL) and polylactic acid (PLA) electrospun nanofibers. In order to observe effects of nanofiber/nanofibrous web morphology and arrangements on the immobilization of bacteria, some of these nanofibers were produced as porous, parallelly arranged, and with different diameters. In the second approach, by using polyvinyl alcohol (PVA) and polyethylene oxide (PEO) polymers, simultaneous encapsulation of bacteria in nanofiber structures was provided. Afterwards, all these different kinds of biocomposites were tested for their remediation potential in accordance with the intended use of the integrated bacteria.

*Keywords:* electrospinning, nanofiber, bacteria, heavy metal, textile dye, surfactant, biocomposite, bioremediation, immobilization, encapsulation

# ÖZET

## ELEKTROSPİN YÖNTEMİ İLE ÜRETİLMİŞ NANOLİF YAPILARA BİYOLOJİK MALZEMELERİN ENTEGRE EDİLEREK ÇEVRESEL UYGULAMALAR İÇİN KULLANILMASI

Ömer Faruk Sarıoğlu

Malzeme Bilimi ve Nanoteknoloji Programı, Doktora

Tez Danışmanı: Tamer Uyar

Ağustos 2016

Elektrospin yöntemi değişik polimerlerden, polimer karışımlarından, inorganik malzemelerden, supramoleküler yapılardan ve kompozitlerden nanolif/nanoağ elde edilen, kolay ve maliyeti düşük bir üretim tekniğidir. Bu nanolifler, yüksek yüzey alanları ve nano boyuttaki gözenekli (boşluklu) yapıları sayesinde sıra dışı fiziksel/kimyasal özellikler göstermektedirler. Üstün özelliklere, birçok işleve sahip olan ve fiziksel/kimyasal yollarla modifiye edilebilen bu nanolifler özellikle membran/filtre uygulamalarında yüksek kullanım potansiyeline sahiptirler.

Biyogiderim yöntemi sudaki kirleticilerin temizlenmesi amacıyla uygulanan yaygın bir tekniktir ve çeşitli türdeki bakteriler sucul sistemlerde biyogiderim yapması amacıyla kullanılmaktadır. Biyoentegre sistemlerin biyogiderim amacıyla kullanımı alternatif bir yaklaşım olup, daha yüksek başarı, uygulama kolaylığı ve tekrar kullanılabilirlik sağlayabilmektedir. Elektrospin edilmiş nanolifler bakteriler için uygun bir tutunma ortamı olabilir, zira elektrospin yöntemi nano/mikro düzeyde kompozit malzemelerin ayarlanabilir fiziksel ve kimyasal özelliklerde üretilmesine olanak sağlamaktadır.

Tez çalışması kapsamında, elektrospin yöntemi ile üretilen nanoliflere, biyogiderim özelliği bulunan bakterilerin immobilizasyon/enkapsülasyon teknikleri kullanılarak entegrasyonu ve elde edilen biyokompozit malzemelerin atık su arıtımındaki potansiyellerinin araştırılması amaçlanmıştır. Amonyum, ağır metal, tekstil boyar maddesi ve surfaktan giderim özelliği gösteren bakterilerin nanoliflerle entegrasyonu iki farklı yaklaşımla gerçekleştirilmiştir. Birinci yaklaşımda, homojen bir morfolojide elde edilen selüloz asetat (CA), polisülfon (PSU), polistiren (PS), polikaprolakton (PCL) ve polilaktik asit (PLA) nanoliflerinin yüzeyine fiziksel yollarla bakteriler immobilize edilmiştir. Nanolif/nanoağ morfoloji veya dizilimdeki değişikliklerin bakteri tutunmasında neden olabileceği farklılıkları incelemek açısından, bu nanoliflerin, gözenekli, paralel dizilimli ve farklı çaplara sahip halleri de üretilerek etkileri incelenmiştir. İkinci yaklaşımda ise, polivinilalkol (PVA) ve polietilenoksit (PEO) polimerleri kullanılarak, bakterilerin eş zamanlı nanolif yapılarına enkapsülasyonu sağlanmıştır. Daha sonra, bu yöntemlerle üretilen biyokompozit malzemelerin entegre edilen bakterinin özelliğine göre endüstriyel atık su arıtımındaki kullanım potansiyelleri test edilmiştir.

*Anahtar kelimeler:* elektrospin, nanolif, bakteri, ağır metal, tekstil boyar maddesi, surfaktan, biyokompozit, biyoremediasyon, immobilizasyon, enkapsülasyon

## ACKNOWLEDGEMENTS

I would like to thank to everyone whoever contributed to my thesis. My special thanks go to my supervisor Prof. Tamer Uyar, for his encouragement, guidance and support during the course of this research. I am sincerely grateful to Prof. Turgay Tekinay for his active collaboration, support and guidance. I would like to thank to Prof. Urartu Şeker, Prof. Ayşe Begüm Tekinay, Prof. Mustafa Özgür Güler for their support and fruitful discussions. I would like to express my special thanks to my senior peers Dr. Aslı Çelebioğlu, Dr. Nalan Oya San Keskin and Dr. Ayşe Özdemir for their partnership and fellowship in this research. I would like to thank to my other senior peers and colleagues in Functional Nanofibers Group, Dr. Ali Demirci, Dr. Osman Arslan, Dr. Bekir Satılmış, Dr. Anitha Senthahizman, Dr. Brabu Balusamy, Dr. Kugalur Shanmugam Ranjith, Dr. Amaresh Chandra Pradhan, Zeynep Aytaç, Yelda Ertaş, Zehra İrem Gürbüz, Şefika Özcan and Ahmet Fatih Işık for their fellowship and helpful discussions. The Scientific and Technological Research Council of Turkey (TUBITAK, project #114Y264) is acknowledged for funding the research and BİDEB 2211-C scholarship.

I would like to thank to Dr. Gökçe Çelik, Mustafa Güler and Zeynep Erdoğan for their technical assistance and fruitful discussions. I would like to express most sincere thanks to my dear friends; İbrahim Murathan Sektioğlu, Nazım Enes Altan, Yavuz Selim Dağdaş, Süleyman Deniz, Tolga Tarkan Ölmez, Ebuzer Kalyoncu, Alper Devrim Özkan, and Ahmet Emin Topal. I would like to thank to my brothers; Abdullah Soylu, Yunus Emre Barun, Akif Bayram,

Hüseyin Enes Salman, İkrâm Orak, Mustafa Ürel, Kadir Akbudak and Hasan Barış Geçer. I would like to thank to Fatma Kayacı, Ali Ekrem Deniz, Ruslan Garifullin, Hasan Güner, Taha Bilal Uyar, Muhammad Aref Khalily, Murat Serhatlıoğlu, Mehmet Girayhan Say, Sami Bolat, Şehmus Tohumeken, Yusuf Keleştemur, Burak Güzeltürk, Talha Erdem, Zeliha Soran Erdem, Burcu Gümüşçü, Berna Şentürk, Pelin Tören, Canan Kurşungöz and Nuray Gündüz. I would like to thank my office mates, Tolga Tarkan Ölmez, Ebuzer Kalyoncu, Mehmet Can Yağcıoğlu, Türkan Gamze Ulusoy and Amir Ghobadi. They helped me to work in such a warm and quiet environment.

I would like to acknowledge UNAM (National Nanotechnology Research Center) and I want to thank to all the other members of UNAM.

Finally, I want to express my gratitude to my beloved family, my altruistic mother Hayriye Sarıoğlu, my dearest brother Fatih Semih Sarıoğlu and my fiancée Merve Gülsüm Keskin for their care, support and understanding.

*Canum babama,*

## LIST OF ABBREVIATIONS

ABS	alkyl benzene sulphonate
CA	cellulose acetate
LAS	linear alkyl sulphonate
LC-MS	liquid chromatography mass spectroscopy
MBAS	methylene blue active substances assay
MB	methylene blue
OD	optical density
PCL	polycaprolactone
PEO	polyethylene oxide
PLA	polylactic acid
PS	polystyrene
PSU	polysulfone
PVA	polyvinyl alcohol
SDS	sodium dodecyl sulfate
VCC	viable cell counting

# TABLE OF CONTENTS

ABSTRACT .....	iii
ÖZET .....	v
ACKNOWLEDGEMENTS .....	vii
LIST OF ABBREVIATIONS .....	x
TABLE OF CONTENTS .....	xi
LIST OF FIGURES .....	xiii
LIST OF TABLES .....	xix
Chapter 1: General Introduction.....	1
1. Water pollution and sustainable water management .....	2
2. Bio-based approaches for water sustainability .....	4
3. Electrospun fibrous networks as carrier matrices for development of biointegrated systems.....	6
Chapter 2: Bacteria immobilized electrospun cellulose acetate fibrous webs for ammonium removal.....	9
1. Introduction.....	10
2. Experimental.....	13
3. Results and discussion .....	17
Chapter 3: Bacteria immobilized electrospun fibrous webs for hexavalent chromium remediation .....	27
1. Introduction.....	28
2. Experimental.....	30
3. Results and discussion .....	35
Chapter 4: An easy and effective method for determination of the number of bacteria that are immobilized on electrospun nanofiber surfaces .....	47
1. Introduction.....	48
2. Experimental.....	49

3. Results and discussion .....	52
Chapter 5: Evaluation of contact time and fiber morphology differences for development of novel surfactant degrading biocomposites .....	60
1. Introduction.....	61
2. Experimental.....	63
3. Results and discussion .....	71
Chapter 6: Evaluation of fiber diameter and morphology differences for electrospun polysulfone fibers on bacterial immobilization and bioremediation performance.....	88
1. Introduction.....	89
2. Experimental.....	91
3. Results and discussion .....	95
Chapter 7: Bacteria immobilized electrospun polycaprolactone and polylactic acid fibrous webs for remediation of textile dyes in water .....	103
1. Introduction.....	104
2. Experimental.....	106
3. Results and discussion .....	112
Chapter 8: Bacteria encapsulated electrospun nanofibrous webs for remediation of methylene blue dye in water .....	123
1. Introduction.....	124
2. Experimental.....	126
3. Results and discussion .....	132
Chapter 9: Conclusion and future perspectives .....	147
LIST OF PUBLICATIONS.....	155
BIBLIOGRAPHY .....	157

## LIST OF FIGURES

<b>Figure 1:</b> Foaming in an industrial effluent due to contamination of surfactants.....	3
<b>Figure 2:</b> Schematic representation of the electrospinning set-up.....	7
<b>Figure 3:</b> Photograph of an electrospun cellulose acetate nanofibrous web.....	7
<b>Figure 4:</b> (a) Schematic representation of electrospinning process for CA nanofibers and photograph of CA nanofibrous web (b) photograph of STB1 immobilized CA nanofibrous web and schematic representation of bacterial cells on nanofiber surfaces. (Copyright © 2013, Reproduced from Ref. [18] with permission from the Royal Society of Chemistry).....	14
<b>Figure 5:</b> General morphology of <i>Acinetobacter calcoaceticus</i> STB1 under Scanning Electron Microscope (SEM) at 5000X (a) and 15000X (b) magnification. (Copyright © 2013, Reproduced from Ref. [18] with permission from the Royal Society of Chemistry).....	19
<b>Figure 6:</b> SEM micrographs of bacteria-free electrospun CA nanofibers at (a) 2500X and (b) 200000X; and STB1 immobilized nanofibers after 35 days of incubation at (c) 5000X and (d) 10000X magnification. (Copyright © 2013, Reproduced from Ref. [18] with permission from the Royal Society of Chemistry).....	19
<b>Figure 7:</b> Ammonium, nitrite and nitrate levels for: (a) free STB1 cells at initial ammonium concentration of 50 mg/L; (b) bacteria-free CA web at initial ammonium concentration of 50 mg/L; (c) STB1 immobilized CA web at initial ammonium concentration of 50 mg/L; (d) STB1 immobilized CA web at initial ammonium concentration of 100 mg/L; (e) STB1 immobilized CA web at initial ammonium concentration of 200 mg/L. Error bars represent mean of three independent replicates. (Copyright © 2013, Reproduced from Ref. [18] with permission from the Royal Society of Chemistry).....	21

<b>Figure 8:</b> Reusability test results of STB1 immobilized CA web for 5 cycles of ammonium removal experiments at initial ammonium concentration of 100 mg/L. Error bars represent mean of three independent replicates. (Copyright © 2013, Reproduced from Ref. [18] with permission from the Royal Society of Chemistry).....	23
<b>Figure 9:</b> SEM micrographs of STB1 immobilized CA web after the reusability tests, showing robust attachment of bacterial biofilms on nanofiber surfaces at (a) 2500X and (b) 10000X magnification. (Copyright © 2013, Reproduced from Ref. [18] with permission from the Royal Society of Chemistry).....	24
<b>Figure 10:</b> (a) Schematic representation of electrospinning process and photographs of PS and PSU webs, (b) photographs of STB5 immobilized PS and (c) STB5 immobilized PSU webs along with SEM micrographs and schematic representations of bacterial cells on fibrous surfaces. (Copyright © 2013, Reproduced from Ref. [53] with permission from Springer).....	31
<b>Figure 11:</b> SEM micrographs of (a) PS and (b) PSU webs without bacterial immobilization, and (c) STB5 immobilized PS and (d) STB5 immobilized PSU webs after 30 days of incubation for bacterial immobilization. (Copyright © 2013, Reproduced from Ref. [53] with permission from Springer).....	36
<b>Figure 12:</b> Cr(VI) bioremoval profiles of (a) free STB5 cells at different pH levels, (b) only STB5, STB5/PS and STB5/PSU samples at different initial Cr(VI) concentrations, (c) only STB5, only PS, only PSU, STB5/PS and STB5/PSU samples at an initial concentration of 25 mg/L. Error bars represent mean of three independent replicates. (Copyright © 2013, Reproduced from Ref. [53] with permission from Springer).....	38
<b>Figure 13:</b> Adsorption isotherm plots of (a) only STB5, (b) STB5/PS, (c) STB5/PSU samples for Freundlich, Langmuir and Toth adsorption models. (Copyright © 2013, Reproduced from Ref. [53] with permission from Springer).....	41

<b>Figure 14:</b> Reusability and post-storage test results of STB5/PS and STB5/PSU biocomposite webs for an initial concentration of 25 mg/L. Error bars represent mean of three independent replicates. (Copyright © 2013, Reproduced from Ref. [53] with permission from Springer).....	43
<b>Figure 15:</b> SEM micrographs of STB5 immobilized (a-b) PS and (c-d) PSU webs after the reusability tests, showing robust attachment of bacterial biofilms on fibrous surfaces at (a-c) 5000X and (b-d) 10000X magnification. (Copyright © 2013, Reproduced from Ref. [53] with permission from Springer).....	44
<b>Figure 16:</b> Photographs of pristine, bacteria immobilized and bacteria detached nanofibers.....	51
<b>Figure 17:</b> SEM micrographs of STB1 immobilized pCA nanofibers after 7 days of incubation at (a) 4000X and (b) 8000X; and bacteria detached pCA nanofibers at (c) 4000X and (d) 20000X magnification.....	54
<b>Figure 18:</b> SEM micrographs of (a) <i>A. calcoaceticus</i> STB1 immobilized and (b) <i>P. aeruginosa</i> ATCC 47085 immobilized nCA nanofibers after 3 days of incubation at 6000X; and bacteria detached CA nanofibers for (c) previously <i>A. calcoaceticus</i> STB1 immobilized and (d) <i>P. aeruginosa</i> ATCC 47085 immobilized web samples at 5000X magnification.....	56
<b>Figure 19:</b> (a) Schematic representation of electrospinning process for nCA and pCA webs, and photographs of nCA and pCA webs, (b) representative images for bacteria immobilized webs including a SEM micrograph and schematic representation of bacterial cells on fibrous surfaces. (Copyright © 2013, Reproduced from Ref. [19] with permission from the Royal Society of Chemistry).....	64
<b>Figure 20:</b> Phylogenetic trees of (a) STB3 and (b) STB4 strains according to 16S rRNA gene sequencing analysis. (Copyright © 2013, Reproduced from Ref. [19] with permission from the Royal Society of Chemistry).....	71
<b>Figure 21:</b> SEM micrographs of (a) pristine nCA and (b) pristine pCA webs. Pores can be seen on a pCA nanofiber in the inset figure. (Copyright © 2013, Reproduced from Ref. [19] with permission from the Royal Society of Chemistry).....	73

<b>Figure 22:</b> SEM micrographs of (a-c) nCA and (b-d) pCA nanofibers showing immobilization of STB3 cells onto (a) nCA nanofibers and (b) pCA nanofibers; and immobilization of STB4 cells onto (c) nCA nanofibers and (d) pCA nanofibers after 7 days of incubation. (Copyright © 2013, Reproduced from Ref. [19] with permission from the Royal Society of Chemistry).....	74
<b>Figure 23:</b> SEM micrographs of (a-c) nCA and (b-d) pCA nanofibers showing immobilization of STB3 cells onto (a) nCA nanofibers and (b) pCA nanofibers; and immobilization of STB4 cells onto (c) nCA nanofibers and (d) pCA nanofibers after 21 days of incubation. (Copyright © 2013, Reproduced from Ref. [19] with permission from the Royal Society of Chemistry).....	74
<b>Figure 24:</b> SDS biodegradation profiles of (a) STB3 and STB4 strains for differential pH levels at 10 mg/L SDS, (b) pristine nCA, pristine pCA, STB3/nCA, STB3/pCA, STB4/nCA and STB4/pCA webs at 10 mg/L SDS, (c) pristine nCA, pristine pCA, STB3/nCA, STB3/pCA, STB4/nCA and STB4/pCA webs at 100 mg/L SDS and (d) STB3/pCA and STB4/pCA webs at 1 g/L SDS. Error bars represent mean of three independent replicates. (Copyright © 2013, Reproduced from Ref. [19] with permission from the Royal Society of Chemistry).....	78
<b>Figure 25:</b> LC-MS spectra of (a) SDS solution in water at 100 mg/L (b) nutrient broth in water (c) STB3 sample having 100 mg/L initial SDS after incubation and suspension of bacterial cells (d) STB4 sample having 100 mg/L initial SDS after incubation and suspension of bacterial cells. (Copyright © 2013, Reproduced from Ref. [19] with permission from the Royal Society of Chemistry).....	83
<b>Figure 26:</b> Reusability test results of STB3/pCA and STB4/pCA webs for 5 cycles of SDS biodegradation at an initial concentration of 100 mg/L. Error bars represent mean of three independent replicates. (Copyright © 2013, Reproduced from Ref. [19] with permission from the Royal Society of Chemistry).....	84

<b>Figure 27:</b> SEM micrographs of (a-b) STB3 immobilized pCA webs and (c-d) STB4 immobilized pCA webs after the reusability test, showing strong bacterial attachments. (Copyright © 2013, Reproduced from Ref. [19] with permission from the Royal Society of Chemistry).....	86
<b>Figure 28:</b> SEM micrographs of (a, e, i) aligned and no salt added PSU fibers, (b, f, j) aligned and salt added PSU fibers (c, g, k) randomly oriented and no salt added PSU fibers (d, h, l) randomly oriented and salt added PSU fibers. (a-d) correspond to pristine PSU fibers, (e-h) correspond to bacteria immobilized PSU fibers after 7 days of incubation (i-l) correspond to bacteria immobilized PSU fibers after 21 days of incubation. As seen in the micrographs, addition of salt reduces the fiber diameters considerably.....	97
<b>Figure 29:</b> VCC (Viable cell counting) assay results of aligned, aligned (with salt), random, random (with salt) PSU fibers after 21 days of incubation period.....	98
<b>Figure 30:</b> MB and $\text{NH}_4^+$ removal profiles of free STB1 cells in a separate system within 72 h of incubation. 50 mg/L of initial $\text{NH}_4^+$ was utilized as the nitrogen source in MB removal experiments.....	99
<b>Figure 31:</b> Simultaneous removal of MB and $\text{NH}_4^+$ by bacteria immobilized PSU fibers at a constant initial MB concentration (25 mg/L) and varying initial $\text{NH}_4^+$ concentrations (25, 50, 100 mg/L) within 72 h of incubation.....	100
<b>Figure 32:</b> $\text{NH}_4^+$ and MB removal profiles of pristine PSU fibers within 72 h of incubation.....	101
<b>Figure 33:</b> Reusability test results of bacteria immobilized PSU fibers in a five consecutive cycle.....	102
<b>Figure 34:</b> Initial characterization of the three isolates ( <i>Enterococcus hermanniensis</i> , <i>Clavibacter michiganensis</i> and <i>Halomonas variabilis</i> ) for their dye removal capabilities against Setazol Blue BRF-X (SBBX) and Setazol Turquoise Blue G (STBG) dyes at an initial concentration of 50 mg/L).....	113

<b>Figure 35:</b> Schematic representation of the electrospinning process and representative images for bacterial immobilization including a photograph of bacteria immobilized electrospun nanofibrous web, a SEM micrograph of bacteria immobilized nanofibers and a schematic representation of the immobilized cells on electrospun nanofibers.....	114
<b>Figure 36:</b> SEM micrographs of (a) pristine PCL (b) pristine PLA (c) bacteria/PCL and (d) bacteria/PLA webs.....	115
<b>Figure 37:</b> (a) Dye removal profiles of free-bacteria, pristine PCL web, pristine PLA web, bacteria/PCL web and bacteria/PLA web samples at initial concentrations of 50, 100 and 200 mg/L. Error bars represent mean of three independent replicates.....	117
<b>Figure 38:</b> Reusability test results of bacteria/PCL and bacteria/PLA webs at an initial dye concentration of 100 mg/L. Error bars represent mean of three independent replicates.....	121
<b>Figure 39:</b> Comparison for OD600 values of bacteria/PCL and bacteria/PLA webs before and after the reusability test.....	121
<b>Figure 40:</b> SEM micrographs of (a) bacteria/PCL and (b) bacteria/PLA webs after the reusability test.....	122
<b>Figure 41:</b> (a) Schematic representation of electrospinning process for bacteria encapsulated PVA and PEO webs, and photographs of PVA and PEO webs, (b) representative images for bacteria encapsulated webs including a SEM micrograph and a schematic representation of a bacterial cell inside PVA/PEO fibers.....	134
<b>Figure 42:</b> SEM micrographs of (a) pristine PVA (b) pristine PEO (c) bacteria/PVA (d) bacteria/PEO webs and fluorescence microscopy images of (e) bacteria/PVA and (f) bacteria/PEO webs.....	135
<b>Figure 43:</b> Raman spectra of (a) pristine PVA and bacteria/PVA and (b) pristine PEO and bacteria/PEO webs.....	136
<b>Figure 44:</b> Growth profiles of bacterial cells which have grown in polymer-free LB medium, PVA containing LB medium or PEO containing LB medium within 18 h. Error bars represent mean of three independent replicates.....	138

<b>Figure 45:</b> (a) MB removal profiles of free-bacteria, bacteria/PVA web and bacteria/PEO web samples at initial concentrations of 10, 15 and 25 mg/L. (b) Concentration vs. time graph of free-bacteria, bacteria/PVA web, bacteria/PEO web, pristine PVA web and pristine PEO web samples at 15 mg/L of initial MB. Error bars represent mean of three independent replicates.....	139
<b>Figure 46:</b> Growth profiles of bacterial cells which have grown in polymer-free LB medium, PVA containing LB medium or PEO containing LB medium within 18 h. Error bars represent mean of three independent replicates.....	139
<b>Figure 47:</b> Viable cell counting (VCC) results of bacteria/PVA and bacteria/PEO web samples for storage at (a) 4 °C for 3 months and (b) 25 °C for 10 days.....	145

## LIST OF TABLES

<b>Table 1.</b> Removal capacities of only STB5, STB5/PS and STB5/PSU samples at equilibrium under different initial Cr(VI) concentrations, measured at the end of the 72 h removal period. T = 30 °C, agitation rate: 150 rpm, average bacterial biomass concentration $0.15 \pm 0.03$ g/L. (Copyright © 2013, Reproduced from Ref. [53] with permission from Springer).....	39
<b>Table 2.</b> Adsorption isotherm coefficients of only STB5, STB5/PS and STB5/PSU samples for each isotherm model. (Copyright © 2013, Reproduced from Ref. [53] with permission from Springer).....	42
<b>Table 3.</b> The $R^2$ values of zero, first, second and third order plots for the removal of Cr(VI) by only STB5, STB5/PS and STB5/PSU samples. (Copyright © 2013, Reproduced from Ref. [53] with permission from Springer).....	42
<b>Table 4.</b> Comparison of VCC values of free and detached STB1 cells (n=4, S.E.M).....	54
<b>Table 5.</b> Comparison of VCC values of free and detached bacterial cells (n=4, S.E.M).....	57

<b>Table 6.</b> Comparison of VCC values of sonicated and non-sonicated free bacterial cells (n=3, S.E.M).....	59
<b>Table 7.</b> Viable cell counting (VCC) results of STB3/nCA, STB3/pCA, STB4/nCA and STB4/pCA webs at different time periods. The results are presented in <i>cfu</i> /mL. The w/v ratio of each web that was utilized for the detachment process was equal (0.5 mg/mL). (Copyright © 2013, Reproduced from Ref. [19] with permission from the Royal Society of Chemistry).....	75
<b>Table 8.</b> Degradation capacities of free STB3 and STB4 cells, and STB3/nCA, STB3/pCA, STB4/nCA, STB4/pCA webs at equilibrium at the end of the degradation period. T = 30 °C, agitation rate: 180 rpm. (Copyright © 2013, Reproduced from Ref. [19] with permission from the Royal Society of Chemistry).....	79
<b>Table 9.</b> Adsorption kinetics coefficients of STB3/pCA and STB4/pCA webs for each isotherm model. (Copyright © 2013, Reproduced from Ref. [19] with permission from the Royal Society of Chemistry).....	80
<b>Table 10.</b> The R <sup>2</sup> values of zero, first, second and third order plots for the removal of SDS by STB3/pCA and STB4/pCA webs.....	81
<b>Table 11.</b> Removal capacities of free-bacteria, bacteria/PCL web and bacteria/PLA web samples at equilibrium at the end of the removal process. T = 30 °C, agitation rate: 150 rpm, incubation time: 48 h.....	116
<b>Table 12.</b> Adsorption isotherm coefficients of free-bacteria, bacteria/PCL web and bacteria/PLA web samples for each isotherm model.....	119
<b>Table 13.</b> The R <sup>2</sup> values of zero, first, second and third order plots for the dye removal by free-bacteria, bacteria/PCL web and bacteria/PLA web samples.....	119
<b>Table 14.</b> Removal capacities of free-bacteria, bacteria/PVA web and bacteria/PEO web samples at equilibrium at the end of the removal process. T = 30 °C, agitation rate: 125 rpm, incubation time: 48 h.....	140
<b>Table 15.</b> Adsorption isotherm coefficients of free-bacteria, bacteria/PVA web and bacteria/PEO web samples for each isotherm model.....	143

<b>Table 16.</b> The $R^2$ values of zero, first, second and third order plots for the removal of MB by free-bacteria, bacteria/PVA web and bacteria/PEO web samples.....	143
<b>Table 17.</b> Viable cell counting (VCC) results of bacteria/PVA and bacteria/PEO web samples after storing at 4 °C or 25 °C for different time periods. The results are presented in cfu/mL. The w/v ratio of each web that was utilized for the VCC assay was equal (5 mg/mL).....	145

# **Chapter 1**

---

## **General Introduction**

# **1. Water pollution and sustainable water management**

Water is the main component of life and its role in international affairs has become of great importance. Although earth has tremendous amounts of water sources, its distribution and availability is the major issue for regular use. Insufficient amount of water sources can lead to drought, famine and health problems. Because of that, water sustainability is a major issue even in water-rich countries, and novel strategies have being developed for sustainable water use.

One of the main area of use for water is in industrial processes. For various operations, water is extensively used and recycling is not in charge for many of them, so that, industrial wastewater releases as effluent to natural water sources (e.g. river, sea) at the end. Although for some wastewater (e.g. food industry), most of the contaminants are highly biodegradable and not harmful for biological organisms, for some of the others (e.g. textile industry), the concentrations of contaminants should be strictly regulated and must be removed before discharge.

In addition to industrial wastewater, domestic wastewater (greywater) needs to be remediated before discharge to natural water sources. Even though this type of wastewater is not generally as harmful as industrial wastewater, because of the potential toxicity of cleaning agents (e.g. detergents, shampoos), it should be properly remediated as well. Cleaning agents may contain various chemicals as ingredients for different purposes. Nevertheless, the toxicity problem is mainly due to the presence of surface active agents (surfactants) in

their formula, hence more biodegradable surfactants are preferred for easier remediation of water sources from surfactants. Because of the biodegradability issue, most of the current cleaning agents contain LAS (Linear Alkyl Sulphonate) type of surfactants, which are relatively more biodegradable than old-fashion ABS (Alkyl Benzene Sulphonate) type of surfactants [1].



**Figure 1:** Foaming in an industrial effluent due to contamination of surfactants.

Today, chemical, physical and biological methods are used for remediation of water systems from contaminants. Some of these methods are used in combination to obtain the highest efficiency. For last decades, bio-based methods have received more attraction because of their eco-friendliness, cost-effectiveness and sustainability. Furthermore, bio-based methods are open for improvement since many types of microorganisms can be used for these purposes, and genetic or material engineering can be performed for improved bioremediation capability or development of bio-hybrid materials. By

integration of specific microorganisms or enzymes with carrier materials, bio-hybrid materials can be generated for intended uses. These types of materials can be more effective than separate systems and can bring some advantages (e.g. reusability).

## **2. Bio-based approaches for water sustainability**

Bio-based approaches have been used for remediation of water systems as alternatives to physical/chemical treatment methods. These approaches are suggested to be more eco-friendly and sustainable for water treatment. Some biotechnology companies market specific bacterial solutions as commercial products for wastewater treatment. Dead or alive biomasses have been used for removal of different contaminants, which may include bacteria, fungi, yeast, agricultural waste and microalgae. These biomasses can remediate water pollutants either by biosorption or bioaccumulation. Although dead biomasses can only be used for biosorption, living cells can possess both bioaccumulation and biosorption, hence higher efficiency for bioremediation could be achieved by living cells in some studies [2]. Some plant species can be used for water cleaning purposes as well, known as phytoremediation, and it can be very effective strategy in some cases. Relatively few numbers of plant species have been used for this purpose and discovery of novel more efficient plant species can make this strategy more favorable for remediation of water systems.

In general, microorganisms in nature do not encounter with water contaminants, so they may have difficulties to remediate them without prior adaptations. Nonetheless, after they encounter with these contaminants, they

may develop new strategies to deal with and survive. By applying genetic engineering techniques, some microorganisms can gain bioremediation capability for certain contaminants or their existing bioremediation capabilities can be enhanced. Using special bacteria for water treatment is both more effective and faster than other methods in some cases. Furthermore, bacteria production and growth is very economical in comparison to other methods. The issues that should be considered before use of bioremediating bacteria for remediation purposes are: growth rate, pathogenicity and rate of metabolism. Bacterial cells should not be pathogenic for use in remediation applications for prevention of potential diseases. Although some bacteria can be used as dead biomass for adsorption purposes, for continuous activity and remediation of more complex contaminants, biodegradation or bioconversion are needed. Dead cell biomasses can be used for heavy metal removal (e.g. hexavalent chromium removal), yet they are not so effective for removal of more complex pollutants such as textile dyes and surfactants.

There are numerous examples in the literature which present specific microorganisms that have tolerance to grow in extreme environments and having bioremediation capability for a specific contaminant. Besides using those microorganisms planktonic in a liquid medium, they can also be used as immobilized on a carrier material, for a specific application. Integration of bioremediating microorganisms to a carrier material makes the final product potentially reusable, more resistant to environmental extremes and more practical. The carrier materials for bio-integration are selected for their biocompatibility, availability, cost-effectiveness and potential biodegradability.

The carrier systems should be non-toxic for biological organisms during and after application. After the end of application, they should be easily recycled.

### **3. Electrospun fibrous networks as carrier matrices for development of biointegrated systems**

In today's world, different types of microorganisms are in use for biotechnological purposes and bioremediation is one of the most common application areas. By the developments in biotechnology field, novel microorganisms have been isolated for treatment of water pollutants. Besides using these microorganisms in a freely floating form, microorganisms can be integrated on a carrier material and their integration makes those carrier materials functional for specific purposes. Biotechnological applications of bio-integrated hybrid systems can be more advantageous than planktonic cells in terms of lower space and growth medium requirements, ease of application and potential reusability of the system. In addition, it may also be advantageous for the resistance of cells to harsh environmental conditions. For instance, for water purification in aquaculture systems, bacteria integrated sand or pebbles can be used for continuous remediation of nitrogenous wastes in the environment.

Electrospun nanofibers are suitable materials for wastewater filtration (detoxification, decoloring, purification etc.) and by different types of modifications, their availability for environmental applications can be augmented. In addition to morphological modifications of electrospun nanofibers, functionalization of those nanofibers with various molecules and microorganisms makes them more available for environmental applications. In

recent years, electrospun fibrous materials have become available candidates as carrier systems for specific microorganisms, since electrospinning is an easy and economical production technique to produce tuneable nanoscale fibrous materials with unique physical/chemical properties.

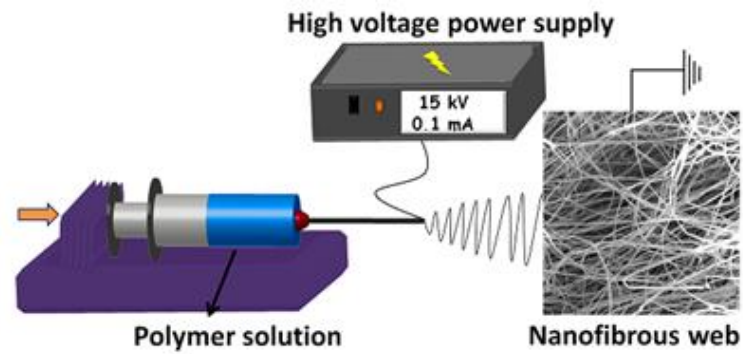


**Figure 2:** Schematic representation of the electrospinning set-up.



**Figure 3:** Photograph of an electrospun cellulose acetate nanofibrous web.

There are some pioneer studies in the literature about integration of different microorganisms to electrospun nanofibers. There are several ways to integrate microorganisms to nanofiber structures, which are: direct encapsulation of microorganisms to nanofiber structures [3-9], encapsulation of microorganisms to core-shell structures [10-13] and physical/chemical attachment of microorganisms to nanofiber surfaces [14-22]. Most of the studies consist of survival and proliferation profiles of the integrated microorganisms, but the number of studies related with the application of those biointegrated nanofibers are very few in the literature.

Electrospun nanofibers have various advantages over other carrier materials such as activated carbon and paper discs. For instance, high surface to volume ratio, porosity and biocompatibility make electrospun nanofibers as ideal carrier materials for the attachment of microorganisms. Since electrospun nanofibers can be produced from different mixtures, they can be produced with desired properties and morphologies for the attachment of different types of microorganisms. In addition, by using encapsulation strategies (direct or core-shell), microorganisms can be encapsulated within electrospun fibrous webs, without a need for post processing step. These systems can be very useful for long term storage, and provide ease of handling and lower space requirements.

## Chapter 2

---

### **Bacteria immobilized electrospun cellulose acetate fibrous webs for ammonium removal**

(Parts of this study was published as “Efficient ammonium removal from aquatic environments by *Acinetobacter calcoaceticus* STB1 immobilized on an electrospun cellulose acetate nanofibrous web”, Omer Faruk Sarioglu, Asli Celebioglu, Tamer Uyar and Turgay Tekinay, *Green Chemistry*, July 9, 2013 (Web), Reproduced (or 'Reproduced in part') from Ref. [18] with permission from the Royal Society of Chemistry. doi: 10.1039/c3gc40885)

## 1. Introduction

Ammonium ( $\text{NH}_4^+$ ), nitrite ( $\text{NO}_2^-$ ) and nitrate ( $\text{NO}_3^-$ ) comprise the most common nitrogenous compounds found naturally in aquatic ecosystems, and are formed by atmospheric decomposition, degradation of organic matter, and  $\text{N}_2$  fixation by certain microorganisms [23]. However, human activities have altered the nitrogen content of aquatic environments for the last two centuries, and the accumulated nitrogenous wastes now have a significant effect on the ecosystem [23]. Among the nitrogenous pollutants released to aquatic environments, ammonia is one of the most toxic ones and exists in water as either non-dissociated ammonia ( $\text{NH}_3$ ) or the ammonium ion ( $\text{NH}_4^+$ ) [24, 25]. Ammonia concentrations between 2 and 10 mg/L are lethal for many aquatic organisms, and concentrations greater than 1.5 mg/L are considered unacceptable in drinking water by the U. S. Environmental Protection Agency (US EPA) [25]. The main metabolic by-products of ammonia are  $\text{NO}_2^-$  and  $\text{NO}_3^-$ , both of which are also toxic for aquatic life. US EPA regulations dictate that the concentrations of nitrite and nitrate in drinking water should not exceed 1 mg/L and 10 mg/L respectively, and the sum of nitrite and nitrate concentrations should be lower than 10 mg/L [26]. Therefore, remediation of high ammonium and nitrogen concentrations in aquatic systems is necessary to maintain the quality of water for human or agricultural use. Conventional wastewater treatment systems include biological applications with both autotrophic nitrifiers and heterotrophic denitrifiers in dynamic aerobic and anaerobic conditions [27]. However, heterotrophic ammonium removal by a single nitrifier/denitrifier strain has many

advantages, such as the simultaneous processing of nitrification and denitrification reactions at equivalent conditions, and novel bacterial species have been isolated from different aquatic environments for that purpose [27-29].

Electrospinning is an emerging nanofiber/nanoweb production technique and has attracted much attention over the past decade due to its simplicity, versatility and cost-effectiveness [30-32]. Electrospun nanofibers and their nanofibrous webs display a variety of unique properties, such as large surface-to-volume ratios and highly porous structures, allowing their use as effective matrices in membranes and filters for environmental applications [30-35]. For instance, the use of immobilized microorganisms on electrospun nanofibrous polymeric mats was recently shown to increase the rate of nitrate removal [14]. In that study, microalgal cells were effectively immobilized on electrospun chitosan nanofiber mats in order to generate a hybrid system for nitrate removal [14]. Nitrate removal by nanofiber-immobilized microorganisms has several advantages over the use of free cells in suspension, including lower space and growth medium requirements, ease of handling, and potential reusability of the same matrix over several treatment cycles [14]. Furthermore, immobilization of bacterial cells on polymeric network systems makes them more resistant to harsh environmental conditions, such as metal toxicity or extremes of salinity, temperature and pH [36]. Covalent coupling, cross-linking, physical entrapment and the natural process of bacterial adhesion can be used for the immobilization of microorganisms to nanofiber networks [37]. Natural adhesion is the most advantageous among these methods, as it enables the formation of biofilms

following surface attachment and results in maximal cell viability and biochemical activity [30].

It was previously shown that *Acinetobacter calcoaceticus* STB1 could remove high concentrations of ammonium at heterotrophic conditions [29]. This strain can successfully remove high concentrations of ammonium in several days, and is non-toxic for aquatic life, hence it can effectively be used for the remediation of aquatic environments.

In the current study, *A. calcoaceticus* STB1 cells were immobilized on electrospun cellulose acetate (CA) nanofibrous web in order to achieve enhanced ammonium removal in aquatic environments. CA was chosen as the fibrous matrix, as it is the most common used regenerative cellulose, and is biodegradable and biocompatible, which renders it advantageous in biological applications [38]. Electrospun CA nanofibers have been used for filtration, drug delivery, enzyme immobilization, artificial tissue matrix formation [39-42], and successful growth of fibroblasts and Schwann cells on CA nanowebs have been reported in the literature [43, 44]. Moreover, CA nanofibers can be converted into more functional and applicable forms by the incorporation of other polymers into the nanofiber mesh, or by the chemical conversion of cellulose into a variety of derivative fibers [45, 46]. Here, we successfully produced a nanofibrous biocomposite web by immobilizing STB1 cells on electrospun CA nanofibers for the removal of ammonium in aqueous systems. Reusability test results indicate that STB1/CA nanofibrous webs can be reused without significant loss of their ammonium removal capacity.

## **2. Experimental**

### **2.1. Preparation of porous CA nanofibers**

The electrospinning of cellulose acetate (CA) nanofibers was performed as detailed in a previous study [47]. While production of porous CA nanofibers generally requires post-treatment of the ultimate nanofiber structure, the porous CA nanofibers described here were produced from a dichloromethane (DCM)/acetone binary solvent system without additional treatment [47]. Constituent solvents of the DCM/acetone binary system were purchased from Sigma-Aldrich (USA) and used without any purification (dichloromethane, DCM,  $\geq 99\%$  (GC); acetone,  $\geq 99\%$  (GC); cellulose acetate, CA, Mw: 30000, 39.8 wt. % acetyl). Briefly, the homogenous electrospinning solution was prepared by dissolving CA in a DCM/acetone (2/1 (v/v)) binary solvent mixture at a 7.5% (w/v) polymer concentration. The clear CA solution was then placed in a 3 mL syringe fitted with a metallic needle of a 0.6 mm inner diameter. The syringe was fixed horizontally on the syringe pump (model SP 101IZ, WPI, USA). The electrode of the high-voltage power supply (Matsusada Precision, AU Series, Japan) was clamped to the metal needle tip, and the cylindrical aluminum collector was grounded. Electrospinning parameters were adjusted as follows: feed rate of solutions = 1 mL/h, applied voltage = 15 kV, tip-to-collector distance = 10 cm. Electrospun nanofibers were deposited on a grounded stationary cylindrical metal collector covered with aluminum foil. The electrospinning apparatus was enclosed in a Plexiglas box, and electrospinning was carried out at 25 °C at 24% relative humidity. Collected

nanofibers/nanowebs were dried overnight at room temperature under the fume hood. The process is summarized in Fig. 4.

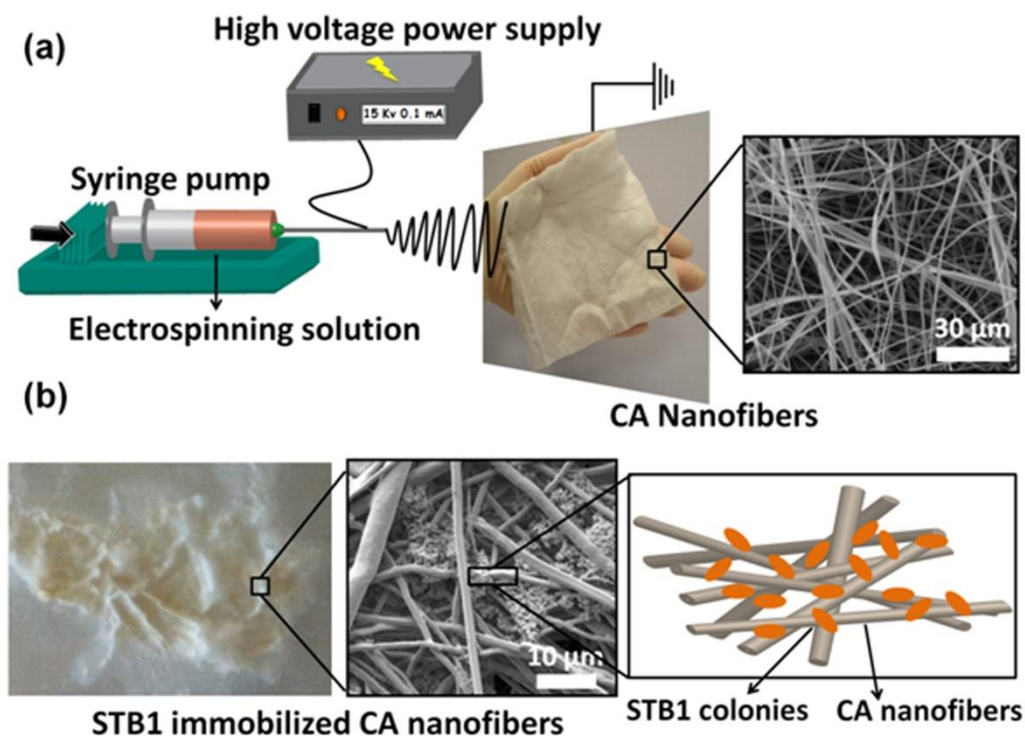


**Figure 4:** (a) Schematic representation of electrospinning process for CA nanofibers and photograph of CA nanofibrous web (b) photograph of STB1 immobilized CA nanofibrous web and schematic representation of bacterial cells on nanofiber surfaces. (Copyright © 2013, Reproduced from Ref. [18] with permission from the Royal Society of Chemistry)

## 2.2. Growth and immobilization of *Acinetobacter calcoaceticus* STB1

The bacterial strain utilized in this study was isolated from brackish water samples collected from a commercial sea bass farm [29]. Immobilization of bacteria was achieved by the inclusion of CA nanofibrous webs in the growth

media of newly inoculated bacteria. Colonies were maintained in 100 mL culture flasks for 30-35 days. The ingredients of the growth medium were: 6.3 g/L  $\text{Na}_2\text{HPO}_4$  ( $\geq 99\%$ ), 3 g/L  $\text{KH}_2\text{PO}_4$  ( $\geq 99\%$ ), 0.5 g/L  $\text{NaCl}$  ( $\geq 99.5\%$ ), 2 g/L glucose (anhydrous), and 300 mL/L of a trace elements solution consisting of 6.1 g/L  $\text{MgSO}_4$  ( $\geq 99.5\%$ ), 3 g/L  $\text{H}_3\text{BO}_3$  ( $\geq 99.5\%$ ), 0.5 g/L  $\text{MnCl}_2$  ( $\geq 99\%$ ), 0.05 g/L  $\text{CaCl}_2$  ( $\geq 93\%$ ), 0.03 g/L  $\text{FeSO}_4 \cdot 7\text{H}_2\text{O}$  ( $\geq 99\%$ ), 0.03 g/L  $\text{CuCl}_2$  ( $\geq 97\%$ ), 0.03 g/L  $\text{ZnCl}_2$  ( $\geq 99.99\%$ ). Ammonium (in the form of  $\text{NH}_4\text{Cl}$ ,  $\geq 99.5\%$ ) was utilized as the nitrogen source during incubation and immobilization, with an initial concentration of 50 mg/L. Following the incubation period, bacterial immobilization was confirmed by SEM imaging and nanofiber samples of equal weights were prepared for further testing. All reagents utilized in this study were purchased from Sigma-Aldrich (USA).

### **2.3. Ammonium removal experiments by using STB1 immobilized CA nanofibers**

The same basal growth medium utilized in bacterial immobilization studies was used in the heterotrophic ammonium removal experiments. Basal growth medium samples were spiked with varying amounts of ammonium (as  $\text{NH}_4\text{Cl}$ ), inoculated with free bacterial samples, bacteria-free nanofibers or bacteria-immobilized nanofibers and incubated for 48 h at 140 rpm and 30 °C. The positive control contained only bacterial inocula at an initial ammonium concentration of 50 mg/L, the negative control contained only nanofibers (0.4 mg of nanofiber per mL) at an initial ammonium concentration of 50 mg/L, and the experimental samples contained bacteria immobilized on CA nanofibers (0.4

mg of nanofiber per mL) at initial ammonium concentrations of 50, 100 and 200 mg/L. Initial ammonium values of the experimental samples were adjusted to 50, 100 and 200 mg/L to represent low, medium and high concentrations of ammonium, and to determine ammonium removal efficiencies at different concentration ranges. Samples were collected periodically to analyze ammonium, nitrite and nitrate values. Bacterial growth rates of the positive control samples were followed by OD<sub>600</sub> measurements. Changes in ammonium, nitrite and nitrate concentrations in the samples were determined by spectrophotometric test kits (Merck Ammonium Cell Test 14559, Merck Nitrate Cell Test 14563 and Merck Nitrite Cell Test 14547). Before performing the tests, samples were centrifuged for 1 min at 12000 rpm at room temperature, and the supernatants were used in analytical measurements of ammonium, nitrite and nitrate. All tests were done in triplicate. Experiments were repeated at least twice.

## **2.4. Scanning Electron Microscopy (SEM)**

Millimeter-length nanofiber pieces with and without bacterial immobilization were cut and prepared for SEM analysis to monitor bacterial attachment before and after ammonium removal experiments. A protocol similar to the Greif and colleagues' was utilized for sample fixation [48]. Briefly, samples were washed twice with PBS buffer and fixed by overnight incubation in 2.5% glutaraldehyde in PBS buffer at room temperature. Following glutaraldehyde fixation, samples were washed twice by PBS buffer and then dehydrated by immersion in a series of ethanol-water solutions ranging from 30% to 96%. Prior to SEM imaging, all

samples were coated with a 5 nm layer of gold-palladium. A Quanta 200 FEG scanning electron microscope (FEI Instruments, USA) was used for the acquisition of SEM images.

## **2.5. Reusability test for STB1 immobilized CA nanofibrous web**

Ammonium removal studies were performed 5 times to assess the reusability of the bacteria-immobilized nanofibers. Prior to each cycle, nanofiber pieces were washed twice with PBS buffer and incubated overnight in PBS to remove any unattached bacteria. The ammonium removal experiments (incubation at 140 rpm and 30 °C for 48 h) described above were performed after each washing step, for a total of 5 cycles. The initial ammonium concentration was fixed at 100 mg/L, since this concentration was found to be more suitable to observe changes in performance values in each cycle compared to low (50 mg/L) and high (100 mg/ L) initial ammonium concentrations. Ammonium concentrations were measured at 0 h and 48 h, and the percentage removal of ammonium was calculated using these results. Each cycle was terminated after 48 h of total incubation and washing steps were repeated for nanofiber samples before the initiation of the next cycle. All tests were done in triplicate.

## **3. Results and Discussion**

### **3.1. Attachment of STB1 strain on CA nanofibrous web**

CA nanofibers can be obtained in smooth or porous morphology depending on the solvent type utilized. While the N,N-dimethylacetamide (DMAc)/acetone blend is one of the most common solvent systems for the electrospinning of

uniform and smooth CA nanofibers [49], we have previously demonstrated the production of nanoporous CA nanofibers by using a highly volatile DCM/acetone solvent mixture [47]. While conventional electrospun CA nanofibers are already suitable for use in biological systems; the rough surface and the higher surface area of porous electrospun CA nanofibers were expected to increase the utility of CA nanowebs in biological applications, and especially for biomedical research. SEM imaging was performed to observe the bacterial adhesion to nanofibers, and 30 days were found to be required for the robust attachment of bacteria onto nanofiber surfaces. Fig. 5a and Fig. 5b show *Acinetobacter calcoaceticus* STB1 cells after 7 days of incubation, wherein no biofilm formation can be observed. SEM images of porous CA nanofibers prior to bacterial attachment are depicted in Fig. 6a and Fig. 6b. The CA fiber diameter range was between 500 nm and 1.5  $\mu\text{m}$ , and the fibers had a ribbon-like morphology [47]. Fig. 6c and Fig. 6d show bacteria strongly attached onto nanofibrous web after 35 days of incubation, and the attached bacteria are observed to form a biofilm structure by adhering to each other and surrounding the filaments of the CA web. This type of attachment was found to be adequate for further studies, and ammonium removal experiments were started with STB1 immobilized CA web samples at this stage.

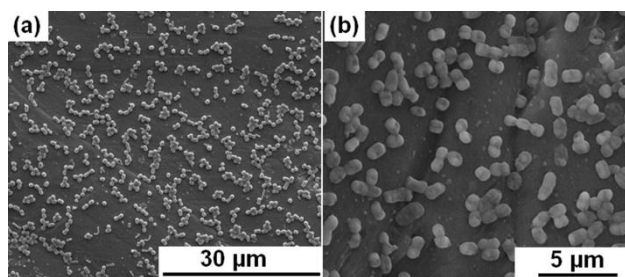


**Figure 5:** General morphology of *Acinetobacter calcoaceticus* STB1 under Scanning Electron Microscope (SEM) at 5000X (a) and 15000X (b) magnification. (Copyright © 2013, Reproduced from Ref. [18] with permission from the Royal Society of Chemistry)

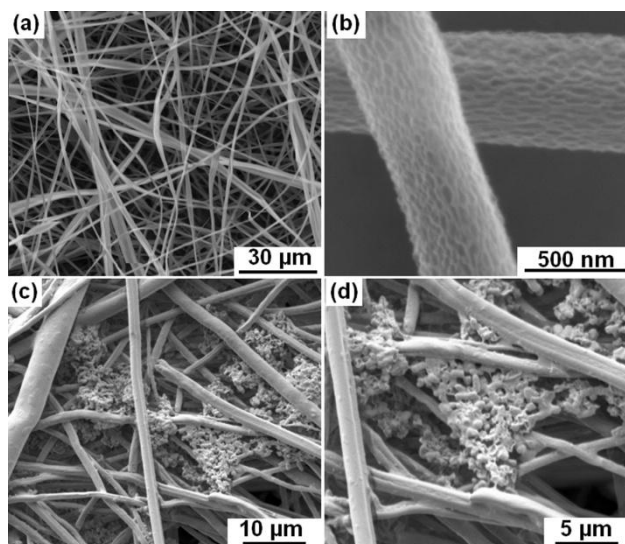


**Figure 6:** SEM micrographs of bacteria-free electrospun CA nanofibers at (a) 2500X and (b) 200000X; and STB1 immobilized nanofibers after 35 days of incubation at (c) 5000X and (d) 10000X magnification. (Copyright © 2013, Reproduced from Ref. [18] with permission from the Royal Society of Chemistry)

### **3.2. Ammonium removal capability of STB1 immobilized CA nanofibrous web**

STB1 immobilized CA nanofibrous webs have shown efficient removal of ammonium at each concentration within 48 h, and the percentile ammonium removal capability of the web samples decreased as the initial ammonium concentrations increased (Fig. 7c, Fig. 7d, Fig. 7e). Bacteria-free CA webs displayed negligible decreases in ammonium concentrations (Fig. 7b), and the removal capability of STB1 immobilized CA nanofibrous web samples were therefore attributed to bacterial nitrogen metabolism. Ammonium removal capability of the STB1/CA nanofibrous web is very similar to that of the free bacteria sample at the initial ammonium concentration of 50 mg/L (Fig. 7a and Fig. 7c), which shows that the STB1/CA nanofibrous web can provide the same outcome as free-suspended bacteria at a defined w/v ratio without including any additional bacterial inocula into the aquatic system. The STB1/CA nanofibrous web was capable of fully remediating an initial ammonium concentration of 50 mg/L, and displayed 98.5% and 72% removal rates at initial ammonium concentrations of 100 mg/L and 200 mg/L, respectively. Increase in nitrate and nitrite concentrations were limited, nitrite concentrations in particular were below detectable limits. Increase in nitrate concentrations was likewise minimal, not exceeding 2 mg/L at the end of 48 h period for each sample. As such, concentrations of nitrite, nitrate and their sum were all below the legal limits for water quality managements [25], which suggests that the production of toxic

metabolic by-products of ammonium is not a problematic issue for STB1/CA nanofibrous webs.

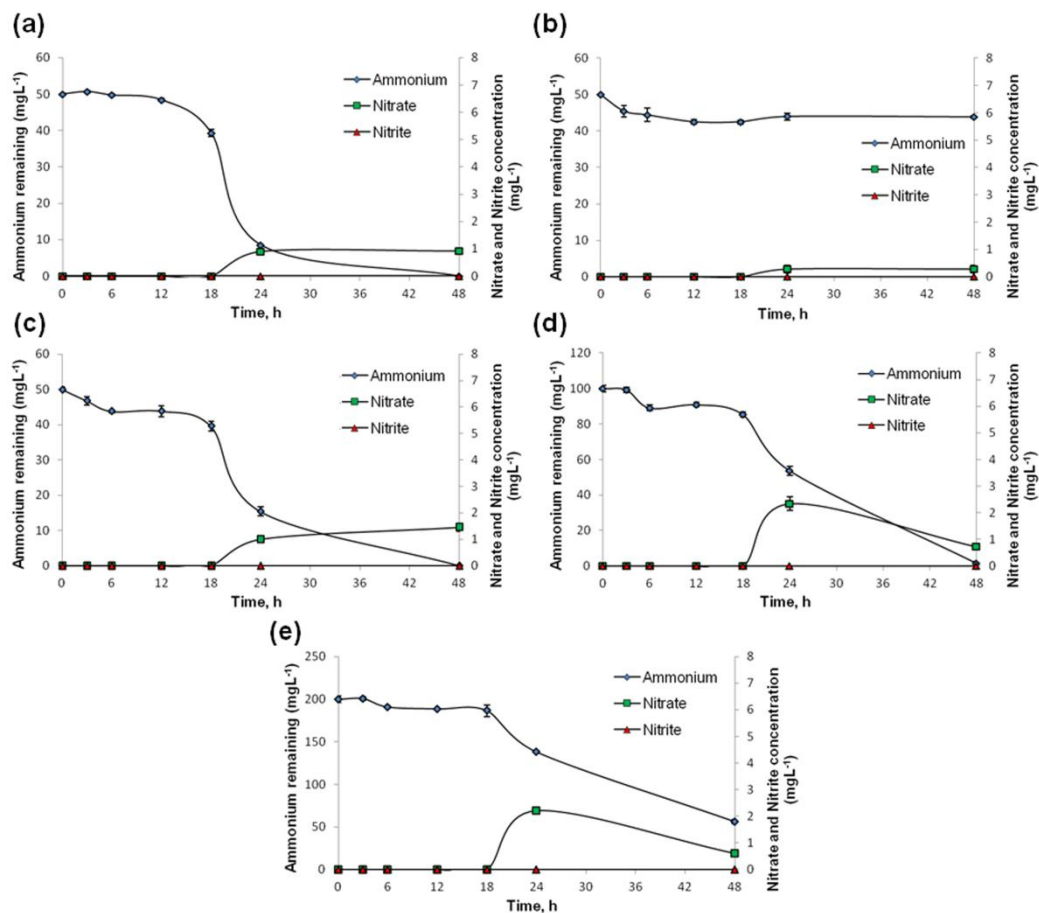


**Figure 7:** Ammonium, nitrite and nitrate levels for: (a) free STB1 cells at initial ammonium concentration of 50 mg/L; (b) bacteria-free CA web at initial ammonium concentration of 50 mg/L; (c) STB1 immobilized CA web at initial ammonium concentration of 50 mg/L; (d) STB1 immobilized CA web at initial ammonium concentration of 100 mg/L; (e) STB1 immobilized CA web at initial ammonium concentration of 200 mg/L. Error bars represent mean of three independent replicates. (Copyright © 2013, Reproduced from Ref. [18] with permission from the Royal Society of Chemistry)

Since nitrite and nitrate levels were minimal for STB1, we have tried to account for the remaining products of ammonium remediation in a previous study by performing Total Nitrogen (TN) analysis with an elemental analyzer [29]. The only nitrogen source in the bacterial growth medium was ammonium for STB1 cells, hence we were able to determine the percentage of ammonium incorporated into cellular biomass for the 100 mg/L sample. Around 22% of the initial ammonium concentration was found to be introduced into the cell biomass; and a further 4% was initially incorporated into cell biomass and subsequently released to the supernatant. For this reason, we have concluded that STB1 cells converted most of the remaining ammonium into gaseous denitrification products [29]. A similar situation was previously observed by Zhao and colleagues, who demonstrated that *Acinetobacter calcoaceticus* strain HNR could convert a considerable amount of ammonium into N<sub>2</sub> gas [27].

### **3.3. Reusability and applicability of STB1 immobilized CA nanofibers**

Ammonium removal capabilities of reused STB1 immobilized CA nanofibrous webs were tested for five cycles of reuse. Fig. 8 shows the performance values of each cycle for the total of 5 cycles. 86% of ammonium removal capacity was obtained for the final cycle (5th cycle) which suggests STB1/CA nanofibrous webs can sustain their ammonium removal capacity under several cycles of reuse. This result is highly promising and with a successful optimization, STB1/CA nanofibrous web may be utilized repeatedly

for ammonium remediation, constituting a reusable material for ammonium remediation from aquatic environments.

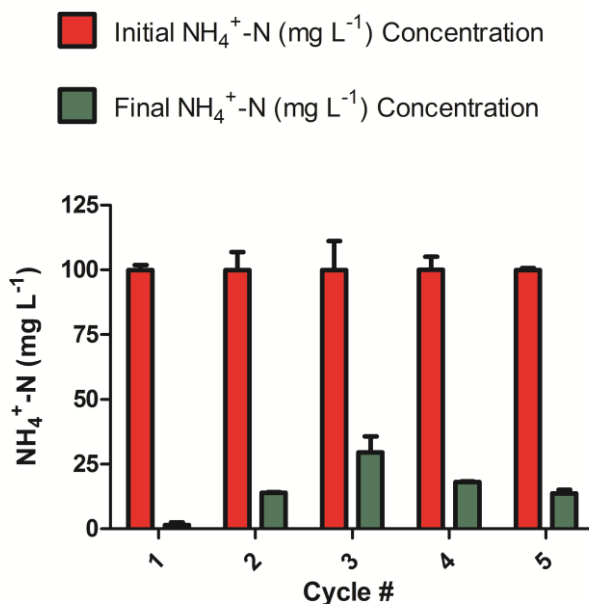


**Figure 8:** Reusability test results of STB1 immobilized CA web for 5 cycles of ammonium removal experiments at initial ammonium concentration of 100 mg/L. Error bars represent mean of three independent replicates. (Copyright © 2013, Reproduced from Ref. [18] with permission from the Royal Society of Chemistry)

After the reusability experiments, CA webs were washed several times with PBS and fixed for SEM imaging. Fig. 9a and Fig. 9b show visible bacterial biofilms on nanofiber surfaces, suggesting that STB1 cells displayed a stronger attachment to CA webs compared to the beginning of the reusability test. As such, washing and reuse of these webs did not lead to a decrease in the quantity of bacterial biofilms, in contrast, the extent of biofilm formation increased and a stronger attachment to the nanofibrous matrix was observed.

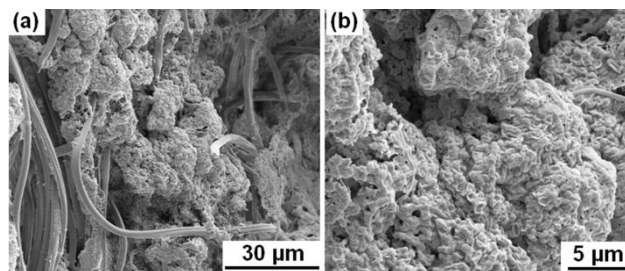


**Figure 9:** SEM micrographs of STB1 immobilized CA web after the reusability tests, showing robust attachment of bacterial biofilms on nanofiber surfaces at (a) 2500X and (b) 10000X magnification. (Copyright © 2013, Reproduced from Ref. [18] with permission from the Royal Society of Chemistry)

The remediation of aquatic systems is an important issue and sustainable solutions, particularly novel and green approaches, for the removal of a wide host of pollutants have received considerable attention in recent times [50, 51]. Since our bacterial isolate is not pathogenic or toxic [29], and biological treatment methods are generally more sustainable and environmentally friendly than their physical and chemical equivalents [52], the use of our bacterial strain is advantageous for ammonium removal. In this study, we immobilized STB1 bacterial strain on electrospun CA nanofibrous webs to analyze the efficiency of these bacteria in ammonium removal, which would be of considerable use in developing novel commercial removal techniques. We deem this approach is successful since bacteria could attach strongly on nanofiber surfaces, STB1 immobilized CA nanofibrous webs could remediate ammonium as effectively as freely floating STB1 bacterial inocula, and the biocomposite material could be used for several cycles for ammonium removal, as shown by reusability test results (Fig. 8). Similar approaches have been proposed in the literature. Eroglu et al. have immobilized microalgal cells on electrospun chitosan nanofiber mats

for the removal of nitrate from liquid effluents [31]. In the present study, ammonium was chosen as the target contaminant due to its high toxicity, and different concentration ranges of ammonium were tested to determine the efficiency of bacteria-immobilized nanofibrous web samples for ammonium removal. The time required for complete removal of 100 mg/L ammonium by STB/CA nanofibrous webs was around 48 h. Zhao et al. reported an *Acinetobacter calcoaceticus* strain capable of completely removing 120/mg L of initial ammonium within 48 h, albeit without the immobilization of bacterial cells on a solid material, which is very similar to our results [26]. The time required for complete removal can be reduced by further modifications, such as increasing the number of bacterial biofilms on nanofiber surfaces or performing optimization studies in heterotrophic conditions for enhanced nitrogen metabolism. However, the presence of embedded bacterial cells within the biofilm complex prevents the estimation of total bacterial count on nanofiber surfaces, and it is therefore difficult to make a quantitative comparison between our results and previous reports in terms of the number of bacteria required for a defined ammonium removal rate.

We observed that, the results of freely floating STB1 cells and STB1 immobilized CA nanofibrous web are quite close however, using STB1/CA nanofibrous web is more advantageous in terms of several points. While a small portion of STB1 immobilized CA nanofibrous web is enough for ammonium bioremoval in a liquid environment, there should be a sufficient number of unimmobilized bacteria in its growth medium for removal of ammonium. STB1/CA nanofibrous web is more applicable and more cost-effective as well,

since when we compare the required amount of STB1/CA nanofibrous web and free STB1 cells for removal of a defined concentration of ammonium, the weight of required STB1/CA nanofibrous web is much lighter in comparison to free STB1 cells (0.4 g of STB1 immobilized CA web is equivalent to 1 L of bacteria containing liquid medium to show the same performance), which provides ease of application for large scale environments and lower transportation costs. In addition, since free STB1 cells are dispersed throughout the medium, it is much more difficult to isolate and reuse them in another ammonium-contaminated area. Finally, biofilm formation in STB1/CA nanofibrous web brings some advantages over free STB1 cells such as higher resistance to environmental extremes and enhanced metabolic activity. Thus, although the results of STB1/CA nanofibrous web and free STB1 cells are very close, the former one is more advantageous for ammonium removal due to aforementioned reasons.

In brief, ammonium removal by STB1 immobilized CA nanofibrous web is very effective and easily applicable to be utilized in a wide variety of environments. The novel biocomposite material described in the present study may therefore assist in the development of alternative green strategies for effective ammonium removal in a variety of freshwater and possibly marine environments.

# Chapter 3

---

## **Bacteria immobilized electrospun fibrous webs for hexavalent chromium remediation**

(Parts of this study was published as “Bacteria-immobilized electrospun fibrous polymeric webs for hexavalent chromium remediation in water”, Omer Faruk Sarioglu, Asli Celebioglu, Turgay Tekinay and Tamer Uyar, *International Journal of Environmental Science and Technology*, June 2, 2016 (Web), Reproduced (or 'Reproduced in part') from Ref. [53] with permission from Springer. doi: 10.1007/s13762-016-1033-0)

## 1. Introduction

Chromium is a commercially important metallic element that is integral for many important industrial processes, such as electroplating, steel production, leather tanning, textile manufacturing and chromate preparation [54]. The trivalent (Cr(III)) and hexavalent (Cr(VI)) forms are the most commonly encountered forms in nature [55]. While Cr(III) is not transported into cells and can be tolerated by many organisms at moderate concentrations, Cr(VI) is a toxic and carcinogenic form that readily permeates through biological membranes and may disrupt the functions of intracellular proteins and nucleic acids [56]. Chromium has been designated as a major pollutant by the United States Environmental Protection Agency (US EPA), and the legal limit defined for all forms of chromium, including Cr(VI), in drinking water is 0.1 mg/L [57]. Heavy metal contamination in water systems can be treated by physical or chemical treatment methods (e.g. chemical oxidation or reduction, ion exchange, reverse osmosis [58]. However, there are several problems related with these techniques such as high operating and maintenance costs, high energy requirements, operational complexity and the production of secondary waste products [59]. Today, biological treatment methods have received considerable attention as potential alternatives to conventional treatment methods [59-61]. In general, bioremediation of heavy metals is performed under acidic pH, since the existence of excess hydrogen ions in the medium facilitates the reduction of metal cations, resulting in higher removal efficiencies [62]. However, these are not self-sustaining and require the constant influx of externally produced

biomass, as most microorganisms cannot tolerate acidic environments and perish rapidly under such conditions. In addition, the water system must be further treated for neutralization before discharge. For that reason, bioremediation at neutral conditions with living microorganisms is a more eco-friendly process, and allows metal removal to occur continuously without external intervention. *Morganella morganii* STB5 is a bacterial strain previously isolated for this purpose and can be used for the effective removal of Cr(VI) at neutral conditions.

Carrier materials can be used to enhance the heavy metal removal capacities of bioremediative organisms [63]. Electrospun nanofibers are popular choices as carrier materials and they have already been studied for pollutant removal [64, 65]. Polystyrene (PS) and polysulfone (PSU) are two common biocompatible polymers [66] that have been used for water filtration, and there are various examples in the literature about the applications of these polymers as electrospun nanofibers for filtering purposes [35, 67-69]. Studies regarding the use of microorganism-integrated electrospun fibrous biocomposites for pollutant removal have recently begun to appear in the literature [10, 11, 14, 18-20, 22]. Lower space and growth medium requirements, ease of handling and potential reusability of these systems are some of the main advantages for using them in remediation studies [14]. Immobilization of microorganisms on a carrier matrix protects them from harsh environmental conditions and stresses associated with heavy metal toxicity [36]. In addition, natural adhesion of bacteria permits the formation of biofilms and maximizes cell viability and biochemical activity [37].

In this study, development of two novel biocomposite materials for Cr(VI) removal in water by immobilization of a previously isolated *Morganella morganii* STB5 strain on electrospun PS and PSU fibrous webs is described. Integration of PS and PSU webs with bacterial cells is aimed to be effective for continuous Cr(VI) remediation in aqueous systems.

## **2. Materials and Methods**

### **2.1. Electrospinning of PS and PSU webs**

The homogenous electrospinning solution was prepared by dissolving 30 % (w/v) polystyrene (PS, Mw ~208,000, Sigma-Aldrich) in N,N-dimethylformamide (DMF, anhydrous, 99.8 %, Sigma-Aldrich) or 32 % (w/v) polysulfone (PSU, Mw ~60,000, Scientific Polymer Products, Inc.) in N,N-dimethylacetamide/acetone (9/1, (v/v)) (DMAC, Sigma-Aldrich, 99 %; acetone, Sigma-Aldrich, ≥99 % (GC)) binary solvent mixture. Each polymer solution was loaded in a syringe with an inner diameter of 0.4 mm. The syringe was fixed horizontally to the syringe pump (model KDS-101, KD Scientific, USA). The electrode of the high-voltage power supply (Spellman, SL30, USA) was clamped to the metal needle tip, and the plate aluminum collector was grounded. Electrospinning parameters were adjusted as follows: feed rate of solutions = 0.5 mL/h, applied voltage = 10 kV, tip-to-collector distance = 10 cm. Electrospun nanofibers were deposited on a grounded stationary plate metal collector covered with aluminum foil. The electrospinning apparatus was enclosed in a Plexiglas box, and electrospinning was performed at 25 °C at 20% relative

humidity. Collected nanofibers/nanowebs were dried in vacuum oven at 50 °C overnight to remove residual solvent. The electrospinning process is schematically represented in Fig. 10.

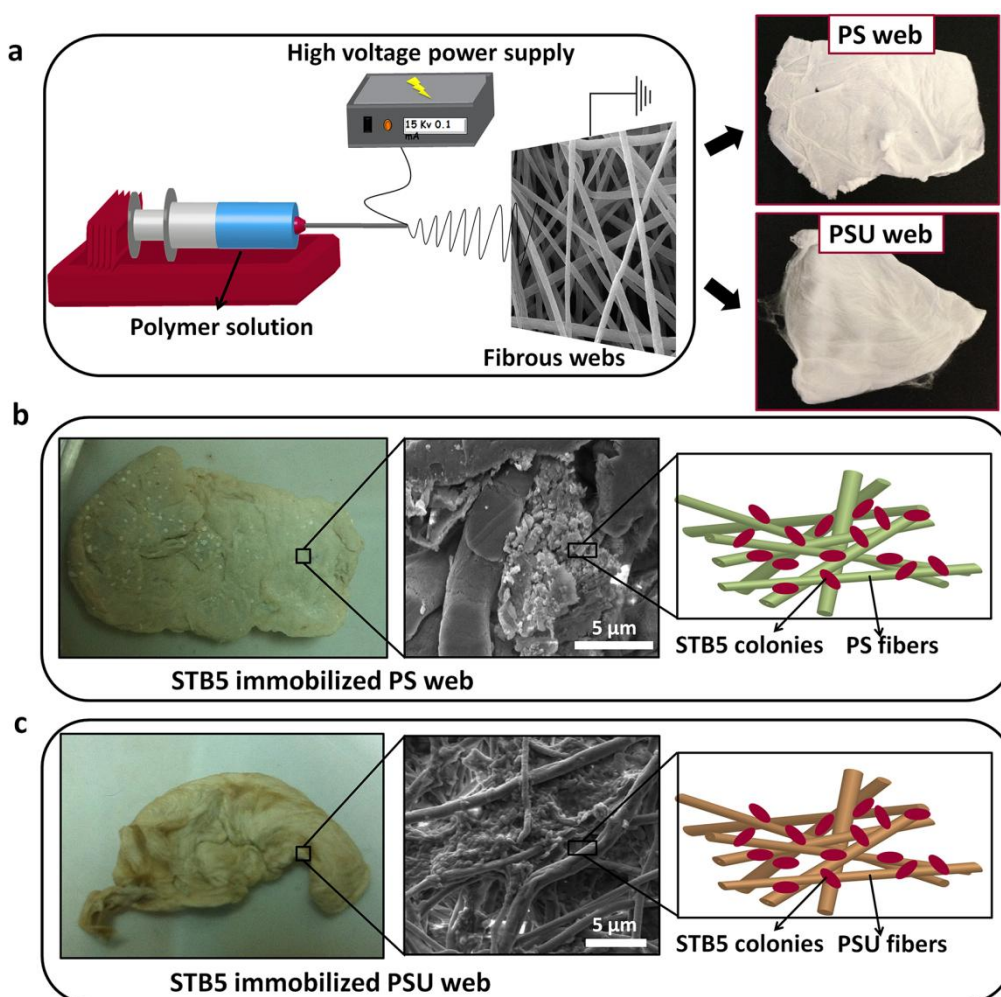


**Figure 10:** (a) Schematic representation of electrospinning process and photographs of PS and PSU webs, (b) photographs of STB5 immobilized PS and (c) STB5 immobilized PSU webs along with SEM micrographs and schematic representations of bacterial cells on fibrous surfaces. (Copyright © 2013, Reproduced from Ref. [53] with permission from Springer)

## **2.2. Contact angle measurements**

Thin surfaces of PS and PSU webs were electrospun on microscope slides to be analyzed with a contact angle measurement system (Dataphysis, OCA 30). Contact angles were measured over a relatively intact and smooth region for each web; three independent measurements were recorded for each sample. Measurements were performed in a closed chamber at ambient temperature.

## **2.3. Growth and immobilization of *Morganella morganii* STB5**

The bacterial strain (*Morganella morganii* STB5) utilized in this study was previously isolated from a local river (Ankara River). Bacterial immobilization was achieved by the inclusion of PS or PSU webs in the growth media of newly inoculated bacteria. Bacterial colonies were maintained for 30 days in 100 mL erlenmayer flasks containing M1 growth medium (pH 7.0). The ingredients of M1 growth medium are: 10 g/L peptone, 2 g/L meat extract, 1 g/L yeast extract and 5 g/L NaCl ( $\geq 99\%$ ) in distilled water. After 30 days of incubation, bacterial immobilization was confirmed by scanning electron microscopy (SEM) analysis. Following confirmation of bacterial immobilization, bacteria-immobilized PS and PSU web samples of equal weights were prepared for Cr(VI) bioremoval experiments. All reagents utilized were purchased from Sigma-Aldrich (USA).

## 2.4. Cr(VI) bioremoval by using STB5/PS and STB5/PSU biocomposite webs

M1 growth medium was used in the Cr(VI) bioremoval studies and all tests were performed in triplicate. The bacterial growth media were spiked with different amounts of Cr(VI) (10, 15 and 25 mg/L, in the form of  $K_2Cr_2O_7$ ,  $\geq 99\%$ , Sigma-Aldrich) and inoculated with free bacterial cells, bacteria-free fibers or bacteria-immobilized fibers prior to incubation at 150 rpm and 30 °C for 72 h. The positive control contained free bacterial cells ( $\sim 10^8$  cfu/mL), the negative control contained pristine fibers and the experimental samples contained bacteria-immobilized PS or PSU fibers, where the w/v ratio of web samples was fixed as 2.8 mg/mL. Samples were collected periodically to determine the remaining amount of Cr(VI). Cr(VI) concentrations were measured via 1,5-diphenylcarbazide, following the EPA protocol [70] for hexavalent chromium detection. The removal capacities ( $Q_{eq}$ ) of free STB5 cells and STB5 immobilized web samples were calculated by Eq. 1 (1)

$$Q_{eq} \text{ (mg/g)} = (C_0 - C_f) \cdot V / M \quad (1)$$

where  $C_0$  is the initial Cr(VI) concentration (mg/L),  $C_f$  is the final Cr(VI) concentration (mg/L),  $V$  is the solution volume (L) and  $M$  is the total bacterial cell biomass (g) at equilibrium [71].

As demonstrated previously, *Morganella morganii* STB5 cells do not store or accumulate Cr(VI) without conversion, as no Cr(VI) release could be observed following the destruction of bacterial cell membranes through sonication [62]. It was therefore assumed that all decreases in Cr(VI)

concentrations are due to reduction and the removed Cr(VI) is reduced entirely to the stable Cr(III).

## **2.5. Adsorption isotherms and kinetics studies**

Adsorption isotherm coefficients were determined upon three isotherm models (Langmuir, Freundlich and Toth) using the isotherm parameter fitting software IsoFit [72]. The order of reactions for Cr(VI) removal were predicted by plotting zero, first, second and third order plots of STB5/PS and STB5/PSU webs to calculate and compare their  $R^2$  values for evaluation of the best fitting models.

## **2.6. Scanning Electron Microscopy (SEM)**

Millimeter-length PS and PSU webs with and without bacterial immobilization were cut and prepared for SEM analysis to evaluate bacterial attachment before and after Cr(VI) bioremoval experiments. A modified protocol was utilized for SEM sample fixation [48]. Briefly, samples were washed twice with PBS (Phosphate-Buffered Saline) buffer and incubated overnight in 2.5% glutaraldehyde solution (prepared in PBS buffer) at room temperature. Samples were then washed twice by PBS buffer and dehydrated by immersion in a series of ethanol-water solutions (30% - 96%). All fixed samples were coated with 5 nm Au-Pd prior to SEM imaging (Quanta 200 FEG SEM, FEI Instruments, USA).

## **2.7. Reusability and post-storage performances of STB5/PS and STB5/PSU fibrous biocomposites**

Cr(VI) bioremoval studies were performed five times to evaluate the reusability of STB5/PS and STB5/PSU fibrous biocomposites. Prior to each cycle, biocomposites were washed with PBS buffer twice and then incubated overnight in this buffer to eliminate any unattached bacteria. Cr(VI) bioremoval experiments were performed with the parameters as described above (incubation at 150 rpm and 30 °C for 72 h). The initial Cr(VI) concentration was fixed at 25 mg/L, the remaining Cr(VI) concentrations were measured at 0 h and 72 h, and the percentile removal of Cr(VI) was calculated using these results. Each cycle was ended after 72 h of incubation and washing steps were repeated for each biocomposite before starting the next cycle. All tests were done in triplicate.

## **3. Results and Discussion**

### **3.1. Attachment of bacterial cells on PS and PSU webs**

Polystyrene (PS) and polysulfone (PSU) based polymeric materials can be used for water purification as membranes or filters, and there are several reports in the literature about the applications of these polymers as electrospun nanofibers for water filtering purposes [35, 67-69]. In this study, high-surface area electrospun PS and PSU fibers were used as substrates for bacterial attachment and the combined system was subsequently utilized for Cr(VI) removal. SEM analysis was performed to assess the extent of bacterial attachment on the fibrous surfaces, and an incubation period of 30 days was found to be required

for robust bacterial adhesion. SEM images of PS and PSU webs before bacterial adhesion are shown in Fig. 11a and 11b.

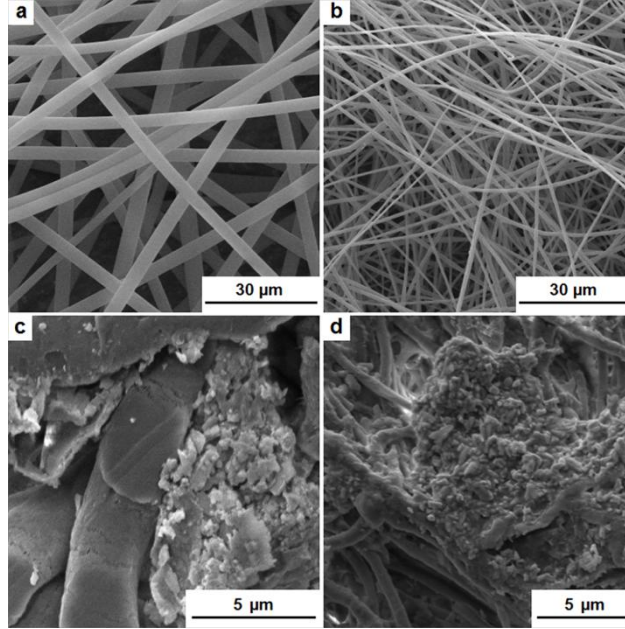


**Figure 11:** SEM micrographs of (a) PS and (b) PSU webs without bacterial immobilization, and (c) STB5 immobilized PS and (d) STB5 immobilized PSU webs after 30 days of incubation for bacterial immobilization. (Copyright © 2013, Reproduced from Ref. [53] with permission from Springer)

The average diameters of PS and PSU fibers were found as 2 μm and 0.8 μm, respectively. Furthermore, both electrospun webs were tested for hydrophobicity differences by contact angle (CA) measurements. PS webs were found to be relatively more hydrophobic (CA:  $146.13^\circ \pm 4.74$ ) compared to PSU webs (CA:  $126.5^\circ \pm 5.91$ ), although both webs have hydrophobic character. Fig. 11c and 11d show that bacterial cells attached strongly on PS and PSU fibrous surfaces after 30 days of incubation, suggesting that both webs are suitable for strong bacterial adhesion. The bacterial cells formed biofilm structures by

adhering to each other and to the surrounding PS and PSU fibers. Bacterial adhesion at this stage was found to be sufficient for further studies, and Cr(VI) bioremoval experiments were started with bacteria-immobilized PS and PSU webs.

### **3.2. Cr(VI) bioremoval capability of STB5/PS and STB5/PSU biocomposite webs**

Initially, free STB5 cells were tested for Cr(VI) removal at five different pH levels to find out the optimal pH level for the removal process (Fig. 12a). Neutral pH (pH 7.0) was found as the optimal level for Cr(VI) remediation by STB5 cells, and the pH levels of further studies were adjusted accordingly. Since the highest Cr(VI) removal performance was achieved at neutral conditions instead of acidic environments, it was inferred that biological removal rather than adsorption is the primary removal practice for STB5 cells. STB5/PS and STB5/PSU biocomposite webs have shown efficient removal of Cr(VI) at three different initial concentrations (10, 15 and 25 mg/L) within 72 h, and their Cr(VI) removal profiles are comparable to free bacterial cells, suggesting that the biocomposites can remediate Cr(VI) as effectively as freely floating cells and the results are highly promising for further Cr(VI) remediation studies (Fig. 12b). Bacteria-free PS and PSU webs have shown very similar and slight decreases (13.5 % and 12.3 %, respectively) in the initial Cr(VI) concentration (Fig. 12c), possibly due to adsorption, implying that the Cr(VI) remediation capability of STB5/PS and STB5/PSU biocomposites are primarily due to on the presence of bacterial cells.

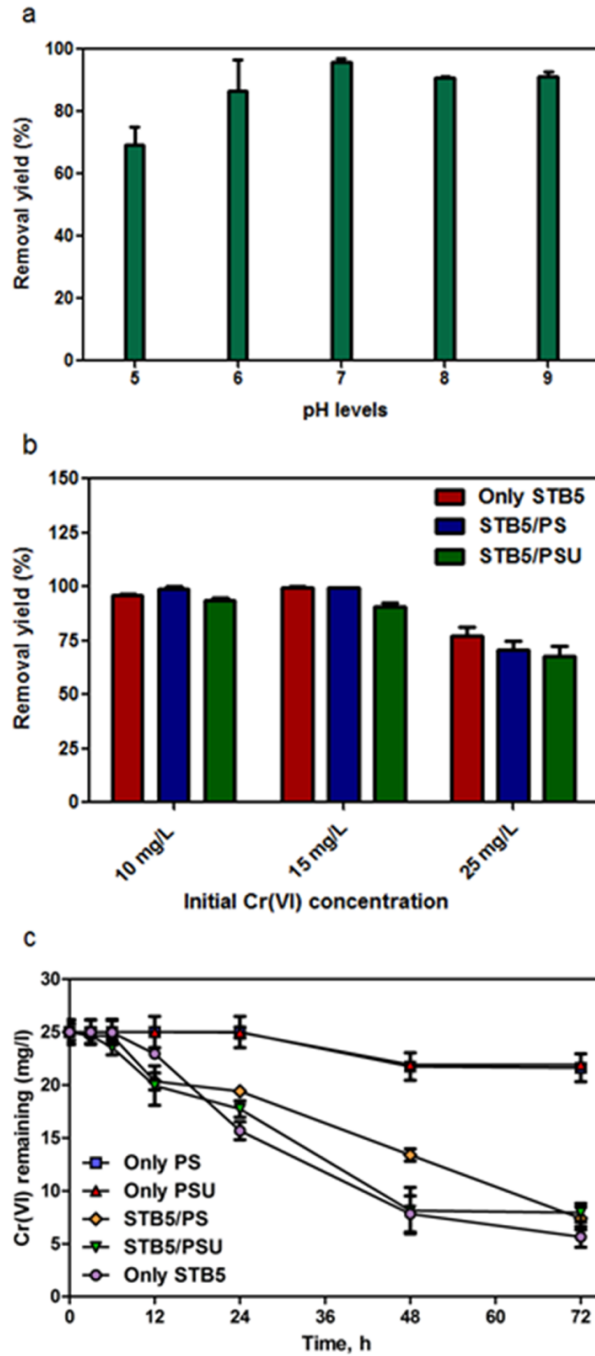


**Figure 12:** Cr(VI) bioremoval profiles of (a) free STB5 cells at different pH levels, (b) only STB5, STB5/PS and STB5/PSU samples at different initial Cr(VI) concentrations, (c) only STB5, only PS, only PSU, STB5/PS and STB5/PSU samples at an initial concentration of 25 mg/L. Error bars represent mean of three independent replicates. (Copyright © 2013, Reproduced from Ref. [53] with permission from Springer)

**Table 1.** Removal capacities of only STB5, STB5/PS and STB5/PSU samples at equilibrium under different initial Cr(VI) concentrations, measured at the end of the 72 h removal period. T = 30 °C, agitation rate: 150 rpm, average bacterial biomass concentration  $0.15 \pm 0.03$  g/L. (Copyright © 2013, Reproduced from Ref. [53] with permission from Springer)

Sample name	Initial concentration (C <sub>0</sub> )	Removed Cr(VI)	Q <sub>eq</sub> (mg/g)	Removal (%)
Only STB5	10 mg/L	9.56 mg/L	64.83 ± 5.68	95.8
STB5/PS	10 mg/L	9.36 mg/L	63.49 ± 4.3	93.6
STB5/PSU	10 mg/L	9.39 mg/L	63.64 ± 7.59	93.79
Only STB5	15 mg/L	14.95 mg/L	101.35 ± 14.5	99.56
STB5/PS	15 mg/L	14.91 mg/L	101.11 ± 15.3	99.47
STB5/PSU	15 mg/L	12.52 mg/L	84.9 ± 4.2	90.78
Only STB5	25 mg/L	19.35 mg/L	131.2 ± 12.4	77.41
STB5/PS	25 mg/L	17.60 mg/L	119.3 ± 7.65	70.41
STB5/PSU	25 mg/L	17.07 mg/L	115.7 ± 11.2	68.27

As demonstrated in Table 1, the Q<sub>eq</sub> (removal capacity at equilibrium) values of free STB5 cells are always higher than STB5/PS and STB5/PSU webs, while Q<sub>eq</sub> values of STB5/PS are following this sample generally. Two different types of polymeric webs were utilized as carrier matrices for bacterial immobilization, and PS was found to be a slightly better carrier matrix in terms of Cr(VI) removal capacity of its bacteria immobilized form, possibly due to its more hydrophobic nature. It is known that gram negative bacteria including *Morganella morganii* have hydrophobic surfaces because of the high lipid content on their cell walls, and hydrophobic bacteria have a preference to adhere on hydrophobic surfaces via hydrophobic interactions [73, 74]. Therefore, hydrophobicity differences might play an important role on the adhesion of STB5 cells, and higher bacterial immobilization on PS web surfaces contributed

to higher Cr(VI) removal performances by STB5/PS samples. Nonetheless, considerable amounts of Cr(VI) were removed in all experiments, suggesting that both biocomposites are promising candidates as supportive systems for conventional Cr(VI) remediation techniques. Since the biocomposites can work under non-acid treated environments, such type of remediation can be applied in natural environments and allow the continuity of the remediation process.

### **3.3. Evaluation of adsorption isotherm coefficients and reaction kinetics**

Adsorption isotherm plots for 3 different tested models (Langmuir, Freundlich and Toth) are presented in Fig. 13 and adsorption isotherm coefficients with their estimated values are listed in Table 2. While STB5/PSU fits well to each of the tested model, only STB5 and STB5/PS samples do not fit to any of the tested models, thus the adsorption isotherm coefficients of these samples were not discussed. It was concluded that, biological removal has the leading role in Cr(VI) remediation by free or immobilized bacteria, since adsorption isotherm coefficients fit only in one sample and the removal process performs best at neutral conditions where biological processes and enzymatic activity are more active usually. The highest correlation was observed in Langmuir model for STB5/PSU sample with the  $R_y^2$  value of 0.997, suggesting that the dye removal process might be homogenous and monolayeric for this sample [62]. The maximum removal capacity ( $Q_{max}$ ) of STB5/PSU was measured as 139.83 mg/g under this model.

The reaction rate can give clues about the reaction mechanism. For instance, while zero order models usually need a catalyst, like enzymes, to proceed, in first order models, the reaction rate depends on only a single reactant concentration [75]. According to the reaction kinetics studies, it was observed that while STB5/PS fits better for zero order reactions, only STB5 and STB5/PSU samples fit better for first order reactions (Table 3). It has been reported that while enzyme-catalyzed reactions often fall under the zero order model [75], Cr(VI) reduction kinetics can fit under the first order model [76], as previously observed by another bacteria immobilized PSU web sample [20].

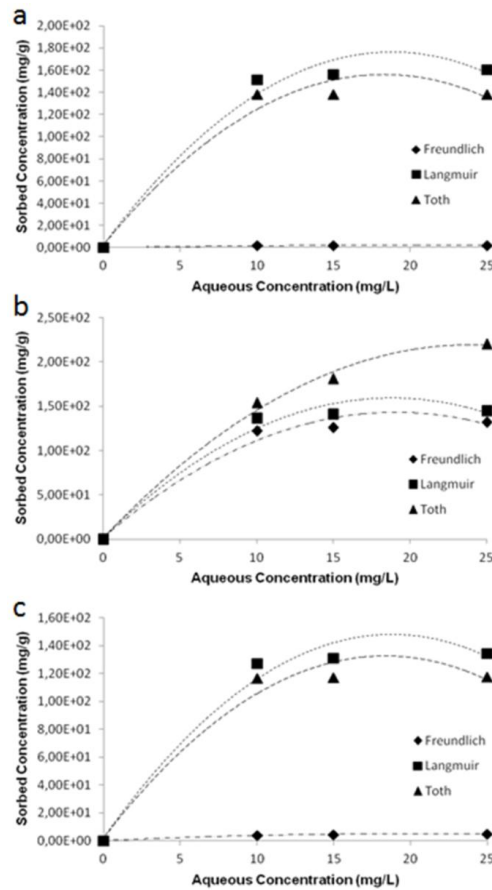


**Figure 13:** Adsorption isotherm plots of (a) only STB5, (b) STB5/PS, (c) STB5/PSU samples for Freundlich, Langmuir and Toth adsorption models. (Copyright © 2013, Reproduced from Ref. [53] with permission from Springer)

**Table 2.** Adsorption isotherm coefficients of only STB5, STB5/PS and STB5/PSU samples for each isotherm model. (Copyright © 2013, Reproduced from Ref. [53] with permission from Springer)

Sample	Isotherm	Parameters	Values	Ry <sup>2</sup> value
Only STB5	Freundlich	Kf	103.4	0.289
		1/n	0.08	
	Langmuir	Q <sub>max</sub>	166.5	0.385
		b	1.00	
	Toth	Q <sub>max</sub>	137.8	0.292
		b	0.99	
STB5/PS	Freundlich	n	4.99	
		Kf	100.61	0.539
		1/n	0.083	
	Langmuir	Q <sub>max</sub>	150.43	0.551
		b	1.00	
	Toth	Q <sub>max</sub>	4576	0.555
b		0.99		
n		0.156		
STB5/PSU	Freundlich	Kf	75.47	0.964
		1/n	0.211	
	Langmuir	Q <sub>max</sub>	139.83	0.997
		b	1.00	
	Toth	Q <sub>max</sub>	117.9	0.986
		b	1.00	
n	1.71			

**Table 3.** The R<sup>2</sup> values of zero, first, second and third order plots for the removal of Cr(VI) by only STB5, STB5/PS and STB5/PSU samples. (Copyright © 2013, Reproduced from Ref. [53] with permission from Springer)

Samples	Model	R <sup>2</sup> values
Only STB5	zero order	0.9465
	first order	0.9790
	second order	0.9758
	third order	0.9390
STB5/PS	zero order	0.9832
	first order	0.9702
	second order	0.9064
	third order	0.8227
STB5/PSU	zero order	0.9291
	first order	0.9346
	second order	0.9219
	third order	0.9054

### 3.4. Reusability and applicability of STB5/PS and STB5/PSU biocomposites

The potential of long-term Cr(VI) removal with STB5/PS and STB5/PSU biocomposites was evaluated through a reuse test where the materials were washed and used for Cr(VI) removal in five consecutive cycles. Fig. 14 shows the performance values of each cycle and the post-storage performances of both biocomposites following 15 days of storage at 4 °C in a closed moist environment.

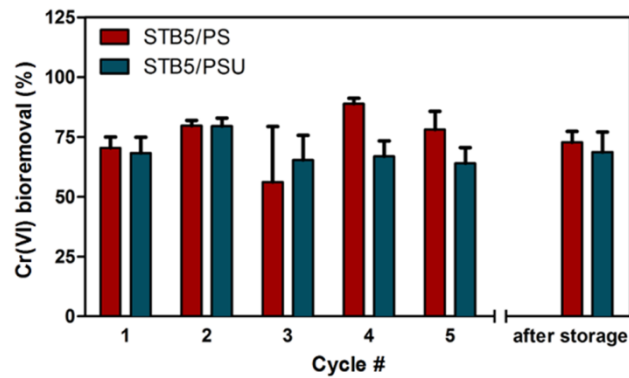


**Figure 14:** Reusability and post-storage test results of STB5/PS and STB5/PSU biocomposite webs for an initial concentration of 25 mg/L. Error bars represent mean of three independent replicates. (Copyright © 2013, Reproduced from Ref. [53] with permission from Springer)

At the end of the reusability test, an average removal capacity of 74.63% was achieved for STB5/PS, while this value was 63.95% for STB5/PSU, indicating that both biocomposites retain their Cr(VI) removal capacity, and the STB5/PS biocomposite was relatively more efficient for continual Cr(VI) bioremoval. The results of the post-storage experiment were also promising, as

72.79% and 68.65% Cr(VI) removal was observed for STB5/PS and STB5/PSU following 15 days of storage, demonstrating that both biocomposites can be stored for short periods of time without losing their Cr(VI) removal capabilities. These results as a whole are very promising and after process optimization, STB5/PS and STB5/PSU biocomposites may be utilized repeatedly for Cr(VI) removal and can be stored for longer periods of time, thus serving as reusable and storable materials for the remediation of Cr(VI) from aqueous environments. Following reusability and storage tests, the biocomposites were washed several times with PBS buffer and fixed for SEM analysis.

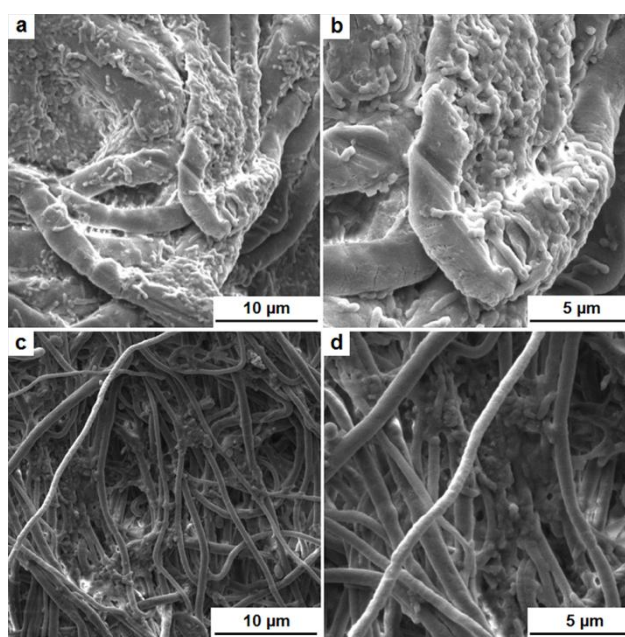


**Figure 15:** SEM micrographs of STB5 immobilized (a-b) PS and (c-d) PSU webs after the reusability tests, showing robust attachment of bacterial biofilms on fibrous surfaces at (a-c) 5000X and (b-d) 10000X magnification. (Copyright © 2013, Reproduced from Ref. [53] with permission from Springer)

Fig. 15 shows bacterial biofilms are present on both PS and PSU webs, indicating that bacterial cells survive throughout the reusability experiments. It can be inferred that washing and reuse of bacteria immobilized PS and PSU web samples did not lead to a viable decrease in the quantity of bacterial biofilms, and the bacterial cells are likely to be preserved on both PS and PSU webs.

Heavy metal remediation of aquatic systems is a substantial issue, and greener approaches are becoming more popular as of late [77-81]. In this study, a Cr(VI)-reducing bacterial strain was immobilized on electrospun PS and PSU webs, and Cr(VI) removal performances of these newly generated biocomposites were evaluated. It was found that bacterial cells could attach strongly on fibrous surfaces, the biocomposites have the capability to remediate Cr(VI) as effectively as free STB5 cells, they can be reused for several cycles of Cr(VI) removal and they can be stored without losing their Cr(VI) bioremoval capabilities. Similar approaches have been proposed in the literature for remediation of water contaminants, and there are some examples for treatment of water systems by using biointegrated electrospun nanofibrous structures. A novel biocomposite have been produced by Eroglu and colleagues for nitrate bioremoval by immobilizing microalgal cells on electrospun chitosan nanofiber mats [14]. In very recent studies, specific bacterial or algal strains have been immobilized on electrospun nanofibrous webs for ammonium bioremoval [18], methylene blue dye biodegradation [22], reactive dye biodegradation [21], anionic surfactant biodegradation [19], and simultaneous removal of Cr(VI) and a reactive dye [20]. In the current study, Cr(VI) was selected as the target contaminant, and two different bacteria-immobilized electrospun fibrous webs

were prepared to evaluate their Cr(VI) remediation profiles. It was found that Cr(VI) removal performance of STB5 strain decreases at higher concentrations, suggesting that this strain and the biocomposites may be more suitable for bioremediation of freshwater systems with lower amounts of Cr(VI) contamination. By increasing the coverage area of immobilized bacteria in STB5/PS and STB5/PSU webs, or optimizing the bacterial growth conditions, it is likely that higher removal rates for Cr(VI) can be achieved for both biocomposites.

In brief, Cr(VI) removal by STB5/PS and STB5/PSU biocomposites is handy, effective and easily applicable. The results suggest that both biocomposites have the potential to be further developed for use in Cr(VI) remediation from aqueous environments.

## **Chapter 4**

---

**An easy and effective method for determination of the number of bacteria that are immobilized on electrospun nanofiber surfaces**

## 1. Introduction

Although there are some studies in the literature about the integration of microorganisms to electrospun fibrous materials, to determine the number of microorganisms that are attached/embedded on the fiber surfaces, there is not a certain protocol to follow. Especially, formation of biofilm structures on the surfaces makes quantification very difficult. Eroglu et al. have given the number of algal cells that are present on chitosan nanofiber mats per  $100\text{ }\mu\text{m}^2$  area (quantified by SEM) to compare algal attachments at different incubation times [14]. In their study, while the average number of algal cells for 3 days of incubation per  $100\text{ }\mu\text{m}^2$  area was 4, this number increased to 20 cells per  $100\text{ }\mu\text{m}^2$  area for 10 days of incubation [14]. Nevertheless, this type of quantification is very difficult and not so reliable since scanning of whole sample is needed and SEM measurements allow analysis of a small sample once, in addition microbial distribution is not uniform for microorganism immobilized samples such that, some regions may be more intense in terms of microbial number and biofilm formation.

Although there are some methods to quantify bacterial biomass or the cell number that are attached on different carrier materials, there is not a single study which gives the amount of bacteria that are attached on electrospun fibrous materials as a result of natural adhesion. Therefore, we tried to apply one of the most reliable method to quantify bacteria that are present on nanofiber surfaces. VCC (Viable Cell Count) is a direct quantification method and it gives only the

number of living cells that are present in the environment. So it allows to estimate the number of active cells that can be used for a specific interest.

To apply this method, first we needed to detach bacterial cells from electrospun fibrous mats with minimal cell viability loss. Based on our survey through the literature and academic forums, we noticed that sonication can be used for bacterial detachment with proper settings. One of the issue that we should consider is preventing or minimizing the excess heat generation due to the sonication process to minimize the cell viability loss, by conducting sonication at cold temperatures. At the end, we generated a protocol to detach bacterial cells from electrospun fibrous mats for further viable cell counting (VCC) assay, by slightly modifying Kobayashi and colleagues' protocol [82].

## **2. Experimental**

### **2.1. Materials and electrospinning**

Cellulose acetate, (CA, Mw: 30000 g/mol, 39.8wt. % acetyl, Sigma-Aldrich), Dichloromethane (DCM,  $\geq 99\%$  (GC), Sigma-Aldrich), acetone ( $\geq 99\%$  (GC), Sigma-Aldrich), methanol (99.7%, Riedel), Sigma-Aldrich), LB broth (Sigma-Aldrich) and Agar (Sigma-Aldrich) were purchased and used without any purification.

Cellulose acetate (CA) nanofibrous webs were produced with porous (nCA) and non-porous (pCA) morphologies by using different binary solvent systems. The electrospinning solutions were prepared by dissolving CA in DCM/methanol (4/1 (v/v)) and DCM/acetone (1/1 (v/v))

mixtures at 12% (w/v) and 10% (w/v) CA concentrations for nCA and pCA, respectively. The electrospinning solutions were loaded in a syringe fitted with a metallic needle which was located horizontally on a syringe pump. One of the electrodes of high-voltage power supply was clamped to the metallic needle and the plate aluminum collector was grounded. The electrospinning parameters were: feed rate = 0.5 mL/h, voltage = 10-15 kV, tip-to-collector distance = 10-12 cm. The grounded stationary metal collector covered with an aluminum foil was used to deposit the electrospun nanofibers. The electrospinning apparatus was enclosed in a Plexiglas box and electrospinning was carried out at about 23 °C at 20% relative humidity. The collected nanofibers/nanowebs were dried overnight at room temperature in a fume hood.

## **2.2. Natural Adhesion on electrospun nanofibers**

Similar/equal weights of nanofiber pieces were added into bacterial growth media (LB) during bacterial growth period for natural adhesion. The bacterial strains utilized in this study were obtained from our culture collections. While *Acinetobacter calcoaceticus* STB1 strain was previously isolated from a hatchery, *Pseudomonas aeruginosa* ATCC 47085 strain was purchased from ATCC (American Type Culture Collection, USA). Both porous (pCA) and non-porous (nCA) cellulose acetate nanofibrous webs were utilized for bacterial immobilization.

### 2.3. Vortexing and Sonication

After successful bacterial immobilization, equivalent nanofiber samples were collected and suspended from the liquid culture. Then they are transferred into 1 mL Tris-HCl (or another buffer) containing eppendorf tubes and vortexed for 30 s before sonication. Sonication was conducted at 40 kHz and 0-4 °C (the cuvette is full of ice). The cycles were 1 min sonication and 30 s rest for each run, till 10 min of sonication is completed. For the initial trials, the sonication step was repeated twice, while this was found to be quite harmful for keeping detached bacterial cells alive, hence this step was performed once for further experiments. After sonication, the samples were vortexed again and the OD<sub>600</sub> values of the liquid samples were measured. Fig. 16 shows the photographs of pristine, bacteria immobilized and bacteria detached nanofibers.

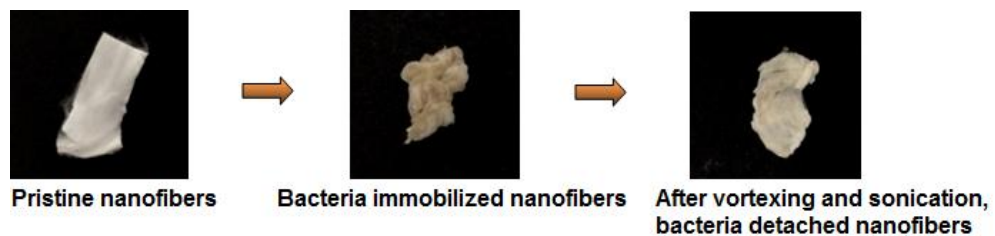


**Figure 16:** Photographs of pristine, bacteria immobilized and bacteria detached nanofibers.

### 2.4. Viable Cell Counting

The liquid samples containing detached bacterial cells were equally diluted ( $10^6$  -  $10^7$ ) and evenly spread on LB or Nutrient agar plates. After overnight incubation, cfu/mL values were determined via direct counting.

## **2.5. Cell growth and monitoring of the bacterial immobilization**

Equal or similar weighted electrospun nanofiber pieces were prepared before starting bacterial growth. Those nanofiber pieces were added to bacterial growth media for each separate sample and incubated with bacterial inocula for a defined period at bacterial growth conditions (e.g. 30 °C, 150 rpm). Bacterial growth and immobilization was followed visually through color change and photographs were taken at different time periods. In addition to the macroscale images, SEM micrographs were taken for each sample to compare the bacterial attachment before and after sonication process. SEM sample fixation and monitoring were performed as presented in the previous chapters.

## **3. Results and discussion**

### **3.1. Immobilization of *Acinetobacter calcoaceticus* STB1 strain on pCA nanofibrous web and detachment of bacterial cells by applying the detachment protocol: 1<sup>st</sup> trial**

An efficient ammonium removing biocomposite, STB1/CA, was presented in Chapter 2, by immobilization of *Acinetobacter calcoaceticus* STB1 cells on porous cellulose acetate nanofibrous webs. In that study, it was noticed that *Acinetobacter calcoaceticus* STB1 strain has a high biofilm formation capability, hence this strain and porous cellulose acetate nanofibers were selected for initial studies of bacterial immobilization and further detachment. For each 1 mL of bacterial growth medium (LB medium), 0.8 mg PCA nanofibers were added. At

the end of incubation period, some samples were separated for SEM analysis and some samples were separated for detachment process. We noticed that, before incubation, the nanofiber pieces were pure white however, they turned brownish as a result of bacterial adhesion, and they turned white again due to the detachment of bacterial cells. Detached and non-detached pCA nanofiber samples were observed under SEM to compare the bacterial adhesion on nanofibers. Fig. 17a and Fig. 17b show strong bacterial biofilms and immobilized *Acinetobacter calcoaceticus* STB1 cells after 7 days of incubation, whereas Fig. 17c and Fig. 17d reveal bacterial detachment from porous cellulose acetate nanofibrous web, showing very few amounts of bacterial cells remained on nanofiber surfaces. By collecting the detached cells in Tris-HCl buffer during sonication process, VCC assay was applied for detached STB1 cells. The results were compared with VCC values of free (planktonic) STB1 cells, revealing the VCC values of free and detached STB1 cells were similar and viability loss of STB1 cells due to the detachment process is negligible (Table 4).

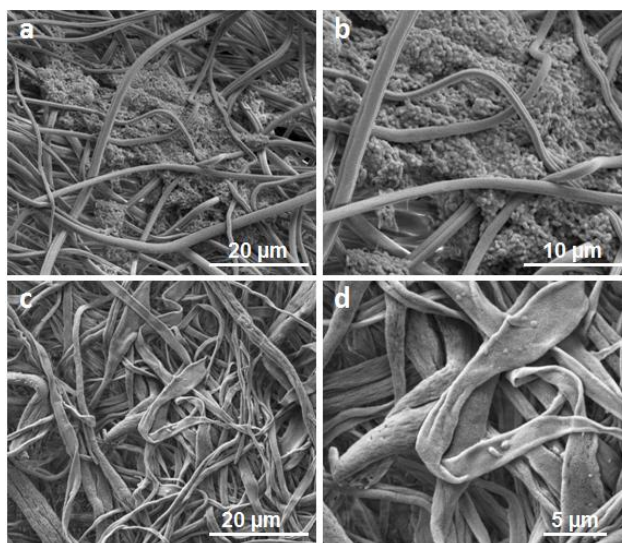


**Figure 17:** SEM micrographs of STB1 immobilized pCA nanofibers after 7 days of incubation at (a) 4000X and (b) 8000X; and bacteria detached pCA nanofibers at (c) 4000X and (d) 20000X magnification.

**Table 4.** Comparison of VCC values of free and detached STB1 cells (n=4, S.E.M).

	NF weight per each mL of growth medium	Average OD <sub>600</sub> values of free cells before VCC	VCC values of free cells (cfu/mL)	Average OD <sub>600</sub> values of detached cells before VCC	VCC values of detached cells (cfu/mL)	Attachment time
1 <sup>st</sup> trial (STB1/pCA)	0.8 mg	0.848	$6.28 \times 10^9 \pm 0.26$	0.547	$4.85 \times 10^9 \pm 1.2$	7 days

### **3.2. Immobilization of *A. calcoaceticus* STB1 and *P. aeruginosa* ATCC 47085 cells on nCA nanofibrous web and detachment of bacterial cells by applying the detachment protocol: 2<sup>nd</sup> trial**

In this trial, in addition to *Acinetobacter calcoaceticus* STB1 strain, *Pseudomonas aeruginosa* ATCC 47085 strain was also utilized for bacterial immobilization and further detachment. nCA nanofibers were utilized as carrier systems for bacterial immobilization and further detachment. For each 1 mL of bacterial growth medium (LB medium), 1 mg nCA nanofibers were added. The OD<sub>600</sub> values of bacterial inocula when starting bacterial incubation of both *A. calcoaceticus* STB1 and *P. aeruginosa* ATCC 47085 cells were equalized and equivalent growth conditions were applied for both cultures to normalize the immobilization conditions of two different bacterial strains. At the end of incubation period, some samples were selected for SEM analysis and some samples were selected for detachment process. Detached and non-detached nCA nanofiber samples were observed under SEM to compare the bacterial adhesion on nanofibers. Fig. 18a shows *A. calcoaceticus* STB1 immobilized and Fig. 18b shows *P. aeruginosa* ATCC 47085 immobilized nCA nanofibers after 3 days of incubation; whereas Fig. 18c and Fig. 18d show bacteria detached nCA nanofibrous webs for previously *A. calcoaceticus* STB1 and *P. aeruginosa* ATCC 47085 immobilized samples, respectively. VCC assay was applied for detached bacterial cells after detachment process, and the results were compared with the VCC values of free bacterial cells. The VCC values of free and detached *A. calcoaceticus* STB1 cells are highly correlated however, the VCC

values of free and detached *P. aeruginosa* ATCC 47085 cells imply not all detached cells were viable after the detachment process, and the dead cells were either came from previously attached but dead cells which were not affected by the detachment process, or the cells were killed because of sonication since detachment protocol might be more lethal for *P. aeruginosa* ATCC 47085 cells (Table 5).

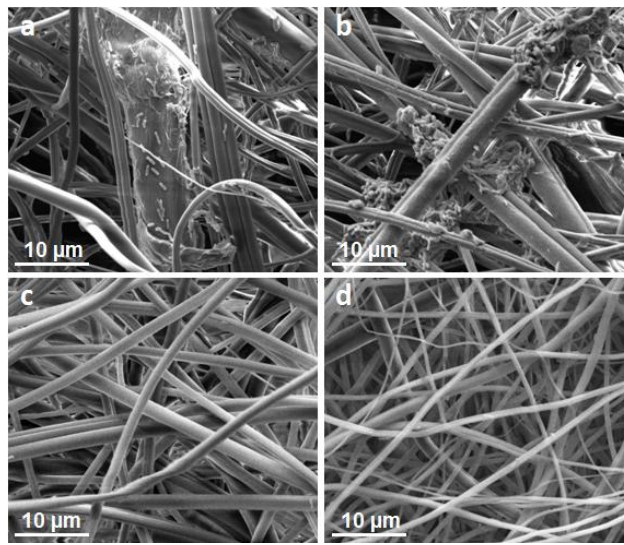


**Figure 18:** SEM micrographs of (a) *A. calcoaceticus* STB1 immobilized and (b) *P. aeruginosa* ATCC 47085 immobilized nCA nanofibers after 3 days of incubation at 6000X; and bacteria detached CA nanofibers for (c) previously *A. calcoaceticus* STB1 immobilized and (d) *P. aeruginosa* ATCC 47085 immobilized web samples at 5000X magnification.

**Table 5.** Comparison of VCC values of free and detached bacterial cells (n=4, S.E.M).

	NF weight per each mL of growth medium	Average OD <sub>600</sub> values of free cells before VCC	VCC values of free cells (cfu/mL)	Average OD <sub>600</sub> values of detached cells before VCC	VCC values of detached cells (cfu/mL)	Attach. Time
2 <sup>nd</sup> trial (STB1/nCA)	1 mg	0.848	$6.28 \times 10^9 \pm 0.26$	0.432	$2.88 \times 10^9 \pm 0.9$	3 days
2 <sup>nd</sup> trial ( <i>P.a</i> /nCA)	1 mg	0.502	$3.95 \times 10^9 \pm 0.75$	1.010	$4.5 \times 10^9 \pm 2$	3 days

### 3.3. Sonication of free bacterial cells to determine fatality of the detachment protocol on free cells of different bacterial species/strains

This study was designed to check the effects of the detachment protocol on free bacterial cells. Although strongly immobilized cells and free cells can differ in terms of resistance to sonication process (since biofilm forming immobilized cells are expected to be more resistant to sonication), it can give an idea about the cell viability differences among different bacterial species/strains when applying the detachment protocol. Our previously utilized bacterial strains, *A. calcoaceticus* STB1 and *P. aeruginosa* ATCC 47085 were selected for this experiment. There were two groups for this experiment; the control group included non-sonicated free bacterial cells and the experimental group included sonicated free bacterial cells. To apply sonication on free bacterial cells, first the liquid samples were collected in microcentrifuge tubes, then they were

centrifuged at 5000 rpm for 5 min, the supernatant solutions were discarded after centrifuge, and 1 mL of buffer solutions were added on bacterial pellets to start vortexing and further sonication. The detachment protocol was applied on experimental samples, and VCC assay was applied on the control and experimental samples (Table 6). The VCC values of control and experimental groups revealed that, while the cell viability loss due to the detachment protocol for free *A. calcoaceticus* STB1 cells is tolerable, for *P. Aeruginosa* ATCC 47085 strain, the cell viability loss is more than 50% for free cells. This result implies that the detachment protocol is not optimum for different kinds of bacteria, and it is better to optimize the parameters for each single bacterial strain. The free cells might be more vulnerable than the immobilized cells to the sonication procedure since biofilm forming cells become much more resistant to harsh environmental conditions. It can be said that, the lower VCC values for *P. aeruginosa* ATCC 47085 detached cells can be explained by the cell viability loss during sonication, where the difference is not such distinctive for *A. calcoaceticus* STB1 cells. Nevertheless, since immobilized bacteria and bacterial biofilms are more resistant to harsh environmental conditions, we cannot precisely estimate the effect of sonication on immobilized bacteria during detachment procedure.

**Table 6.** Comparison of VCC values of sonicated and non-sonicated free bacterial cells  
(n=3, S.E.M).

	OD <sub>600</sub> values of non- sonicated free cells	VCC values of non-sonicated free cells	OD <sub>600</sub> values of sonicated free cells	VCC values of sonicated free cells	% cell viability loss
<i>A. calcoaceticus</i> STB1	0.288	$2.2 \times 10^9 \pm 0.7$	0.236	$1.8 \times 10^9 \pm 0.15$	18
<i>P. aeruginosa</i> ATCC 47085	0.657	$7.2 \times 10^9 \pm 2.4$	0.619	$2.9 \times 10^9 \pm 0.7$	60

# Chapter 5

---

## **Evaluation of contact time and fiber morphology differences for development of novel surfactant degrading biocomposites**

(Parts of this study was published as “Evaluation of contact time and fiber morphology on bacterial immobilization for development of novel surfactant degrading nanofibrous webs”, Omer Faruk Sarioglu, Asli Celebioglu, Turgay Tekinay and Tamer Uyar, *RSC Advances*, November 16, 2015 (Web), Reproduced (or 'Reproduced in part') from Ref. [19] with permission from the Royal Society of Chemistry. doi: 10.1039/c5ra20739h)

## 1. Introduction

Surface active agents (surfactants) are the major components of detergents and commonly used in various industrial and domestic applications, leading a significant contribution to water pollution [83]. According to the United States Environmental Protection Agency (USEPA), surfactants may negatively influence the endocrine system of both animals and humans, so constituting a considerable health hazard [84]. Therefore, decontamination of water sources from surfactants is of substantial importance.

There are different methods to treat surfactant contaminated environments and bioremediation is becoming an emerging technology for decontamination of these pollutants, since it is cost-effective, eco-friendly and effective for a wide variety of pollutants such as petroleum hydrocarbons, heavy metals and surfactants [85]. Although there are numerous reports in the literature about isolation and discovery of novel surfactant degrading microorganisms, their *in situ* application is not so simple, since the environmental parameters are highly variable and the rate of surfactant degradation is very low under natural conditions [86]. Therefore, alternative application procedures should be studied and the degradation conditions should be optimized for specific microorganisms to obtain better remediation performances under variable physical and environmental conditions.

The genus *Achromobacter* comprises Gram-negative, aerobic, non-fermentative and rod-shaped bacteria [87]. It has been reported that

*Achromobacter xylosoxidans* has petroleum hydrocarbon degrading capability and resistant to grow in crude oil contaminated environments [88], which may indicate the potential surfactant degrading capability of this species, since high amounts of industrial surfactants are derived from petroleum. The genus *Serratia* is a member of the Enterobacteriaceae, and comprises Gram-negative, non-spore forming, glucose fermenting, facultatively anaerobic and rod-shaped bacteria [89, 90]. *Serratia odorifera*, a member of the genus *Serratia*, has shown efficient surfactant degrading capability in consortia against two different common surfactants, LAS and SLES [91, 92], highlighting the potential of this family for applications of surfactant bioremediation.

Bioremediation techniques can be applied with either free microorganisms or immobilized microorganisms which are adhered on a carrier matrix. Application of immobilized microorganisms is more advantageous than the freely floating cells in terms of lower space and growth medium requirements and potential reusability of the system [14]. Furthermore, it is also advantageous for the resistance of cells to harsh environmental extremes [36]. As a carrier material, electrospun fibrous webs have become a promising candidate since electrospinning is a simple, versatile and cost-effective technique and electrospun fibrous webs can have unique properties such as large surface-to-volume ratio and high porosity, hence these materials have a potential to be used in membrane/filter applications [30-35]. Among different immobilization procedures, natural adhesion is the most advantageous one since it provides the formation of biofilms, maximizes the cell viability and biochemical activity [37]. In recent years, few studies regarding environmental

applications of microorganism immobilized electrospun fibrous webs have been published [11, 14, 18, 20-22].

In the current study, *Serratia proteamaculans* STB3 and *Achromobacter xylosoxidans* STB4 cells, which have biodegradation capabilities on a known anionic surfactant: sodium dodecyl sulfate (SDS), were immobilized onto cellulose acetate nanofibers that have either non-porous or porous morphology to obtain reusable materials for surfactant remediation in aqueous systems. We describe here the development procedure of bacteria immobilized biocomposites and their potential reusability. Our reusability test results indicate that the biocomposites have a potential to be reused for continuous remediation of surfactants in water.

## **2. Experimental**

### **2.1. Materials**

The chemicals that were used in this study were: dichloromethane (DCM,  $\geq 99\%$  (GC), Sigma-Aldrich), acetone ( $\geq 99\%$  (GC), Sigma-Aldrich), methanol (99.7%, Riedel), cellulose acetate, (CA, Mw: 30000 g/mol, 39.8wt. % acetyl, Sigma-Aldrich), sodium dodecyl sulfate (SDS,  $\geq 98.5\%$  (GC), Sigma-Aldrich), methylene blue ( $\geq 82\%$ , Sigma-Aldrich), Nutrient broth (Sigma-Aldrich), LB broth (Sigma-Aldrich) and Agar (Sigma-Aldrich). All of them were used without any additional purification.

## 2.2. Electrospinning of non-porous and porous cellulose acetate webs

The electrospinning of non-porous (nCA) and porous (pCA) cellulose acetate nanofibrous webs were performed by applying the protocol mentioned in Chapter 4. The electrospinning process and bacterial immobilization are schematically represented in Fig. 19.

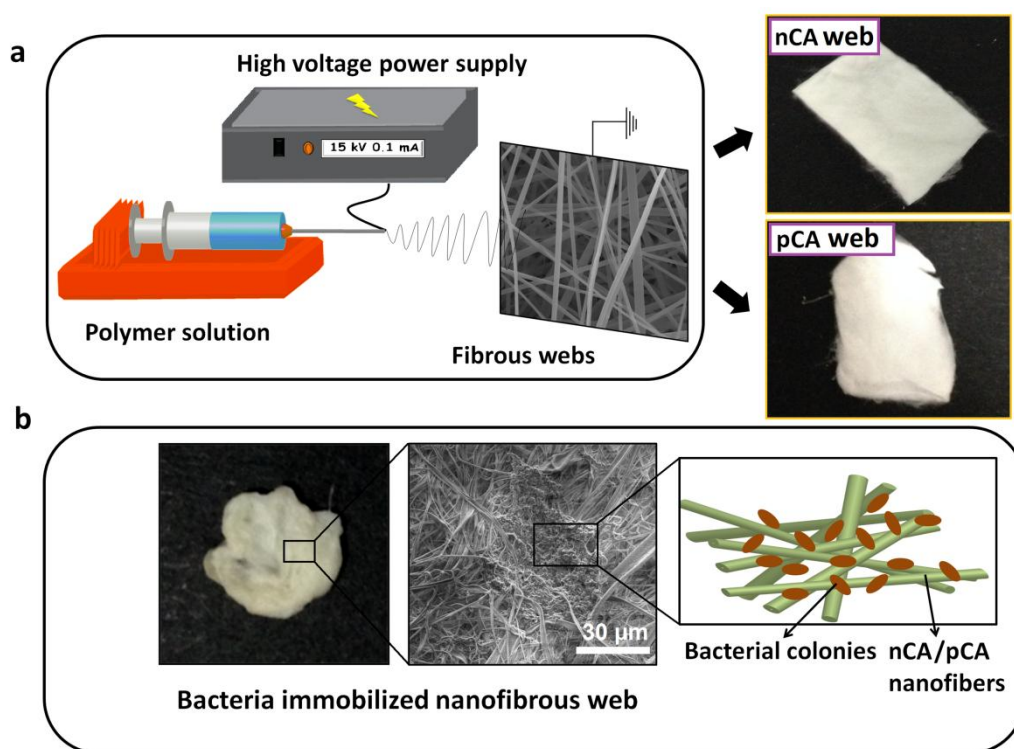


**Figure 19:** (a) Schematic representation of electrospinning process for nCA and pCA webs, and photographs of nCA and pCA webs, (b) representative images for bacteria immobilized webs including a SEM micrograph and schematic representation of bacterial cells on fibrous surfaces. (Copyright © 2013, Reproduced from Ref. [19] with permission from the Royal Society of Chemistry)

### **2.3. Isolation, preliminary characterization and 16S rRNA gene sequence analysis of STB3 and STB4 strains**

It was aimed to find and isolate specific and efficient bacterial strains for surfactant remediation and therefore, different water samples were collected from the area nearby the wastewater effluent (which contain low amounts of anionic surfactants) of a glassware producing factory (Trakya Glass Bulgaria EAD). The bacterial isolates were then enriched in LB medium (Luria-Bertani: 10 g/L tryptone, 5 g/L yeast extract, 10 g/L NaCl in 1 L of distilled water) and plated on LB-agar plates to obtain pure cultures. All reagents utilized in this study were purchased from Sigma-Aldrich (USA). The pure cultures were collected from the plates, enriched in LB medium, named with the designation “STB” and their preliminary characterization for surfactant remediation were performed with lower amounts of (5-10 mg/L) SDS containing LB growth media. The remaining concentrations of SDS in the culture media were measured by MBAS (methylene blue active substances) assay in each biodegradation experiment, in which methylene blue binds with anionic surfactants in an aqueous medium and the mixture gives an absorbance peak at 652 nm [93]. The most efficient bacterial isolates for SDS remediation were selected as STB3 and STB4 strains.

The species identity of STB3 and STB4 were determined via 16S rRNA gene sequencing analysis. Bacterial DNA isolation was carried out via DNeasy Blood & Tissue Kit (QIAGEN, Germany). A modified protocol for PCR amplification and further sequencing was utilized with the concentrations of:

1.25 U Platinum Taq polymerase, 0.2 mM dNTP, 0.4 pmol T3 (ATTAACCCTCACTAAAGGGA) and T7 (TAATACGACTCACTATAGGG) primers which encompass the entire 16S gene, 1.5 mM MgCl and 1X Taq buffer [94]. The PCR steps were adjusted as: initial denaturation at 96 °C for 5 min and further 30 cycles of denaturation at 96 °C for 30 s, annealing at 55 °C for 30 s, elongation at 72 °C for 30 s and a final elongation at 72 °C for 5 min. The sequencing was done via a 3130xl Genetic Analyzer by using BigDye Terminator v3.1 Cycle Sequencing Kit (Applied Biosystems, USA), and the analysis was performed with ABI 3130xl Genetic Analyzer. The 16S rRNA gene sequences of the isolates were analyzed by NCBI's Bacterial Blast Tool (<http://www.ncbi.nlm.nih.gov>) and an online phylogenetic tree printer (Phylohendron, <http://iubio.bio.indiana.edu/treeapp/treeprint-form.html>) was utilized to construct and visualize the phylogenetic trees.

## **2.4. Growth and immobilization of STB3 and STB4 cells**

Immobilization of STB3 and STB4 cells was provided by the inclusion of cellulose acetate nanofibrous webs (which have either porous (pCA) or non-porous (nCA) morphology) into the growth media of newly inoculated bacteria. Nutrient broth (1 g/L meat extract, 2 g/L yeast extract, 5 g/L peptone, 5 g/L NaCl in 1 L of distilled water) was utilized as the bacterial growth medium. Bacterial growth was maintained in 100 mL culture flasks for about 25 days at 25 °C and 180 rpm, and the growth media were refreshed for every 7 days. For the evaluation of bacterial attachment, equivalent samples with equal weights (w/v ratio of 0.5 mg/mL) were taken at day 7, 21 and at the end of the

reusability test; and the bacterial quantity was determined via a modified protocol in which the immobilized bacterial cells were detached via sonication and viable cell counting was applied on the detached cells [82]. Briefly, the bacteria immobilized web samples were first collected and gently washed via PBS (Phosphate-Buffered Saline) to remove unattached cells. The web samples were then transferred to 1 mL buffer containing sterile microcentrifuge tubes and vortexed for 30 s before sonication. Sonication was conducted at 40 kHz and 4 °C (the sonication bath was pre-cooled and the temperature was kept constant to prevent excess heat generation and subsequent cell viability loss) by using an ultrasonic cleaner (B2510, Branson Ultrasonics, USA). The cycles were adjusted at 1 min sonication and 30 s rest for each run, till 10 min of sonication was completed. At the end of sonication, the web samples were vortexed for 30 s and the detached bacteria containing buffer samples were transferred to new sterile microcentrifuge tubes. The sonication was repeated once again with fresh buffers and the detached cells for each sample were combined in single tubes. Viable cell counting (VCC) assay was applied for detached cells by spreading them on Nutrient-Agar plates. After overnight incubation, *cfu* (colony forming unit) values for each sample were determined. Bacterial immobilization was also checked with SEM microscopy, which is detailed in further sections. After deciding 25 days of incubation is enough for both STB3 and STB4 cells' attachment, equivalent bacteria immobilized nCA and pCA web samples (with equal w/v ratios) were prepared for SDS biodegradation experiments.

## **2.5. SDS biodegradation experiments**

Nutrient broth was utilized as the bacterial growth medium for SDS biodegradation experiments. Samples were collected periodically to analyze remaining SDS concentrations by MBAS assay. In the first experiment, free STB3 and STB4 cells were tested for SDS biodegradation capability at variable pH levels (6.0-8.0). The initial SDS concentration was 10 mg/L and the bacterial samples were incubated for 72 h at 180 rpm and 30 °C. For further experiments, the pH level was adjusted at 7.0, since it was the optimum level for STB4 strain which exhibited the highest degradation capacity. In the second and third experiment, pristine nCA and pCA webs, STB3 immobilized nCA and pCA webs, and STB4 immobilized nCA and pCA webs were tested for their SDS remediation capability at 10 and 100 mg/L of initial SDS, with the same conditions of the first experiment. In the fourth experiment, STB3 immobilized pCA webs and STB4 immobilized pCA webs were tested for SDS biodegradation capability at a high concentration (1 g/L) and the samples were incubated for 168 h at 180 rpm and 30 °C. Only STB3 immobilized pCA webs and STB4 immobilized pCA webs were selected for this experiment since they have shown the highest biodegradation capability among STB3 and STB4 immobilized web samples in the previous experiment. In each experiment, the utilized web samples were washed gently with PBS before the initiation of the experiment. The w/v ratios were equal for each web sample (0.5 mg/mL). All tests were done in triplicate.

The removal capacities ( $Q_{eq}$ ) of free STB3 and STB4 cells, and bacteria immobilized web samples were calculated by Eq. 1 (1)

$$Q_{eq} \text{ (mg/g)} = (C_0 - C_f) \cdot V / M \quad (1)$$

where  $C_0$  is the initial SDS concentration (mg/L),  $C_f$  is the final SDS concentration (mg/L),  $V$  is the solution volume (L) and  $M$  is the total bacterial cell biomass (g) at equilibrium [71].

## **2.6. Adsorption isotherms and kinetics studies**

Adsorption coefficients of STB3/pCA and STB4/pCA webs were estimated for three isotherm models (Freundlich, Langmuir and Toth) by using the calculated  $Q_{eq}$  and  $C_f$  values, that are required for the isotherm parameter fitting software IsoFit [72] to generate adsorption isotherms from three different experiments. The orders of reactions for SDS removal were evaluated by plotting zero, first, second and third order plots of STB3/pCA and STB4/pCA webs, and comparing their  $R^2$  values afterwards.

## **2.7. LC-MS (Liquid Chromatography - Mass Spectroscopy)**

LC-MS analysis was performed without column separation for the samples; SDS only, nutrient broth only, STB3 post-incubation and STB4 post-incubation by using a TOF LC/MS system (6224, Agilent Technologies, USA). SDS only sample was containing 100 mg/L of SDS, while STB3 and STB4 samples were containing 100 mg/L of SDS before starting bacterial growth at 72 h and 30 °C. STB3 and STB4 post-incubation samples were prepared by first collecting the bacterial cultures after incubation period in sterile centrifuge tubes, centrifuging

them at 6000 rpm for 5 min, and then transferring the supernatant portions to HPLC vials to be analyzed with LC-MS. The experimental parameters were; ion polarity: negative, LC stream: MS, mass range: 50-3000 m/z, acquisition rate: 1.03 spectra/s, acquisition time: 966.5 ms/spectrum, flow: 0.5 ml/min, pressure limit: 0-400 bar.

## **2.8. Scanning Electron Microscopy (SEM)**

Millimeter-length nCA and pCA webs were prepared for SEM analysis to evaluate bacterial attachment. The sample fixation was done by using a modified protocol, similar to the Greif and colleagues'[48]. Briefly, web samples were washed twice with PBS and then incubated overnight in 2.5% glutaraldehyde (prepared in PBS) for sample fixation. After overnight incubation, the web samples were washed twice with PBS and a dehydration protocol was applied on those samples by immersion in a series of EtOH solutions (30% - 96%). At the end of dehydration, samples were coated with 5 nm Au-Pd for SEM imaging (Quanta 200 FEG SEM, FEI Instruments, USA).

## **2.9. Reusability test**

Reusability of STB3/pCA and STB4/pCA biocomposites was tested for remediation of SDS. Prior to each cycle, the web samples were washed gently with PBS to remove unattached bacteria. The experiments were performed at an initial SDS concentration of 100 mg/L with the parameters of: incubation at 180 rpm and 30 °C for 72 h. SDS concentrations in the media were measured at the beginning and at the end for each run, and the percentile removal of SDS was

calculated upon these results. The washing step was repeated for each web sample before starting the next one. All tests were done in triplicate.

### 3. Results and discussion

#### 3.1. Identification and preliminary characterization of the bacterial isolates

STB3 and STB4 isolates were collected nearby an industrial effluent which contains low amounts of anionic surfactants, and therefore thought as potential candidates for bioremediation of anionic surfactants. According to the preliminary characterization studies, both strains have shown biodegradation capability against SDS at the concentrations of 5-10 mg/L. 16S rRNA gene sequencing analysis was applied on these two strains and the neighbor-joining phylogenetic tree of STB3 and STB4 strains are shown in Fig. 20.

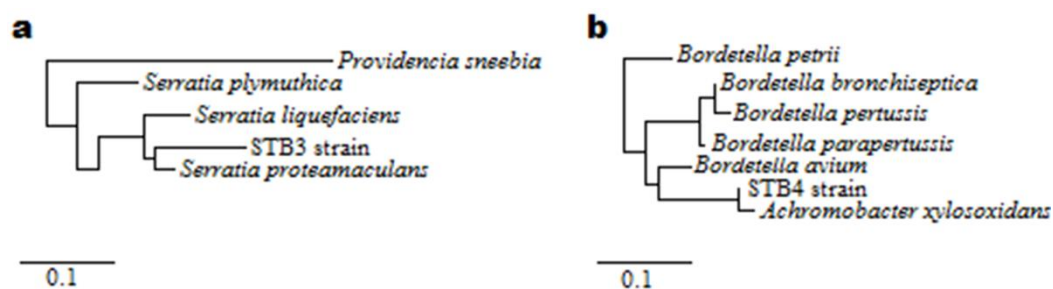


**Figure 20:** Phylogenetic trees of (a) STB3 and (b) STB4 strains according to 16S rRNA gene sequencing analysis. (Copyright © 2013, Reproduced from Ref. [19] with permission from the Royal Society of Chemistry)

STB3 strain shows closest identity (95%) with *Serratia proteamaculans* and STB4 strain shows closest identity (97%) with *Achromobacter xylosoxidans*, hence the isolates were designated as *Serratia proteamaculans* STB3 and *Achromobacter xylosoxidans* STB4. The strains STB3 and STB4 were deposited in GenBank with the accession numbers of KR094855 and KR094856, and the gene sequences are accessible with those accession numbers.

### **3.2. Immobilization of bacterial cells on nCA and pCA webs and evaluation of contact time on bacterial integration**

Depending on the solvent type for the electrospinning solution, CA nanofibers can be obtained in non-porous (nCA) or porous (pCA) morphology. It is known that electrospun CA nanofibers are suitable matrices for biological use, and the high porosity along with the higher surface area of pCA nanofibers may have a greater potential to be utilized in biological applications [18]. The morphologies of nCA and pCA nanofibers are shown in Fig. 21, demonstrating nanoscale pores are present on pCA nanofibers. The fiber diameters of nCA and pCA nanofibers were ranging between 0.5 to 3  $\mu\text{m}$ .

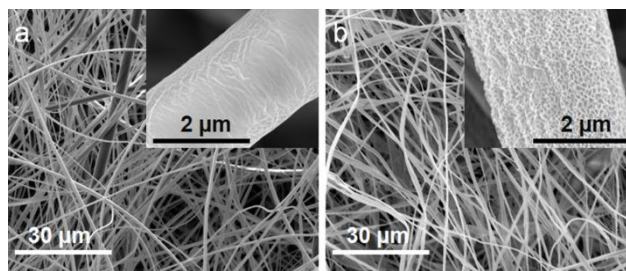


**Figure 21:** SEM micrographs of (a) pristine nCA and (b) pristine pCA webs. Pores can be seen on a pCA nanofiber in the inset figure. (Copyright © 2013, Reproduced from Ref. [19] with permission from the Royal Society of Chemistry)

A modified protocol [82] was applied for web samples to quantify the approximate amount of the attached bacteria at different time periods, and SEM imaging was performed to support these results. Fig. 22a and 22b show *Serratia proteamaculans* STB3 cells on nCA and pCA nanofibers after 7 days of incubation, wherein the bacterial attachment was not sufficient. Fig. 22c and Fig. 22d show *Achromobacter xylosoxidans* STB4 cells on nCA and pCA nanofibers, which revealed bacterial cells attached more strongly on nCA nanofibers. Fig. 23a and Fig. 23b show *Serratia proteamaculans* STB3 cells on nCA and pCA nanofibers, while Fig. 23c and Fig. 23d show *Achromobacter xylosoxidans* STB4 cells on nCA and pCA nanofibers after 21 days of incubation, which all revealed bacterial attachment became adequate for each sample to initiate biodegradation studies, this was also supported by the viable cell counting results (Table 7). Therefore, at least 21 days was found to be required for both STB3 and STB4 strains, and the web samples were collected after 25 days of incubation.

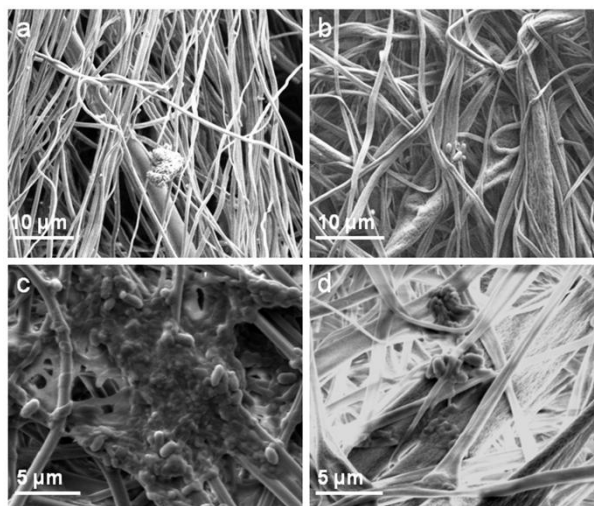


**Figure 22:** SEM micrographs of (a-c) nCA and (b-d) pCA nanofibers showing immobilization of STB3 cells onto (a) nCA nanofibers and (b) pCA nanofibers; and immobilization of STB4 cells onto (c) nCA nanofibers and (d) pCA nanofibers after 7 days of incubation. (Copyright © 2013, Reproduced from Ref. [19] with permission from the Royal Society of Chemistry)

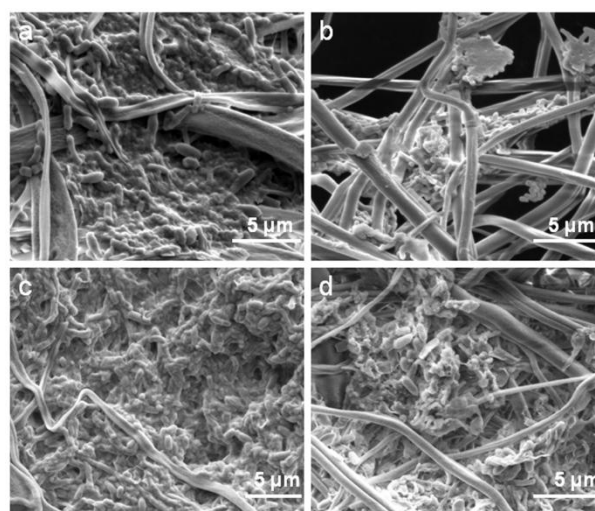


**Figure 23:** SEM micrographs of (a-c) nCA and (b-d) pCA nanofibers showing immobilization of STB3 cells onto (a) nCA nanofibers and (b) pCA nanofibers; and immobilization of STB4 cells onto (c) nCA nanofibers and (d) pCA nanofibers after 21 days of incubation. (Copyright © 2013, Reproduced from Ref. [19] with permission from the Royal Society of Chemistry)

**Table 7.** Viable cell counting (VCC) results of STB3/nCA, STB3/pCA, STB4/nCA and STB4/pCA webs at different time periods. The results are presented in *cfu/mL*. The w/v ratio of each web that was utilized for the detachment process was equal (0.5 mg/mL). (Copyright © 2013, Reproduced from Ref. [19] with permission from the Royal Society of Chemistry)

Attachment time	STB3/nCA	STB3/pCA	STB4/nCA	STB4/pCA
7 days	$0.3 \times 10^9 \pm 0.04$	$0.25 \times 10^9 \pm 0.04$	$3.1 \times 10^9 \pm 1.2$	$1.4 \times 10^9 \pm 0.17$
21 days	$1.15 \times 10^9 \pm 0.4$	$0.6 \times 10^9 \pm 0.11$	$3.15 \times 10^9 \pm 0.85$	$2.65 \times 10^9 \pm 0.54$
After reusability test	–	$2.97 \times 10^9 \pm 0.42$	–	$2.8 \times 10^9 \pm 0.33$

From the viable cell counting results, it was inferred that, bacterial cells have difficulty to adhere on nanoporous surfaces since lower number of bacterial immobilization was achieved for pCA samples at days 7 and 21. A similar behavior was also observed for different kinds of Gram-negative bacteria (*Pseudomonas fluorescens* and two different strains of *Escherichia coli*), which showed that bacterial cells attach preferably on nanosmooth silica surfaces rather than patterned, nanoporous surfaces at mature biofilm stage, and it has been elucidated by the tendency of bacterial cells to maximize their contact area with the substrate surface during immobilization [95]. Since bacterial attachment came into saturation in STB4/nCA sample after 7 days, no significant increase in bacterial number could be observed after 21 days for this sample; nevertheless, the bacterial attachment on STB4/pCA sample was not saturated after 7 days, hence the bacterial number highly increased and became closer to the STB4/nCA sample's, barely after adequate time of incubation (21 days). This result implies that, while the nanoporous morphology of pCA webs complicates bacterial cells' initial colonization, it might not lead to a significant

effect on the maximal bacterial attachment capacity, since higher numbers of bacterial attachment was obtained on pCA samples latterly.

To summarize, morphological difference in CA webs was found to be effective on bacterial adhesion and the required contact time. After finishing the bacterial immobilization process at day 25, the web samples were collected and SDS biodegradation experiments were started with those samples.

### **3.2. SDS biodegradation capability of STB3/nCA, STB3/pCA, STB4/nCA and STB4/pCA webs**

*Serratia proteamaculans* STB3 and *Achromobacter xylosoxidans* STB4 cells have shown slight differences in SDS biodegradation profiles at different pH levels (6.0-8.0) for an initial SDS concentration of 10 mg/L (Fig. 24a), suggesting both strains can be utilized efficiently within this pH range. For further studies, the pH was adjusted at 7.0, since the best SDS biodegradation profile was obtained by *Achromobacter xylosoxidans* STB4 cells at this pH level. In the second experiment (Fig. 24b), STB4/nCA and STB4/pCA biocomposite webs have shown better SDS biodegradation profiles than free STB4 cells and the other webs, STB3/nCA and STB3/pCA biocomposite webs have shown similar SDS biodegradation profiles with free STB3 cells, and pristine nCA and pCA webs have shown only slight decreases in the initial SDS concentration (10 mg/L) with a relatively more decrease for pristine pCA webs. This result suggests the biocomposite webs can provide the same remediation performance without adding any additional bacterial inocula to the aqueous

system. In the third experiment (Fig. 24c), the same samples were tested at a higher concentration of SDS (100 mg/L) with the same conditions of the previous experiment. Interestingly, it was observed that, STB3/pCA web has shown the best SDS biodegradation profile among different samples for degradation of 100 mg/L of SDS. STB4/pCA and STB3/nCA samples have shown very similar SDS biodegradation profiles, while STB4/nCA web has shown the lowest SDS biodegradation among four different biocomposite webs. Similar to the previous experiment, pristine nCA and pCA webs have shown slight decreases in the initial SDS concentration, which occurred possibly due to adsorption. In this case, decreases in SDS concentrations for pristine nCA and pCA webs were observed as very similar, which contradicted our previous thought that pCA webs may have a higher adsorption capability for SDS due to their higher porosity. In the final SDS biodegradation experiment (Fig. 24d), we increased both the initial SDS concentration and incubation time to test the SDS biodegradation capability of our best biocomposite webs (including both bacterial strains) at considerably high concentrations of SDS (1 g/L). Similar to the third experiment, STB3/pCA web has shown a better SDS biodegradation profile (85%) than STB4/pCA web (63%) within 168 h, which suggests STB3 cells may have a higher SDS biodegradation capability than STB4 cells at higher concentrations of SDS.

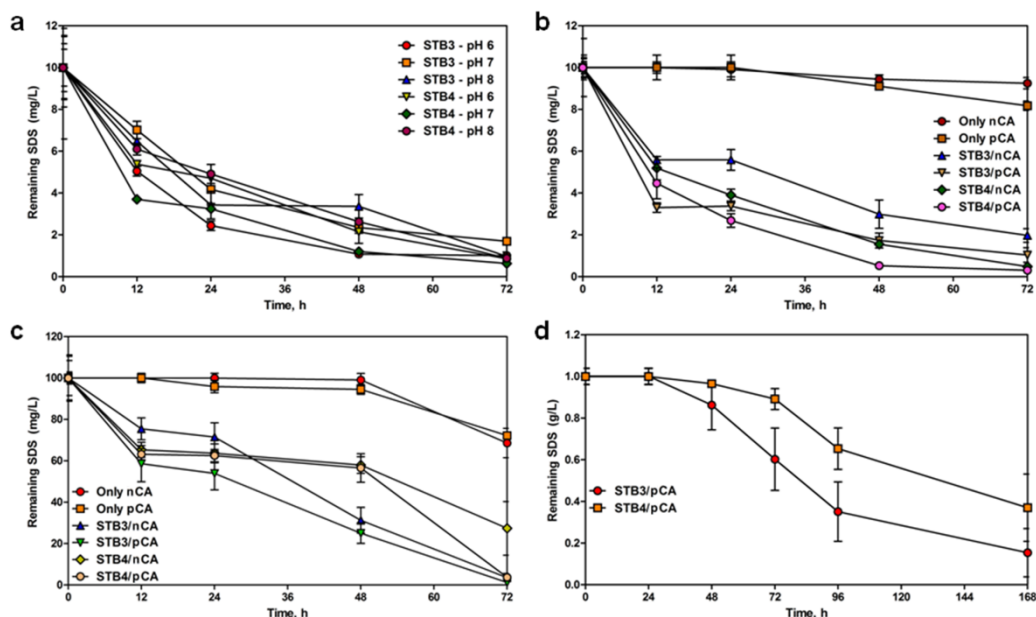


**Figure 24:** SDS biodegradation profiles of (a) STB3 and STB4 strains for differential pH levels at 10 mg/L SDS, (b) pristine nCA, pristine pCA, STB3/nCA, STB3/pCA, STB4/nCA and STB4/pCA webs at 10 mg/L SDS, (c) pristine nCA, pristine pCA, STB3/nCA, STB3/pCA, STB4/nCA and STB4/pCA webs at 100 mg/L SDS and (d) STB3/pCA and STB4/pCA webs at 1 g/L SDS. Error bars represent mean of three independent replicates. (Copyright © 2013, Reproduced from Ref. [19] with permission from the Royal Society of Chemistry)

Degradation capacities ( $Q_{eq}$ ) of free cells and biocomposite webs were calculated at pH 7.0 for the concentrations of 10 and 100 mg/L wherein nearly complete degradation of SDS was observed, and they are presented in Table 8. The  $Q_{eq}$  value of free STB3 cells was higher than free STB4 cells at both 10 and 100 mg/L SDS, which was also observed in STB3 immobilized web samples. Furthermore, it was observed that,  $Q_{eq}$  values of both STB3 and STB4 immobilized webs increased with an increase in the initial SDS concentration, but more notable increases in  $Q_{eq}$  values occurred in STB3 immobilized webs

and the percentile degradation of these webs were highly increased (96.5% for STB3/nCA and 98.8% for STB3/pCA) and reached or surpassed the percentile degradation levels of STB4 immobilized webs at 100 mg/L of initial SDS. This result may support our previous statement that, STB3 cells have a higher SDS biodegradation capability than STB4 cells at higher concentrations.

**Table 8.** Degradation capacities of free STB3 and STB4 cells, and STB3/nCA, STB3/pCA, STB4/nCA, STB4/pCA webs at equilibrium at the end of the degradation period. T = 30 °C, agitation rate: 180 rpm. (Copyright © 2013, Reproduced from Ref. [19] with permission from the Royal Society of Chemistry)

Sample name	Initial amount ( $C_0$ )	Removed SDS	$Q_{eq}$ (mg/g)	Removal (%)
STB3 only	10 mg/L	8.3 mg/L	$29.66 \pm 0.54$	83%
STB4 only	10 mg/L	9.37 mg/L	$20.06 \pm 0.23$	93.7%
STB3/nCA	10 mg/L	8.03 mg/L	$28.68 \pm 1.15$	80.3%
STB3/pCA	10 mg/L	8.96 mg/L	$32.02 \pm 1.24$	89.6%
STB4/nCA	10 mg/L	9.52 mg/L	$20.38 \pm 0.29$	95.2%
STB4/pCA	10 mg/L	9.7 mg/L	$20.76 \pm 0.02$	97%
STB3 only	100 mg/L	95 mg/L	$339.46 \pm 1.53$	95%
STB4 only	100 mg/L	66.8 mg/L	$142.97 \pm 27.7$	66.8%
STB3/nCA	100 mg/L	96.5 mg/L	$344.63 \pm 6.3$	96.5%
STB3/pCA	100 mg/L	98.8 mg/L	$352.88 \pm 1.7$	98.8%
STB4/nCA	100 mg/L	72.4 mg/L	$155.55 \pm 27.8$	72.4%
STB4/pCA	100 mg/L	96.28 mg/L	$206.16 \pm 3.98$	96.28%
STB3/pCA	1 g/L	846.47 mg/L	$3023.01 \pm 413.5$	84.66%
STB4/pCA	1 g/L	630.61 mg/L	$1350.34 \pm 345.9$	63.01%

### 3.3. Adsorption isotherms and order of reactions

The estimated values of adsorption coefficients for three isotherm models (Langmuir, Freundlich and Toth) are listed in Table 9. All of the tested models in two different samples have shown good fitting properties. For STB3/pCA sample, Langmuir and Toth isotherms have shown slightly better correlation with the  $R_y^2$  value of 0.992, while this value is 1.000 for STB4/pCA sample in all three models. Since Langmuir model is not a single best fitting model in both samples, the SDS removal process is not likely to be monolayeric, rather it is heterogenous and multilayeric by bacteria immobilized web samples [62]. The maximum removal capacities ( $Q_{\max}$ ) of web samples were estimated to be 3367 mg/g for STB3/pCA and 1464 mg/g for STB4/pCA under the Langmuir model, while they were 3023 mg/g for STB3/pCA and 1350 mg/g for STB4/pCA under the Toth model, implying STB3/pCA has a much higher removal capacity for SDS.

**Table 9.** Adsorption kinetics coefficients of STB3/pCA and STB4/pCA webs for each isotherm model. (Copyright © 2013, Reproduced from Ref. [19] with permission from the Royal Society of Chemistry)

Samples	Isotherm	Parameters	Values	$R_y^2$ value
STB3/pCA	Freundlich	Kf	184.98	0.991
		1/n	0.555	
	Langmuir	$Q_{\max}$	3367	0.992
		b	0.057	
	Toth	$Q_{\max}$	3023	0.992
		b	0.06	
STB4/pCA	Freundlich	n	4.9	
		Kf	76.78	1.000
	Langmuir	1/n	0.48	
		$Q_{\max}$	1464	1.000
	Toth	b	0.032	
		$Q_{\max}$	1350	1.000
		b	0.031	
		n	4.58	

The  $R^2$  values of different order plots for STB3/pCA and STB4/pCA are listed in Table 10. STB3/pCA and STB4/pCA samples have shown the highest correlation for the zero order model with the  $R^2$  values of 0.9319 and 0.8531, respectively; suggesting the SDS removal process by both web samples is an enzyme-catalyzed degradation, as enzyme-catalyzed reactions often fall under the zero order model [75]. Since the total surface area has an essential role in the zero order model, the higher SDS removal capacities of bacteria/pCA samples can also be attributed to the higher surface area of the immobilized bacteria, in contrast to the bacteria/nCA samples where higher bacterial immobilization might lead to aggregation and decrease in the total surface area.

**Table 10.** The  $R^2$  values of zero, first, second and third order plots for the removal of SDS by STB3/pCA and STB4/pCA webs.

Samples	Model	$R^2$ values
STB3/pCA	zero order	0.9319
	first order	0.8583
	second order	0.6515
	third order	0.6246
STB4/pCA	zero order	0.8531
	first order	0.7414
	second order	0.6434
	third order	0.6249

### 3.4. LC-MS analysis

LC-MS analysis was performed to monitor the remaining SDS and its byproducts in bacterial growth media after the incubation process. Biodegradation of SDS has been studied previously and the known byproducts of SDS before proceeding to the fatty acid metabolism are 1-dodecanol,

dodecanal and laurate [96]. According to the LC-MS analysis results, SDS (molar mass: ~288 g/mol) was observed at around 265 m/z by releasing sodium ions (Fig. 25), and nutrient broth gave various peaks in the range of 100-180 m/z. For post-incubation samples, no explicit peaks at around 184, 186 and 199 m/z were observed, corresponding to the molar masses of dodecanal, 1-dodecanol and laurate, respectively. It was concluded that, while the remaining SDS in media can be monitored by LC-MS analysis, the byproducts cannot be seen since these metabolites have very short lifetime and they are quickly processed for further fatty acid metabolism. The counts (%) ratio for the remaining SDS at around 265 m/z was higher for the STB4 sample, revealing lower SDS degradation was occurred for this sample, which was also observed in the SDS biodegradation experiments of free STB4 cells (Table 8).

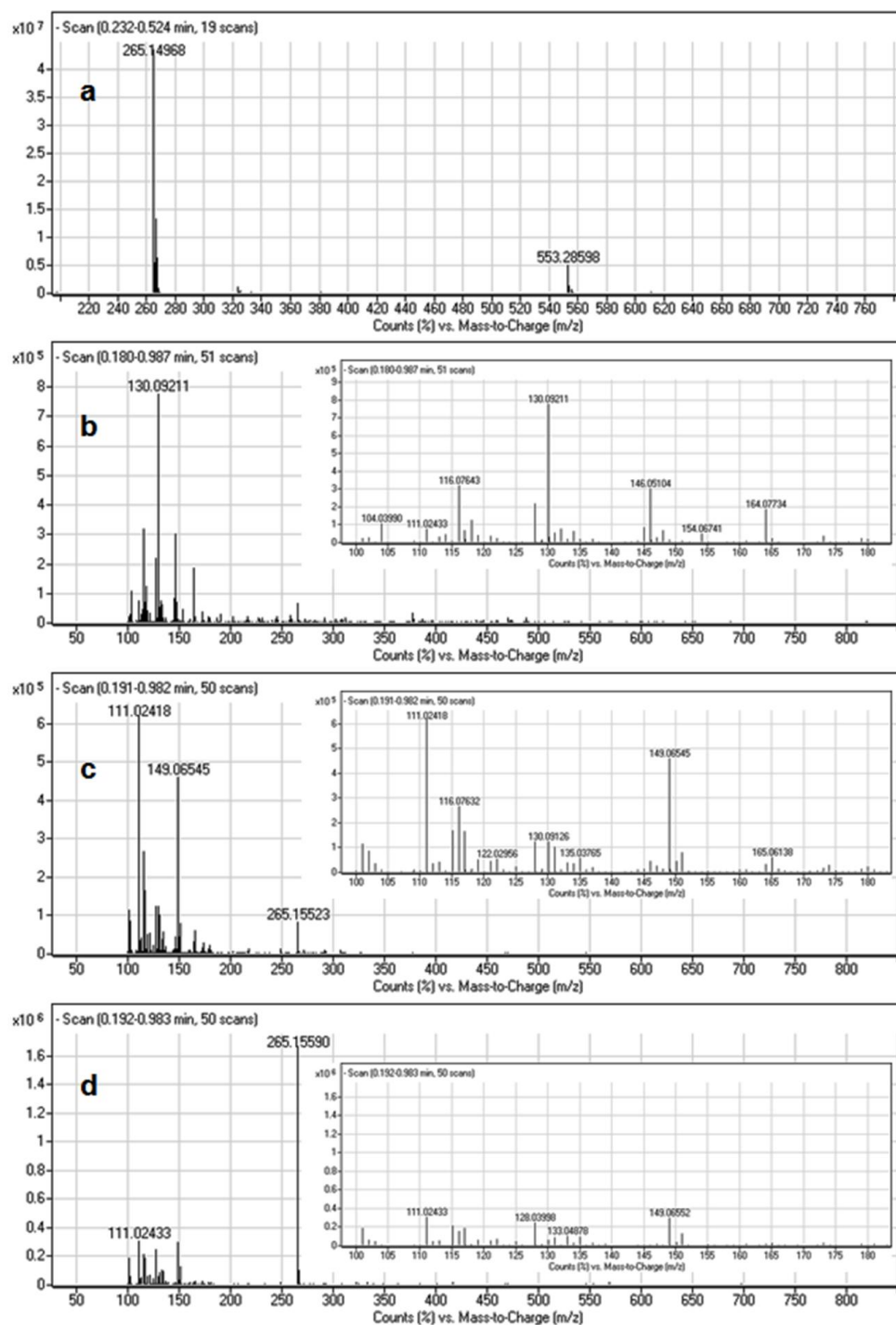


**Figure 25:** LC-MS spectra of (a) SDS solution in water at 100 mg/L (b) nutrient broth in water (c) STB3 sample having 100 mg/L initial SDS after incubation and suspension of bacterial cells (d) STB4 sample having 100 mg/L initial SDS after incubation and suspension of bacterial cells. (Copyright © 2013, Reproduced from Ref. [19] with permission from the Royal Society of Chemistry)

### 3.5. Reusability and applicability of STB3/pCA and STB4/pCA biocomposites

After the end of biodegradation experiments, the same web samples were tested for reusability in five consecutive cycles. Although significant portions of SDS were degraded by STB3/pCA and STB4/pCA webs at 1 g/L, 100 mg/L was selected as the initial concentration for the reusability test rather than 1 g/L, since complete degradation could not be achieved and the degradation time highly increased at 1 g/L of SDS. As seen in Fig. 26, while the SDS biodegradation capabilities of STB3/pCA and STB4/pCA webs were considerably low for the initial cycles, they recovered in the following cycles, especially for the STB3/pCA web.

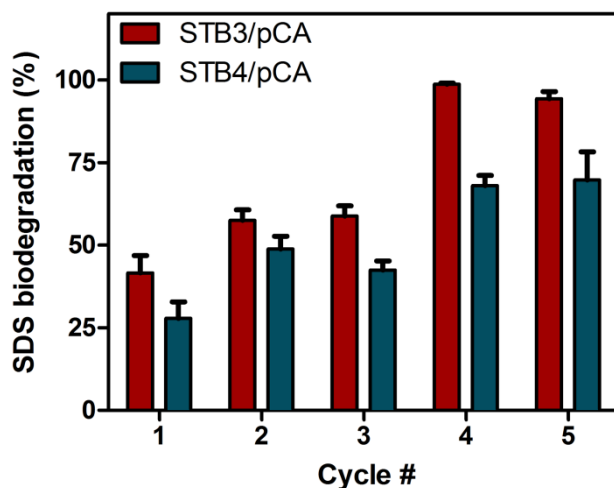


**Figure 26:** Reusability test results of STB3/pCA and STB4/pCA webs for 5 cycles of SDS biodegradation at an initial concentration of 100 mg/L. Error bars represent mean of three independent replicates. (Copyright © 2013, Reproduced from Ref. [19] with permission from the Royal Society of Chemistry)

This result might be related with losses of viable bacterial cells and metabolic activity for the biocomposite webs, after exposure to a very high concentration of SDS (1 g/L) in the previous experiment. On the other hand, the degradation performances and viable cell counts started to recover at convenient conditions, during the test period at an initial SDS concentration of 100 mg/L where bacterial cells can rapidly grow and immobilize on the fibrous surfaces with a high metabolic activity, leading higher bacterial attachment and higher degradation efficiencies, and indeed at the end of the reusability test, higher numbers of viable cells were counted for both STB3/pCA and STB4/pCA web samples (Table 7). The test results indicated that, STB3/pCA has a more efficient SDS biodegradation profile than STB4/pCA during the reusability test, and has a higher recovery capability for long term use at the tested concentration. Since the viable cell numbers increased for both samples (especially for STB3/pCA) during the reusability test, their removal capacities have altered and differed from the pre-reusability test conditions. It was inferred that, while 1 g/L of initial SDS might be toxic and constrain the metabolic activities of bacterial cells, 100 mg/L of initial SDS is appropriate for seeing the maximal biodegradation performances of the bacteria immobilized webs and for their repeated use. SEM imaging was applied on STB3/pCA and STB4/pCA webs to monitor the presence of immobilized bacteria at the end of the reusability test. As seen in Fig. 27, robust attachment of bacterial cells and biofilm-like structures on both web samples were observed, supporting the viable cell counting results of STB3/pCA and STB4/pCA after the reusability test (Table 7).

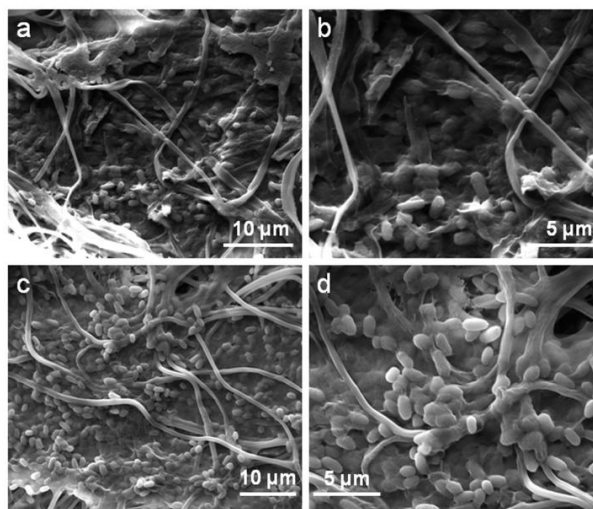


**Figure 27:** SEM micrographs of (a-b) STB3 immobilized pCA webs and (c-d) STB4 immobilized pCA webs after the reusability test, showing strong bacterial attachments. (Copyright © 2013, Reproduced from Ref. [19] with permission from the Royal Society of Chemistry)

Remediation of anionic surfactants from water systems is a critical issue and greener approaches have been received more attention [86, 91, 92, 97, 98]. In addition, use of biointegrated functional electrospun fibrous webs for remediation of contaminated water systems has been explored in recent years and there are few examples in the literature for the applications of these kinds of materials. For remediation of nitrate in aqueous systems, Eroglu et al. produced a novel biocomposite by immobilization of microalgal cells on electrospun chitosan nanofiber mats [14]. In recent studies performed by our group, specific bacterial or algal strains have been attached on electrospun fibrous webs for ammonium bioremoval [18], methylene blue dye biodegradation [22], reactive dye biodegradation [21] and simultaneous removal of hexavalent chromium and a reactive dye [20]. In the present study, we focused on anionic surfactant

bioremediation and therefore produced novel biocomposite webs by immobilization of two different SDS degrading bacterial strains on electrospun nCA and pCA webs. It was observed that, bacterial cells strongly immobilized on nCA and pCA fibrous surfaces, the bacteria immobilized webs exhibited similar biodegradation performances with free STB3 and STB4 cells and can be reused for several cycles of SDS biodegradation with recovery capabilities. 1 g/L of SDS was found as potentially toxic for STB3 and STB4 cells since the degradation profiles of STB3/pCA and STB4/pCA highly decreased right after this experiment as seen in Fig. 26, still STB3/pCA and STB4/pCA webs were able to degrade significant portions of SDS at this concentration. The bacterial strains have shown efficient biodegradation profiles at differential pH levels for the initial SDS concentration of 10 mg/L, indicating the biodegradation performances of both strains were not significantly affected by pH differences within 6.0-8.0. Although highly efficient results could be achieved at different concentrations for SDS biodegradation, the bacteria immobilized webs are still improvable by increasing the number of attached bacteria or optimizing the bacterial growth conditions. Overall, these results are highly promising and with successful optimizations, STB3/pCA and STB4/pCA webs may be utilized continually for SDS biodegradation in aqueous environments.

# Chapter 6

---

**Evaluation of fiber diameter and morphology differences for electrospun polysulfone fibers on bacterial immobilization and bioremediation performance**

## 1. Introduction

Industrial wastewater contains different types of contaminants and nitrogenous wastes and dyes are two common types of water contaminants. Ammonia ( $\text{NH}_3$ ), or the ionized form ammonium ( $\text{NH}_4^+$ ), is one of the most popular nitrogenous water contaminant that is found naturally in aquatic ecosystems or produced as a result of industrial processes, and is highly toxic for many organisms above certain thresholds. U. S. Environmental Protection Agency (US EPA) regulates the acceptable limits for ammonia and its two main metabolic byproducts, nitrite and nitrate, so that ammonia concentration should not exceed 1.5 mg/L, nitrite concentration should not exceed 1 mg/L, nitrate concentration should not exceed 10 mg/L, and the sum of nitrite and nitrate concentration should not exceed 10 mg/L in drinking water [25, 26]. Therefore, remediation of ammonia and its derivatives from aquatic systems is essential for sustainable water use. Bioremediation is a very common procedure for removal of nitrogenous wastes in water due to its sustainability and biofriendliness, and specific microorganisms have been used for this purpose. Among different types of systems, heterotrophic ammonium removal by a single nitrifier/denitrifier system is advantageous since simultaneous processing of nitrification and denitrification can be possible in this system and due to contamination of different organic wastes as potential carbon sources, industrial wastewater is more favorable for heterotrophic removal. In addition to nitrogenous wastes, dyes also comprise a great portion of industrial contaminants. Dyes have diverse application areas and are widely used for many industrial processes. Nevertheless, their decontamination is an important issue and novel strategies

are in search for greener treatment. Bioremediation is an alternative green approach for removal of dyes in water systems, and it enables efficient, environmentally friendly, cost-effective and sustainable remediation [2].

In addition to free-bacteria cells, bacteria immobilized bio-hybrid systems have also been utilized for water treatment. These bio-hybrid materials can bring certain advantages over free-bacteria such as lower space and growth medium requirements, easier handling and potential reusability of the system. As carrier matrices, electrospun fibrous webs are promising candidates for immobilization of bacteria cells since electrospinning is a low-cost and versatile fabrication method and it enables tunable production of fibrous networks (e.g. higher porosity) [7]. Polysulfone (PSU) is a common biocompatible polymer that has been used in water filtration applications, and electrospun PSU fibers can be used as a carrier matrix for bacterial immobilization, to be further used in bioremediation of water systems [53].

*Acinetobacter calcoaceticus* STB1 strain was previously presented as promising for ammonium remediation in water, and it can remove even high concentrations of ammonium at heterotrophic conditions [18]. The dye removal capability of this strain was unknown and therefore was aimed to be evaluated in this study for potential dye removal applications.

In the present study, different types of electrospun PSU fibers (with different morphologies and different fiber diameters) were produced to determine the most favorable system for bacterial integration. The most successful sample was then tested for simultaneous removal of ammonium and

methylene blue dye at differential concentrations. Reusability of this sample was also evaluated for the potential reusability of the system. This type of system is supposed to be promising for potential wastewater treatment applications after successful optimizations.

## **2. Experimental**

### **2.1. Electrospinning of PS fibers**

Aligned and randomly oriented PSU fibers were produced by different systems. The homogenous electrospinning solutions were prepared by dissolving 32% (w/v) polysulfone (PSU, Mw ~60,000, Scientific Polymer Products, Inc.) in N,N-dimethylacetamide/acetone (9/1, (v/v)) (DMAC, Sigma-Aldrich, 99%; acetone, Sigma-Aldrich,  $\geq 99\%$  (GC)) binary solvent mixture, and 2% of NaCl (Sigma-Aldrich,  $\geq 99\%$ ) was added to some samples to increase conductivity of the solution and decrease the fiber diameter. Polymer solutions were loaded in a syringe with inner diameters of 0.4-0.6 mm. The syringe was located horizontally and connected with a syringe pump (model KDS-101, KD Scientific, USA), and the electrode of the high-voltage power supply (Spellman, SL30, USA) was clamped to the metal needle tip, while the aluminum collectors were grounded. Electrospinning parameters were adjusted as follows: feed rate of solutions = 0.5 mL/h, applied voltage = 10-15 kV, tip-to-collector distance = 10-12 cm. For the production of randomly oriented PSU fibers, electrospun fibers were deposited on a grounded stationary plate metal collector covered with aluminum foil. For the production of aligned PSU fibers, electrospun fibers were deposited on a grounded cylindrical collector covered with aluminum foil,

which was rapidly rotating by the aid of a rotary motor (3000 rpm) to align electrospun fibers in a parallel orientation. The electrospinning apparatus was inside a Plexiglas box, and the process was performed at room temperature and 20% relative humidity. Collected PSU fibers were then dried in a fume hood for overnight to remove residual solvent.

## **2.2. Procurement of the *Acinetobacter calcoaceticus* STB1 strain and initial characterization**

The bacterial strain (*Acinetobacter calcoaceticus* STB1) utilized in this study was previously isolated from a hatchery and found in our culture collection. This strain is known to be capable of  $\text{NH}_4^+$  removal and was also tested for methylene blue dye removal in this study. All bacterial cultures were grown in a specific growth medium, which does not contain nitrogenous sources besides external addition of  $\text{NH}_4^+$ . The ingredients of the bacterial growth medium were: 6.3 g /L  $\text{Na}_2\text{HPO}_4$  ( $\geq 99\%$ ), 3 g/L  $\text{KH}_2\text{PO}_4$  ( $\geq 99\%$ ), 0.5 g/L  $\text{NaCl}$  ( $\geq 99.5\%$ ), 2 g/L glucose (anhydrous), and 300 mL/ L of a trace elements solution consisting of 6.1 g/L  $\text{MgSO}_4$  ( $\geq 99.5\%$ ), 3 g/L  $\text{H}_3\text{BO}_3$  ( $\geq 99.5\%$ ), 0.5 g/L  $\text{MnCl}_2$  ( $\geq 99\%$ ), 0.05 g/L  $\text{CaCl}_2$  ( $\geq 93\%$ ), 0.03 g/L  $\text{FeSO}_4 \cdot 7\text{H}_2\text{O}$  ( $\geq 99\%$ ), 0.03 g/L  $\text{CuCl}_2$  ( $\geq 97\%$ ), 0.03 g/L  $\text{ZnCl}_2$  ( $\geq 99.99\%$ ).  $\text{NH}_4^+$  removal capability of STB1 strain was tested by external addition of  $\text{NH}_4\text{Cl}$  ( $\geq 99.5\%$ ) to the bacterial growth media, to provide the initial  $\text{NH}_4^+$  concentrations of 25, 50 and 100 mg/L. Methylene blue (MB,  $\geq 82\%$ ) dye removal capability of STB1 strain was also tested separately, with having a constant concentration of  $\text{NH}_4^+$  (50 mg/L) and varying

concentrations of MB (25, 50, 100 mg/L) in the growth media. All reagents utilized were purchased from Sigma-Aldrich (USA).

### **2.3. Immobilization of bacteria on PSU fibers**

Bacterial immobilization was achieved by the inclusion of equivalent PSU fibers (2.8 mg per mL) in newly inoculated STB1 cells containing LB growth medium (Luria-Bertani: 10 g/L tryptone, 5 g/L yeast extract, 10 g/L NaCl in 1 L of distilled water, pH 7.0). Bacterial colonies were maintained for 21 days at 150 rpm and 30 °C for immobilization onto the fiber surfaces. After 7 and 21 days of incubation, bacterial immobilization was checked by scanning electron microscopy (SEM) imaging, and the quantitative analysis of bacterial adhesion was evaluated by a specific procedure, in which immobilized bacteria were detached from the fiber surfaces via sequential vortexing and sonication, and the detached bacteria were utilized for cell viability assessments [19]. After this evaluation, the sample showing the highest bacterial cell viability at equivalent conditions was selected for use in application studies.

### **2.4. MB and ammonium bioremoval experiments**

Bacterial cultures were grown in the same basal growth medium with external additions of both  $\text{NH}_4^+$  and MB into the solution. Equivalent pieces of bacteria immobilized PSU fibers (with w/v ratio of 0.5 mg/mL) were added directly to the bacteria containing growth media, and the samples were incubated for 72 h at 150 rpm and 30 °C. Pristine PSU fibers were also tested for simultaneous removal of MB and  $\text{NH}_4^+$  to determine the role of bacterial presence for the

removal of these contaminants. The initial MB concentration was fixed at 25 mg/L for bacteria immobilized PSU fibers, while the initial  $\text{NH}_4^+$  concentrations were varying (25, 50, 100 mg/L). The initial MB concentration was also same for pristine PSU fibers, while the initial  $\text{NH}_4^+$  concentration was 100 mg/L. Liquid samples were collected periodically to measure the remaining concentrations of  $\text{NH}_4^+$  and MB. Changes in  $\text{NH}_4^+$  concentrations were determined by a spectrophotometric test kit (Merck Ammonium Cell Test 14559), and changes in MB concentrations were also determined spectrophotometrically at 660 nm absorbance. Before performing the tests, samples were centrifuged for 5 min at 8000 rpm at room temperature, and the supernatants were used to measure the remaining concentrations of  $\text{NH}_4^+$  or MB to prevent the interference coming from bacterial cells. All tests were done in triplicate.

## **2.5. Scanning Electron Microscopy (SEM)**

Small PSU fiber samples with and without bacterial immobilization were prepared for SEM analysis. The samples were fixed by incubation in a 2.5% glutaraldehyde solution, and then dehydrated by immersion in a series of ethanol water solutions (30%-96%). All samples were coated with 5-10 nm layer of gold-palladium prior to the analysis, and a Quanta 200 FEG scanning electron microscope (FEI Instruments, USA) was used for imaging.

## **2.6. Reusability test for STB1 immobilized CA nanofibrous web**

The reusability of bacteria immobilized PSU fibers were tested for  $\text{NH}_4^+$  removal in a five consecutive cycles. Prior to each cycle, PSU fibers were washed with Tris-HCl buffer and incubated overnight in it to remove any unattached bacteria. The initial  $\text{NH}_4^+$  concentration was constant (100 mg/L) and the incubation conditions were same with the previous experiments. The remaining  $\text{NH}_4^+$  concentrations were measured at 0 h and 72 h, and the percentage removal of  $\text{NH}_4^+$  was calculated using these results. Each cycle was terminated after 72 h and the same steps were repeated before the initiation of the next cycle. All tests were done in triplicate.

## **3. Results and discussion**

### **3.1. Fiber morphology and diameter differences on bacterial immobilization**

Polysulfone (PSU) has already been used for water filtering applications and bio-integrated application studies [53]. Electrospun PSU fibers were used as substrates for bacterial immobilization and the hybrid system was utilized for water cleaning purposes. In order to preserve the parallel orientation for aligned PSU fibers, both aligned and randomly oriented PSU fibers were not detached from the aluminum foil and equivalent pieces (with w/v ratio of 2.8 mg/mL) were cut and prepared from those samples. These samples were added to bacterial cultures and immobilization of bacteria onto fiber surfaces was aimed

during incubation. At days 7 and 21, equivalent samples were taken and SEM analysis was applied on these samples. In addition, bacterial immobilization was quantitatively evaluated by a protocol after finishing the incubation, which allows quantification of previously immobilized bacteria by viable cell counting assay (VCC). According to SEM imaging (Fig. 28), there are some disruptions in the parallel orientation for aligned PSU fibers at days 7 and 21, which might be caused by shaking and fixation, though still these fibers have more aligned morphology and the morphology difference at the initial contact was supposed to be meaningful for characteristic immobilization. It was found that addition of salt to the system considerably decreased the fiber diameters, so that the fiber diameters of PSU fibers were measured as:  $1517 \pm 54$  nm for parallel oriented and no salt added sample,  $864 \pm 84$  nm for parallel oriented and salt added sample,  $1455 \pm 83$  nm for randomly oriented and no salt added sample, and  $1066 \pm 140$  nm for randomly oriented and salt added sample.

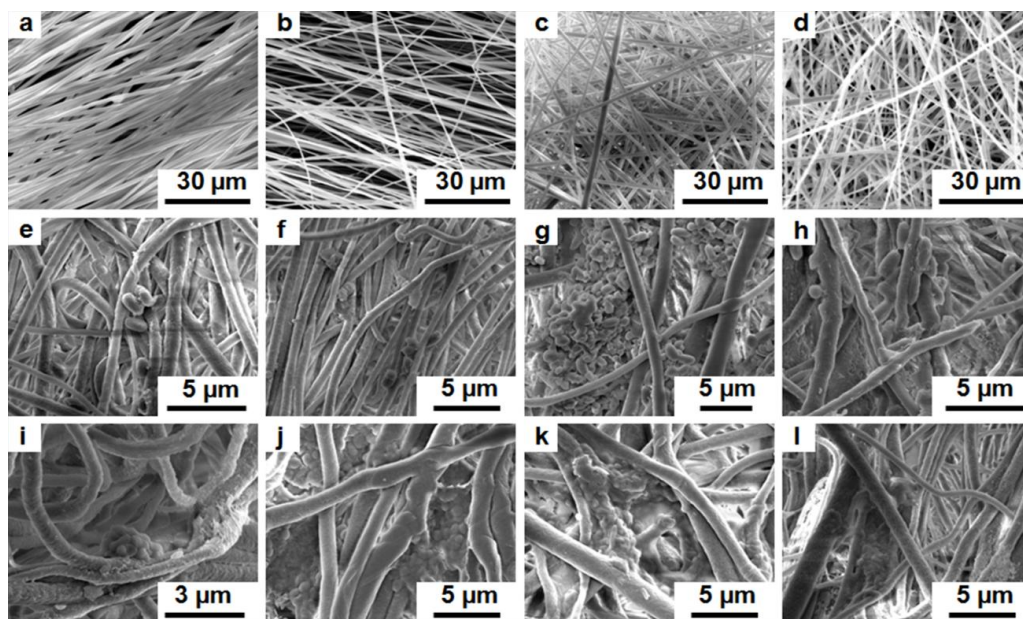


**Figure 28:** SEM micrographs of (a, e, i) aligned and no salt added PSU fibers, (b, f, j) aligned and salt added PSU fibers (c, g, k) randomly oriented and no salt added PSU fibers (d, h, l) randomly oriented and salt added PSU fibers. (a-d) correspond to pristine PSU fibers, (e-h) correspond to bacteria immobilized PSU fibers after 7 days of incubation (i-l) correspond to bacteria immobilized PSU fibers after 21 days of incubation. As seen in the micrographs, addition of salt reduces the fiber diameters considerably.

7 days of bacterial immobilization was found as inadequate and therefore bacterial incubation was maintained for 21 days. Bacterial immobilization was found as sufficient after 21 days of incubation, and therefore equivalent samples were utilized for cell viability assessments. As seen in Fig. 29, the cell viabilities were found as higher for thinner PSU fibers, plus randomly oriented and thinner PSU fiber sample was the best sample showing the highest bacterial cell viability for the immobilized cells. It was deduced that this result was due to the size of bacteria and the presence of more available spaces for attachment in randomly oriented fibers. At the end of this experiment, randomly oriented and

thinner PSU fiber sample was selected as the carrier matrix for bacterial integration, and further studies were performed on this sample.

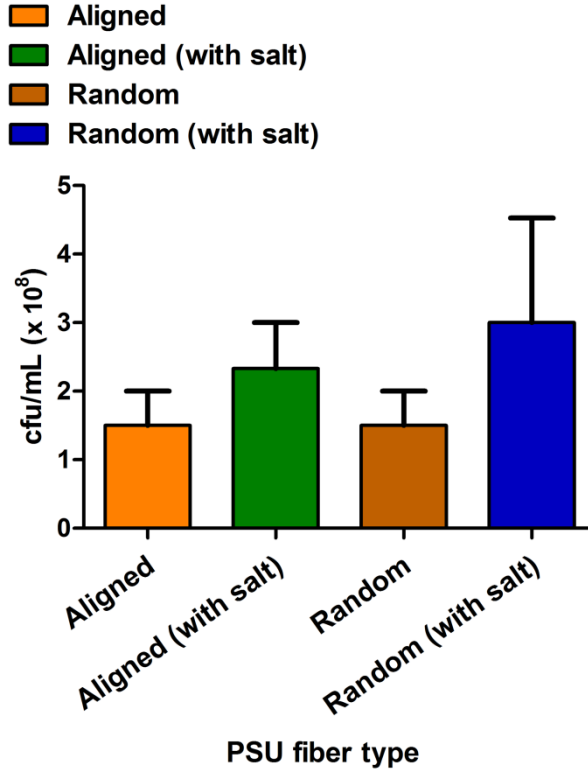


**Figure 29:** VCC (Viable cell counting) assay results of aligned, aligned (with salt), random, random (with salt) PSU fibers after 21 days of incubation period.

### **3.2. Simultaneous removal of MB and NH<sub>4</sub><sup>+</sup> by bacteria immobilized PSU fibers**

STB1 strain was initially tested for MB and NH<sub>4</sub><sup>+</sup> removal for use in further studies. MB removal by STB1 strain was tested at a constant NH<sub>4</sub><sup>+</sup> concentration (50 mg/L), which was the only nitrogen source in the medium for bacteria. As seen in Fig 30, the removal efficiency decreases with an increase in the MB concentration, and the highest removal yield was observed at 25 mg/L of initial

MB (~40%). Nevertheless, complete removal of  $\text{NH}_4^+$  was observed for each sample at the tested concentrations. Based on this result, it was aimed to test the simultaneous removal of MB and  $\text{NH}_4^+$  by bacteria immobilized PSU fibers while keeping the initial MB concentration constant at 25 mg/L.

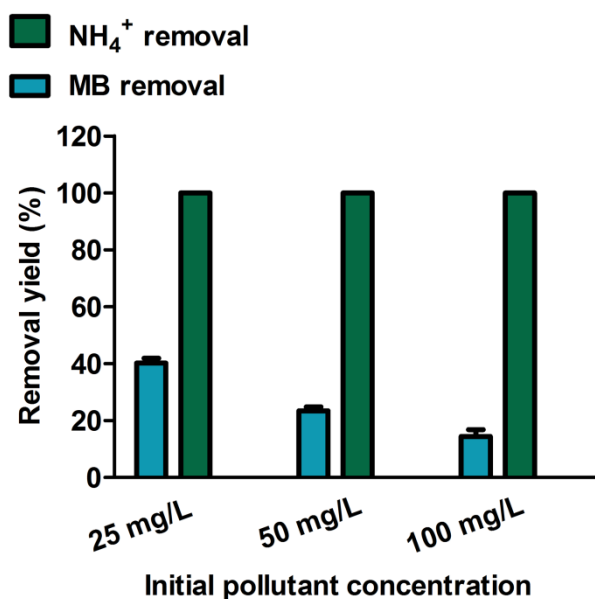


**Figure 30:** MB and  $\text{NH}_4^+$  removal profiles of free STB1 cells in a separate system within 72 h of incubation. 50 mg/L of initial  $\text{NH}_4^+$  was utilized as the nitrogen source in MB removal experiments.

Fig. 31 shows that, bacteria immobilized PSU fibers have shown efficient removal of  $\text{NH}_4^+$  at three different initial concentrations (25, 50 and 100 mg/L) within 72 h and complete removal was achieved for each concentration, while the removal efficiencies were lower for MB and the highest removal yield was achieved for the sample having 100 mg/L of initial  $\text{NH}_4^+$  (55%). It was found that, MB removal yield increased with an increase in the initial  $\text{NH}_4^+$  concentration at the tested concentrations, which suggests

simultaneous removal of MB and  $\text{NH}_4^+$  might be achieved with desirable removal efficiencies after successful optimizations.

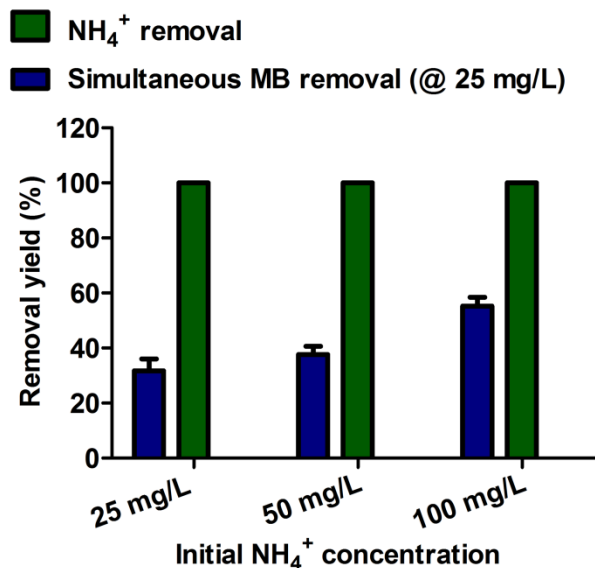


**Figure 31:** Simultaneous removal of MB and  $\text{NH}_4^+$  by bacteria immobilized PSU fibers at a constant initial MB concentration (25 mg/L) and varying initial  $\text{NH}_4^+$  concentrations (25, 50, 100 mg/L) within 72 h of incubation.

The removal capability of pristine PSU fiber sample was tested for MB and  $\text{NH}_4^+$  at initial concentrations of 25 mg/L and 100 mg/L, respectively. As seen in Fig. 32, the removal performances of pristine PSU fiber sample were very low, such that the MB removal capability was minimal and the  $\text{NH}_4^+$  removal capability was much lower than the bacteria immobilized samples. The higher adsorption capability against  $\text{NH}_4^+$  might be due to the interaction between positively charged  $\text{NH}_4^+$  and negatively charged sulfone groups. Nevertheless, this kind of removal was much lower than biological removal, therefore it was deduced that, MB and  $\text{NH}_4^+$  removal capabilities of bacteria immobilized fibers were primarily due to the bacterial presence.

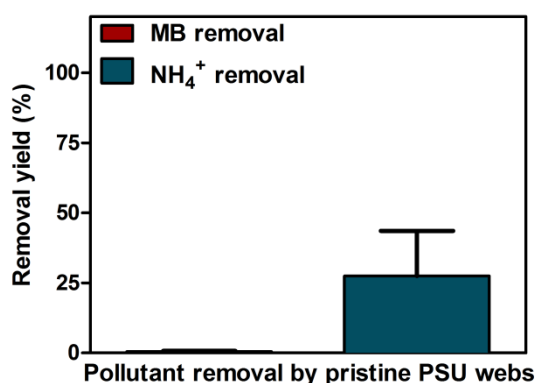


**Figure 32:** NH<sub>4</sub><sup>+</sup> and MB removal profiles of pristine PSU fibers within 72 h of incubation.

### 3.3. Reusability of bacteria immobilized PSU fibers

The potential of continuous NH<sub>4</sub><sup>+</sup> removal by bacteria immobilized PSU fibers were evaluated through a reuse test for five consecutive cycles. Since the removal yields for MB were low in the previous study, just the continuous NH<sub>4</sub><sup>+</sup> removal performance was tested in this reusability test. Fig. 33 shows the performance values of each cycle, in which, ~95% of an average removal yield was obtained, suggesting that bacteria immobilized PSU fibers have a potential for continuous remediation. After successful optimizations, these fibers are supposed to be used for simultaneous removal of NH<sub>4</sub><sup>+</sup> and MB from water systems in a continuous mode of application.

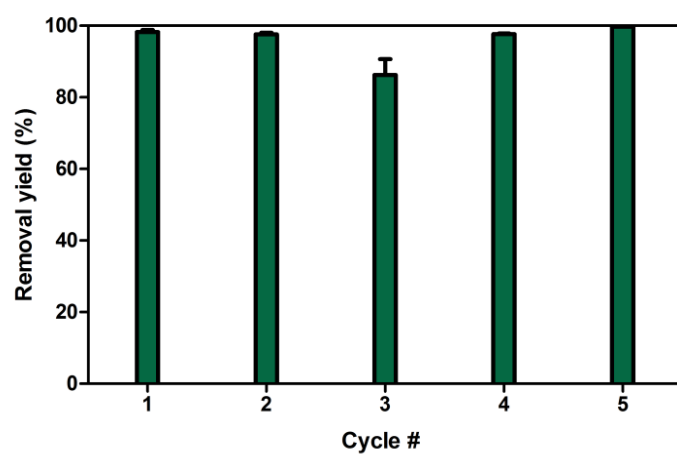


**Figure 33:** Reusability test results of bacteria immobilized PSU fibers in a five consecutive cycle.

## **Chapter 7**

---

**Bacteria            immobilized            electrospun  
polycaprolactone and polylactic acid fibrous  
webs for remediation of textile dyes in water**

## 1. Introduction

Dyes comprise a great portion of industrial contaminants and their removal from wastewater systems is of substantial importance. Because of their diverse application areas (e.g. textile and leather industries), synthetic dyes have a great usage, whereas decontamination of them is still a major challenge and their incomplete removal from water systems can lead to environmental problems [22]. Dyes can be removed from wastewater systems by using conventional treatment methods such as reverse osmosis [99], advanced oxidation process [100] and photocatalysis [101]; tough alternative technologies have been proposed for increased sustainability and biofriendliness. Bioremediation is an alternative technique for removal of water contaminants from wastewater systems by use of specific microorganisms, and it provides low-cost, efficient, green and sustainable remediation [2]. Therefore, there are many attempts for bioremediation of coloring agents in the literature, and specific microorganisms have been used for this purpose [21, 22, 31, 102, 103].

The genus *Enterococcus* comprises Gram-positive, non-sporulating and facultative aerobe cocci which are tolerant to environmental extremes [104]. The genus *Halomonas* comprises Gram-negative, rod shaped and halophilic bacteria that have the ability to grow at extreme conditions [105]. *Clavibacter michiganensis* is the only member of the genus *Clavibacter*, and it comprises Gram-positive and aerobic bacteria [106].

Bioremediation process can be performed with either free microorganisms or microorganism immobilized bio-integrated materials.

Although free microorganisms can efficiently remove water contaminants, use of bio-integrated materials can bring some advantages over free microorganisms such as lower space and growth medium necessities, potential reusability and higher resistance to environmental extremes [14, 36]. Due to their versatile nature, electrospun fibrous webs have been used as carrier matrices for immobilization of specific microorganisms for decontamination of water systems [18-21, 53, 107]. Since electrospinning is a low-cost and versatile technique and it enables optimization in fiber morphology (e.g. higher surface area and porosity), electrospun fibrous webs are promising candidates for bio-integration and water filtering applications [7].

In the present study, a dye bioremediating bacterial strain was successfully immobilized onto polycaprolactone (PCL) and polylactic acid (PLA) polymeric matrices, which are known as biocompatible and biodegradable [108, 109], to be used in applications of dye bioremediation. These novel bacteria encapsulated nanofibrous webs were tested for their removal capacities against a commercial reactive textile dye, and the results have shown that these webs have the potential for dye remediation in water. Reusability of bacteria immobilized nanofibrous webs was also tested and the results suggest that these webs can be reused for several times while increasing the number of immobilized bacteria and reducing the time required for bioremediation. These types of bio-integrated materials are supposed to be promising candidates for potential wastewater treatment applications.

## **2. Experimental**

### **2.1. Materials**

The chemicals and reagents (polycaprolactone (PCL, Mw ~70.000-90.000, Scientific Polymer Products, Inc.), polylactic acid (PLA, NatureWorks LLC Co.), dichloromethane (DCM, ≥99% (GC), Sigma-Aldrich), N,N-Dimethylformamide (DMF, ≥99% (GC), Sigma-Aldrich), textile dyes (Setazol Blue BRF-X, Setazol Turquoise Blue G (Setaş, Turkey)), LB broth (Luria-Bertani, Sigma-Aldrich) and Agar (Sigma-Aldrich)) were procured and used without any purification (all of them were of high purity available and were of analytical grade). Millipore Milli-Q Ultrapure Water System was used for providing deionized water.

### **2.2. Procurement of the bacterial strains and 16S rRNA gene sequencing analysis**

The bacterial strains utilized in this study were isolated from different resources. *Enterococcus hermanniensis* and *Clavibacter michiganensis* isolates were isolated from İvedik wastewater treatment plant (Ankara, Turkey), while *Halomonas variabilis* isolate was isolated from Salt Lake (Ankara, Turkey). The isolates were enriched in LB medium (Luria-Bertani: 10 g/L tryptone, 5 g/L yeast extract, 10 g/L NaCl in 1 L of distilled water) and then stock cultures were prepared. These three bacterial strains were chosen due to their capability to grow in extreme conditions and their fast growing abilities. The stock cultures

were stored for short periods (at 4 °C) and fresh cultures were prepared from those samples prior to the further use.

The species identities of the isolates were determined via 16S rRNA gene sequencing analysis. DNeasy Blood & Tissue Kit (QIAGEN, Germany) was utilized for bacterial DNA isolation. PCR amplification and further sequencing were performed with the following concentrations: 1.25 U Platinum Taq polymerase, 0.2 mM dNTP, 0.4 pmol T3 (ATTAACCCTCACTAAAGGGA) and T7 (TAATACGACTCACTATAGGG) primers encompassing the entire 16S gene, 1.5 mM MgCl and 1X Taq buffer [94]. The PCR steps were as follows: initial denaturation at 96 °C for 5 min and further 30 cycles of denaturation at 96 °C for 30 s, annealing at 55°C for 30 s, elongation at 72 °C for 30 s and a final elongation at 72 °C for 5 min. DNA sequencing and analysis was done via ABI 3130xl Genetic Analyzer by using BigDye Terminator v3.1 Cycle Sequencing Kit (Applied Biosystems, USA). The 16S rRNA gene sequences of the isolates were analyzed by NCBI's Bacterial Blast Tool (<http://www.ncbi.nlm.nih.gov>) for determination of the species identities.

### **2.3. Electrospinning of PCL and PLA nanofibrous webs**

PCL and PLA nanofibers were produced by using different binary solvent systems. The homogenous electrospinning solutions were prepared by dissolving PCL and PLA in DCM/DMF (1/1 (v/v)) and DCM/DMF (7/3 (v/v)) solvent mixtures at 15% (w/v) polymer concentrations for PCL and PLA nanofibers, respectively. The electrospinning solutions were loaded

in a 3 mL syringe fitted with a metallic needle of 0.4-0.6 mm inner diameter, and these were located horizontally on a syringe pump (model KDS-101, KD Scientific, USA). The metallic needle of the syringe was clamped by one of the electrode of high-voltage power supply (Spellman, SL30, USA) and the aluminum foil covered metal collector (to deposit electrospun nanofibers onto it) was grounded. Electrospinning parameters were adjusted as follows: feed rate of solutions = 0.5 mL/h, applied voltage = 10-15 kV, tip-to-collector distance = 10-12 cm. The electrospinning apparatus was put in a Plexiglas box and electrospinning was performed at  $24 \pm 1$  °C and 20% relative humidity. The deposited nanofibers/nanowebs were dried overnight at room temperature in a fume hood before use in application studies.

## **2.4. Dye bioremoval experiments**

LB broth was utilized as the bacterial growth medium for dye bioremoval experiments. The pH levels were neutral (pH 7.0). Initially, three different bacterial isolates (*Enterococcus hermanniensis*, *Clavibacter michiganensis* and *Halomonas variabilis*) were tested against two different commercial reactive textile dyes (Setazol Blue BRF-X, Setazol Turquoise Blue G) to determine the dye with the higher biodegradability and the isolate with the highest bioremoval capacity. The remaining dye concentrations were determined by spectrophotometric measurements and it was found that, Setazol Blue BRF-X gives specific absorbance at 609 nm and Setazol Turquoise Blue G gives specific absorbance at 626 nm. For this test, all initial dye concentrations were

kept constant at 50 mg/L and all isolates were incubated at 30 °C for 48 h. Since *Clavibacter michiganensis* isolate has shown the highest bioremoval performance among three different isolates especially against Setazol Blue BRF-X in this test, further dye bioremoval studies were performed by *Clavibacter michiganensis* isolate against Setazol Blue BRF-X dye. Equivalent samples of pristine PCL and PLA webs with equal weights (w/v ratio of 0.5 mg/mL) were prepared for bacterial immobilization and consecutive application studies. These webs were added directly to bacteria containing ( $\sim 10^7$ - $10^8$  cfu/mL) LB broth for bacterial attachment. Bacterial incubation was ended after 7 days and bacterial immobilization was monitored by SEM (Scanning Electron Microscopy) analysis. Since *Clavibacter michiganensis* isolate is a rapid growing strain, bacterial immobilization at this stage was found as sufficient to initiate dye bioremoval studies. The bacterial immobilization was also checked by detachment of the immobilized bacterial cells from equivalent samples and further OD<sub>600</sub> measurements. The detachment protocol includes sequential vortexing and sonication at cold temperatures (to preserve bacterial cell viability) [19]. For testing the bioremoval capabilities of bacteria/PCL and bacteria/PLA webs, three different (50, 100, 200 mg/L) initial dye concentrations were selected and bacteria immobilized web samples were added to dye containing LB media as inoculants. The bacteria immobilized web samples were incubated for 48 h at 150 rpm and 30 °C. Free bacteria cells and pristine web samples were also tested for their dye removal capabilities, as positive and negative controls, respectively. Liquid samples were collected periodically and then centrifuged at 8000 rpm for 5 minutes, and the supernatant

fractions were used for spectrophotometric measurement of the dye, to avoid optical density interference from bacterial cells. All tests were done in triplicate.

The removal capacities ( $Q_{eq}$ ) of free bacteria cells, and bacteria immobilized web samples were calculated by Eq. 1 (1):

$$Q_{eq} \text{ (mg/g)} = (C_0 - C_f) \cdot V / M \quad (1)$$

where  $C_0$  is the initial dye concentration (mg/L),  $C_f$  is the final dye concentration (mg/L),  $V$  is the volume of the solution (L) and  $M$  is the total bacterial biomass (g) at equilibrium [71].

## **2.5. Scanning electron microscopy (SEM)**

Millimeter-length PCL and PLA webs were prepared for SEM analysis to evaluate bacterial immobilization on nanofibrous webs. The sample fixation was done as previously mentioned [19]. In brief, bacteria immobilized web samples were washed several times with PBS buffer and incubated overnight in 2.5% glutaraldehyde solution (prepared in PBS buffer) for sample fixation. Then the web samples were washed again with PBS buffer and the samples were dehydrated by immersion in a series of EtOH solutions (30% - 96%). At the end, samples were coated with 5 nm Au-Pd for SEM imaging (Quanta 200 FEG SEM, FEI Instruments, USA). While the fixation protocol was not applied for Pristine PCL and PLA webs, they were also coated with 5 nm Au-Pd prior to SEM imaging.

## **2.6. Adsorption isotherms and kinetics studies**

Adsorption isotherm coefficients and their estimated values were determined upon three isotherm models (Langmuir, Freundlich, and Toth) using the isotherm parameter fitting software IsoFit [72]. The reactions orders were evaluated upon the  $R^2$  values of zero, first, second and third order plots of free bacteria, bacteria/PCL and bacteria/PLA samples.

## **2.7. Reusability test**

Reusability of bacteria/PCL and bacteria/PLA web samples were tested for bioremoval of Setazol Blue BRF-X dye. Prior to each cycle, the web samples were washed gently with Tris-HCl buffer to remove unattached bacteria. The experiments were performed at an initial dye concentration of 100 mg/L with the parameters: incubation at 150 rpm and 30 °C for 48 or 24 h. The remaining dye concentrations were measured at the beginning and at the end of each run, and the percentile removal of dye was calculated. All tests were done in triplicate.

## **3. Results and discussion**

### **3.1. Identification and preliminary characterization of the bacterial isolates**

The bacterial isolates were isolated from different resources where they were growing in extreme conditions, therefore they were assumed as potential

candidates for bioremediation of water contaminants. 16S rRNA gene sequencing analysis was applied on these strains and the species identities of the isolates were determined to be *Enterococcus hermanniensis*, *Clavibacter michiganensis* and *Halomonas variabilis*, and they were deposited in NCBI's GenBank with the accession numbers of GU907677, GQ466171 and KX351792.1, respectively. These three isolates were then tested for their potential textile dye bioremediation capability. At the end of this test, all of the isolates have shown higher bioremoval performance against Setazol Blue BRF-X dye, while only 25-40% of removal was observed for Setazol Turquoise Blue G dye (Fig. 34). In addition, among three different isolates, *Clavibacter michiganensis* isolate has shown the highest bioremoval performances against both Setazol Blue BRF-X and Setazol Turquoise Blue G dyes. Therefore, Setazol Blue BRF-X dye was selected as the target contaminant and *Clavibacter michiganensis* isolate was selected as the remediating organism for further textile dye bioremediation studies.

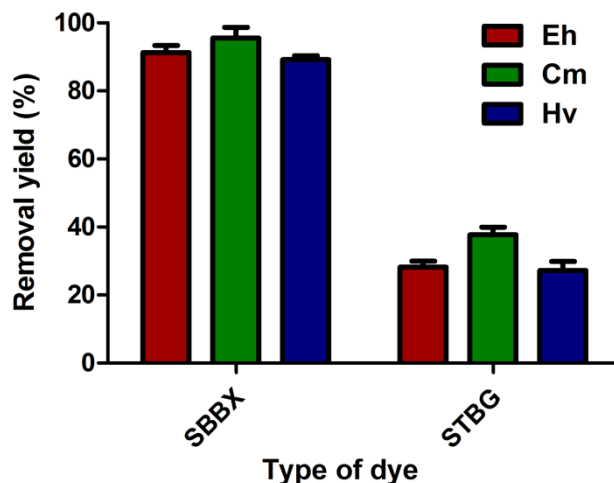


**Figure 34:** Initial characterization of the three isolates (*Enterococcus hermanniensis*, *Clavibacter michiganensis* and *Halomonas variabilis*) for their dye removal capabilities against Setazol Blue BRF-X (SBBX) and Setazol Turquoise Blue G (STBG) dyes at an initial concentration of 50 mg/L).

### 3.2. Bacterial immobilization on PCL and PLA webs

Two biodegradable and biocompatible polymers [108, 109], PCL and PLA were selected for producing electrospun fibrous webs. These webs were then utilized as carrier matrices for bacterial integration. The electrospinning process and subsequent bacterial adhesion are summarized in Fig. 35 schematically. Bacterial immobilization was achieved by natural adhesion process in which, bacterial cells attach on the surface via physical and chemical interactions after the initial contact, then they start to colonize throughout the surface after stabilizing their location, and finally forming biofilm structures [110].

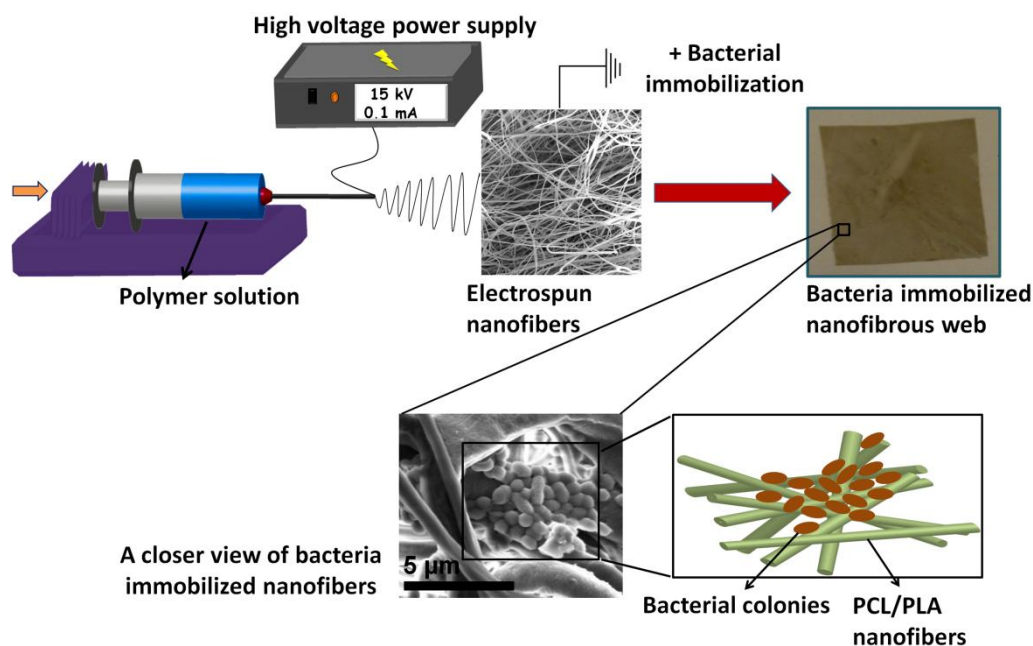


**Figure 35:** Schematic representation of the electrospinning process and representative images for bacterial immobilization including a photograph of bacteria immobilized electrospun nanofibrous web, a SEM micrograph of bacteria immobilized nanofibers and a schematic representation of the immobilized cells on electrospun nanofibers.

The morphologies of pristine PCL and PLA nanofibers along with their bacteria immobilized versions are shown in Fig. 36. The average fiber diameters of PCL and PLA webs were measured as  $1280 \pm 90$  and  $840 \pm 80$  nm, respectively ( $n=10$ ). As shown in Fig. 36c and 36d, strong bacterial adhesion and biofilm structures were observed, hence 7 days of incubation was found as adequate for each sample to initiate bioremediation studies. In addition to SEM imaging, bacterial immobilization was followed by a protocol in which immobilized bacterial cells were detached from equivalent web samples and then  $OD_{600}$  measurements were applied on these detached cells to determine the approximate number of the immobilized bacteria (where  $OD_{600}=0.1$  corresponds

to  $\sim 10^8$  cfu/mL). The results of this experiment will be mentioned in a following section. After ending the bacterial immobilization process at day 7, equivalent samples of bacteria/PCL and bacteria/PLA webs (w/v ratio of 0.5 mg/mL) were collected to initiate dye removal experiments.

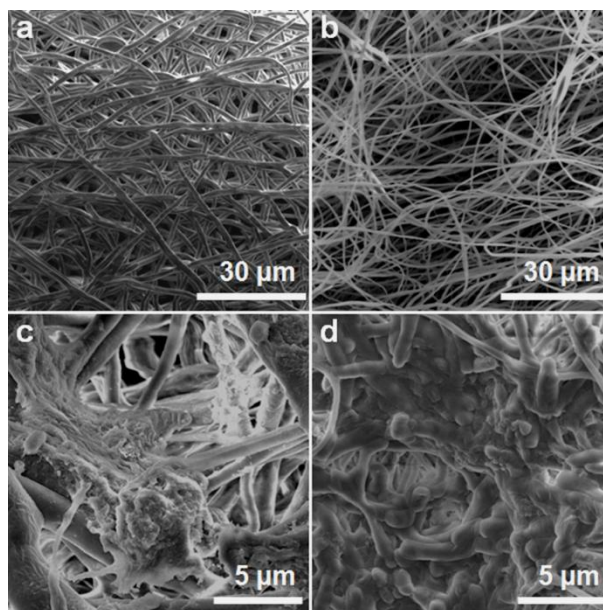


**Figure 36:** SEM micrographs of (a) pristine PCL (b) pristine PLA (c) bacteria/PCL and (d) bacteria/PLA webs.

### 3.3. Dye removal capabilities of bacteria/PCL and bacteria/PLA webs

Bacteria/PCL and bacteria/PLA webs were tested for their dye removal capabilities at different initial dye concentrations (50, 100 and 200 mg/L). Removal capacities ( $Q_{eq}$ ) of free-bacteria cells and bacteria immobilized webs were also calculated and are presented in Table 11.

**Table 11.** Removal capacities of free-bacteria, bacteria/PCL web and bacteria/PLA web samples at equilibrium at the end of the removal process. T = 30 °C, agitation rate: 150 rpm, incubation time: 48 h.

Sample name	Initial concentration (C <sub>0</sub> )	Removal (%)	Q <sub>eq</sub> (mg/g)
Free-bacteria	50 mg/L	95.56 ± 3.16	119.56 ± 5.6
	100 mg/L	89.04 ± 3	296.56 ± 8
	200 mg/L	90.49 ± 0.31	603.23 ± 11.64
Bacteria/PCL web	50 mg/L	87.88 ± 2.79	109.75 ± 3.92
	100 mg/L	92.52 ± 1.98	307.89 ± 6.05
	200 mg/L	93.18 ± 1.29	621.52 ± 20.86
Bacteria/PLA web	50 mg/L	89.57 ± 4.08	112.15 ± 8.6
	100 mg/L	91 ± 3.6	301.65 ± 9.67
	200 mg/L	93.60 ± 3.13	623.28 ± 20.25

Both webs have shown efficient removal yields at each concentration, while there were slight differences between them (Fig. 37, Table 11). For 50 mg/L of initial dye concentration, free-bacteria sample has shown the highest removal yield with 95.56%, while bacteria/PLA and bacteria/PCL webs followed this with the removal yields of 89.57% and 87.88%, respectively. The Q<sub>eq</sub> values of the samples were in the same sequence, 119.56 mg/g for free-bacteria, 112.15 mg/g for bacteria/PLA web and 109.75 mg/g for bacteria/PCL web samples. For 100 mg/L of initial dye concentration, bacteria immobilized webs have shown higher removal yields than free-bacteria sample, where bacteria/PCL web has shown 92.52% removal with a Q<sub>eq</sub> value of 307.89 mg/g,

bacteria/PLA web has shown 91% removal with a  $Q_{eq}$  value of 301.65 mg/g, and free-bacteria sample has shown 89.04% removal with a  $Q_{eq}$  value of 296.56 mg/g. For 200 mg/L of initial dye concentration, bacteria immobilized webs have shown once more higher removal yields than free-bacteria sample, where bacteria/PCL web has shown 93.18% removal with a  $Q_{eq}$  value of 621.52 mg/g, bacteria/PLA web has shown 93.60% removal with a  $Q_{eq}$  value of 623.28 mg/g, and free-bacteria sample has shown 90.49% removal with a  $Q_{eq}$  value of 603.23 mg/g.

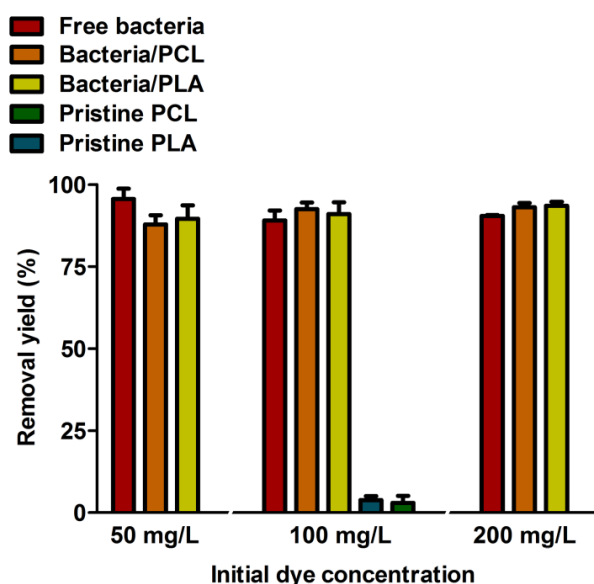


**Figure 37:** (a) Dye removal profiles of free-bacteria, pristine PCL web, pristine PLA web, bacteria/PCL web and bacteria/PLA web samples at initial concentrations of 50, 100 and 200 mg/L. Error bars represent mean of three independent replicates.

Pristine PCL and PLA webs were also tested as negative controls for dye removal, and the results revealed that PCL and PLA webs had negligible effects on dye removal, which suggests that the dye removal capabilities of bacteria

immobilized webs were primarily based on the bacterial cells. The results of dye removal experiments were found as promising and henceforth bacteria immobilized web samples were further tested for their potential reusability.

### **3.4. Evaluation of adsorption isotherm coefficients and reaction kinetics**

Adsorption isotherm coefficients and their estimated values are given in Table 12. All of the samples have shown good fits for each isotherm model. No distinctive fitting was observed for the Langmuir model in each sample, suggesting the dye removal process might be heterogeneous and multilayeric through bacteria [62]. The maximum removal capacities ( $Q_{\max}$ ) were estimated to be  $1.41 \times 10^4$  mg/g for free-bacteria,  $1.77 \times 10^3$  mg/g for bacteria/PCL web and  $3.24 \times 10^3$  mg/g for bacteria/PLA web samples under the Toth model.

The  $R^2$  values of different order plots for dye removal are listed in Table 13. All of the samples have shown the highest correlation with the zero order model with the  $R^2$  values of 0.9909 for free-bacteria, 0.9877 for bacteria/PCL web and 0.9944 for bacteria/PLA web samples. It has been reported that enzyme-catalyzed reactions often fall under the zero order model [75], hence the dye removal process by bacterial cells was supposed to be enzymatic.

**Table 12.** Adsorption isotherm coefficients of free-bacteria, bacteria/PCL web and bacteria/PLA web samples for each isotherm model.

Samples	Isotherm	Parameters	Values	Ry <sup>2</sup> value
Free-bacteria	Freundlich	K <sub>f</sub>	30.72	0.967
		1/n	0.99	
	Langmuir	Q <sub>max</sub>	2.15 x 10 <sup>4</sup>	0.964
		b	1.46 x 10 <sup>-3</sup>	
	Toth	Q <sub>max</sub>	1.41 x 10 <sup>4</sup>	0.967
		b	2.18 x 10 <sup>-3</sup>	
		n	2.07	
Bacteria/PCL web	Freundlich	K <sub>f</sub>	41.02	0.961
		1/n	1.00	
	Langmuir	Q <sub>max</sub>	1.62 x 10 <sup>5</sup>	0.961
		b	2.54 x 10 <sup>-4</sup>	
	Toth	Q <sub>max</sub>	1.77 x 10 <sup>3</sup>	0.961
		b	2.31 x 10 <sup>-2</sup>	
		n	4.95	
Bacteria/PLA web	Freundlich	K <sub>f</sub>	40.37	0.957
		1/n	1.00	
	Langmuir	Q <sub>max</sub>	6.51 x 10 <sup>5</sup>	0.957
		b	6.2 x 10 <sup>-5</sup>	
	Toth	Q <sub>max</sub>	3.24 x 10 <sup>3</sup>	0.957
		b	1.24 x 10 <sup>-2</sup>	
		n	4.79	

**Table 13.** The R<sup>2</sup> values of zero, first, second and third order plots for the dye removal by free-bacteria, bacteria/PCL web and bacteria/PLA web samples.

Samples	Model	R <sup>2</sup> values
Free-bacteria	zero order	0.9909
	first order	0.9689
	second order	0.8692
	third order	0.8061
Bacteria/PCL web	zero order	0.9877
	first order	0.9594
	second order	0.9448
	third order	0.9425
Bacteria/PLA web	zero order	0.9944
	first order	0.9810
	second order	0.9496
	third order	0.9430

### **3.5. Reusability and applicability of bacteria/PCL and bacteria/PLA webs**

Bacteria/PCL and bacteria/PLA web samples were tested for reusability in five consecutive cycles (Fig. 38). At the end of the reusability test, the average removal capacities of these two webs were found as very similar, 95.36% for bacteria/PCL and 95.41% for bacteria/PLA web samples, showing that both webs retained their dye removal capacities during the test period. In addition, it was found that, while bioremediation needed more time in initial cycles, it decreased after the second run from 48 h to 24 h, implying that the number of immobilized bacteria increased during the test. This deduction was also supported by OD<sub>600</sub> measurements, in which OD<sub>600</sub> values of detached bacteria for equivalent web samples were measured before and after the reusability test. As shown in Fig. 39, the bacterial numbers highly increased during the test for both web samples, which might be the primary reason for faster bioremediation by bacteria immobilized webs after the second run. Following the reusability test, bacteria/PCL and bacteria/PLA webs were evaluated for bacterial adhesion by SEM imaging. Fig. 40 shows strong bacterial biofilms retained on both PCL and PLA webs, indicating that bacterial cells have survived and grown throughout the reusability test. These results were found as promising for continuous remediation of textile dyes from aqueous environments by use of bacteria immobilized electrospun fibrous webs.

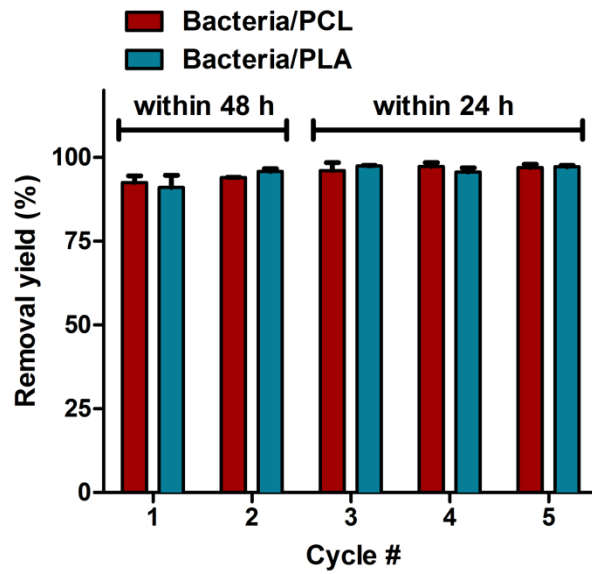


**Figure 38:** Reusability test results of bacteria/PCL and bacteria/PLA webs at an initial dye concentration of 100 mg/L. Error bars represent mean of three independent replicates.

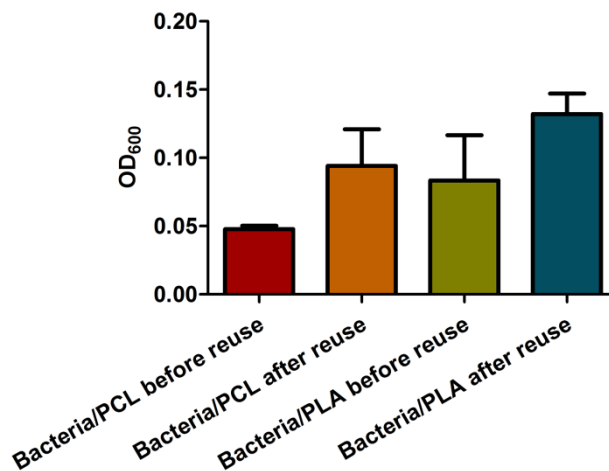


**Figure 39:** Comparison for OD<sub>600</sub> values of bacteria/PCL and bacteria/PLA webs before and after the reusability test.

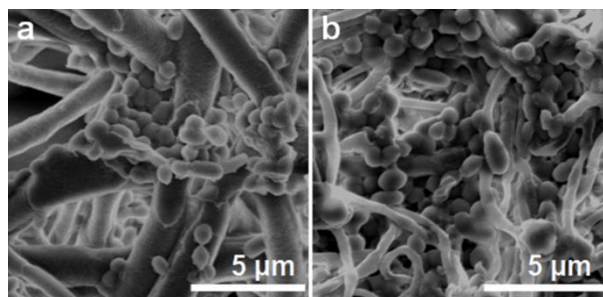


**Figure 40:** SEM micrographs of (a) bacteria/PCL and (b) bacteria/PLA webs after the reusability test.

Dye bioremoval in aqueous solutions by use of different organisms have been extensively studied in the literature. [21, 102, 103, 111-114]. On the other hand, alternative approaches as in this study are relatively few, hence the objective of this study was the development of novel bio-hybrid materials with distinct features for dye bioremoval. The bacteria immobilized webs have lower space and weight requirements compare to free-bacteria in liquid media, thereby providing lower transportation costs and easier handling as in lyophilized bacteria. In addition, as demonstrated, bacteria immobilized webs are potentially reusable for continuous remediation of contaminated areas. By optimization of environmental parameters and increasing the number of immobilized bacteria, more efficient biocomposites can be produced for continuous, environmentally friendly and cost-effective dye bioremoval in water.

## Chapter 8

---

### **Bacteria encapsulated electrospun nanofibrous webs for remediation of methylene blue dye in water**

(Parts of this study was submitted as “Bacteria encapsulated electrospun nanofibrous webs for remediation of methylene blue dye in water”, Omer Faruk Sarioglu, Nalan Oya San Keskin, Asli Celebioglu, Turgay Tekinay and Tamer Uyar, *Colloids and Surfaces B: Biointerfaces*, August 25, 2016

## 1. Introduction

There are different types of contaminants in wastewater effluents which are utilized in industrial processes, and dyes comprise a great portion in those industrial contaminants. Synthetic dyes have a great usage in various industries (e.g. textile, leather, paper) and dyeing process can lead to many environmental problems [22]. Methylene blue (MB) is a common basic, cationic dye with a broad application area in textile industry, paper industry, chemistry, biology and medicine [22, 115-120]. Nevertheless, decontamination of MB from water systems after use is still a major challenge. Conventional wastewater treatment methods can be used for remediation of MB such as photocatalysis [101], advanced oxidation processes [100], reverse osmosis [99] and electrochemical treatment [107]. Some of these techniques can be used efficiently for MB remediation, though each of them has their own limitations, hence innovative approaches have been presented in the literature for development of sustainable, environmentally friendly, cost-effective and efficient treatment methods [22]. Bioremediation is an alternative technology for decontamination of water systems by use of specific microorganisms, and it can provide green, efficient, cost-effective and sustainable remediation of water contaminants [2]. Microalgae, fungi and bacteria can be utilized for bioremediation. These microorganisms can remediate water pollutants either by biosorption or bioaccumulation. Although dead cell biomasses can only be used for biosorption, living cells can possess both bioaccumulation and biosorption,

hence higher efficiency for bioremediation could be achieved by living cells in some studies [2].

The genus *Pseudomonas* comprises Gram-negative, aerobic, rod-shaped bacteria and has a broad metabolic diversity [121], having a potential to be used in bioremediation studies. A popular member of this genus, *Pseudomonas aeruginosa* has already been used effectively in bioremediation of organic contaminants [22, 122-124], implying this species as a potential candidate for further bioremediation studies.

Application of microorganisms for use in bioremediation can be performed with either free microorganisms or microorganism immobilized bio-hybrid materials. Immobilized microorganisms can bring advantages than free cells in terms of their potential reusability, lower space and growth medium necessities, and higher resistance to environmental extremes [14, 36]. Electrospun fibrous webs have become a popular carrier matrix for immobilization of specific microorganisms for bioremediation of water systems [18-21, 107]. Electrospinning can allow simple, versatile and cost-effective production of fibrous webs with unique properties such as high surface area and porosity, making electrospun fibrous webs as promising candidates for microbial integration and membrane/filter applications [7]. In recent years, a number of studies have been reported about encapsulation of microorganisms into electrospun fibrous matrices [4, 7, 11, 125, 126]. While viability or bioactivity of encapsulated microorganisms has been checked in all of these

studies, just only very few of them have reported applications of bioremediation [11, 126].

In the present study, bioremediating bacterial cells were successfully encapsulated into polyvinyl alcohol (PVA) and polyethylene oxide (PEO) polymeric matrices while keeping the bacteria bioactive and the viable cell numbers in desirable amounts. Two water based and biocompatible polymeric matrices were selected for encapsulation of bacterial cells to reduce the effects of exterior environment on the viable bacterial numbers. These newly produced bacteria encapsulated nanofibrous webs were tested for their removal capacities against MB dye. It was found that, bacteria encapsulated webs have the potential to successfully remediate MB in water. In addition, the storability of bacteria encapsulated nanofibrous webs was tested in terms of the viable bacterial numbers. The results have shown that the encapsulated bacteria can be stored safely for long time periods without significant losses in their cell viability. These types of bio-hybrid materials could be of interest due to easy and safe preservation of bioremediating bacteria for potential wastewater treatment applications.

## **2. Experimental**

### **2.1. Materials**

The chemicals and reagents (polyvinyl alcohol (PVA, Mw ~125.000, Scientific Polymer Products, Inc.), polyethylene oxide (PEO, Mw ~900.000, Sigma-Aldrich), methylene blue (MB,  $\geq 82\%$ , Sigma-Aldrich), Nutrient broth (Sigma-

Aldrich), LB (Luria-Bertani) broth (Sigma-Aldrich) and Agar (Sigma-Aldrich)) were purchased and used without any purification. The deionized water was obtained from a Millipore Milli-Q Ultrapure Water System. All the chemicals were of high purity available and were of analytical grade.

## **2.2. Procurement of the bacterial strain**

The commercial bacterial strain utilized in this study (*Pseudomonas aeruginosa* ATCC 47085) was purchased from ATCC (American Type Culture Collection, USA). The bacterial culture was enriched in LB medium (Luria-Bertani: 10 g/L tryptone, 5 g/L yeast extract, 10 g/L NaCl in 1 L of distilled water) and stock cultures were prepared from the initial broth. The stock cultures were stored at 4 °C for short periods and fresh cultures were prepared from those samples prior to the further use.

## **2.3. Electrospinning of bacteria encapsulated PVA and PEO nanofibrous webs**

PVA and PEO nanofibers were produced by using a single solvent system (water), but with different polymer concentrations. While for PVA nanofibers, the polymer concentration was 7.5% (w/v) in the electrospinning solution, it was 3.5% (w/v) for PEO nanofibers. The materials used for preparation of electrospun nanofibers were all sterilized by autoclave, and the inside of the Plexiglas box where electrospinning was carried out was sterilized by UV-C light to avoid contamination. Before electrospinning process, 2X concentrations of polymer mixtures were prepared and then equal amounts of either bacteria-

free distilled water or bacteria containing distilled water were mixed with these mixtures to obtain 1X electrospinning solutions. In order to encapsulate sufficient amounts of bacteria within polymer matrices, the required bacterial amount was determined by dry cell biomass (~4 mg of bacterial biomass per mL of electrospinning solution, corresponding to  $\sim 10^{10}$  cfu/mL). The electrospinning solutions were loaded in 1 mL syringe fitted with a metallic needle of 0.6 mm inner diameter and they were located horizontally on a syringe pump (model KDS-101, KD Scientific, USA). One of the electrodes of high-voltage power supply (Matsusada Precision, AU Series) was clamped to the metallic needle and the other one was clamped to the grounded aluminum collector which was covered with an aluminum foil to deposit the PVA and PEO electrospun nanofibers. The electrospinning parameters were applied as: feed rate of solutions = 1 mL/h, applied voltage = 10-15 kV, tip-to-collector distance = 10-12 cm. The electrospinning apparatus was enclosed in a Plexiglas box and electrospinning was carried out at  $24\text{ }^{\circ}\text{C} \pm 1$  and ~20% relative humidity. The collected bacteria encapsulated nanofibrous webs were stored in a refrigerator ( $+4\text{ }^{\circ}\text{C}$ ) for quick or longer-term use. Only in one experiment, the bacteria encapsulated nanofibrous webs were stored at room temperature as well. Bacteria-free (pristine) nanofibers were stored at room temperature.

## **2.4. Viability and storage tests**

In order to evaluate whether bacterial cells were properly encapsulated within PVA and PEO nanofibers, the *Pseudomonas aeruginosa* ATCC 47085 cells were stained with fluorescent stains (LIVE/DEAD BacLight™ kit) before

mixing with the 2X concentrations of polymer mixtures. After preparation of electrospinning solutions, PVA and PEO nanofibers were collected on glass slides to observe under a fluorescence microscope. Microscopic evaluation of LIVE/DEAD-stained bacterial cells was made by the general assessment: bright green fluorescence emitting cells correspond to living cells and bright red fluorescence emitting cells correspond to dead ones. Photographs were taken by using a Leica optical microscope (Leica, DMI 4000 B) which has an attached fluorescence unit.

In addition to fluorescence microscopy, the viability of *Pseudomonas aeruginosa* ATCC 47085 cells in either electrospinning solutions or encapsulated within nanofibrous webs was determined via viable cell counting (VCC) assay. To find the encapsulation efficiency, equivalent pieces of the nanofibrous material was weighed which contain the encapsulated bacterial cells. Distilled water was added to these pieces and they dissolved rapidly in water, serial 10-fold dilutions were made and then the bacterial solutions were spread on LB agar plates. After overnight incubation at 30 °C, the number of colony-forming units (CFU) was counted. All tests were done in triplicate.

For storage test, equivalent pieces were prepared for same samples and their viabilities were checked regularly for defined time periods. Bacteria encapsulated nanofibrous webs were tested for storability at 4 °C for 3 months and at 25 °C for 10 days.

## **2.5. Methylene blue (MB) bioremoval experiments**

LB broth was utilized as the bacterial growth medium for MB bioremoval experiments. The pH levels were constant and neutral (pH 7.0). Bacteria encapsulated PVA and PEO webs were added directly to MB containing LB broth for initiating bacterial growth. The effect of PVA and PEO in the growth media of dissolved webs on bacterial growth was evaluated by OD<sub>600</sub> measurements. After achieving the bacterial cell viabilities of each bacteria encapsulated PVA and PEO webs in the range of  $10^7$ - $10^8$  cfu/mL per 10 mg, equivalent web samples (with w/v ratio of 1 mg/mL) were prepared for initiating MB bioremoval experiments. The initial bacterial cell viabilities of bacteria/PVA and bacteria/PEO webs were around  $10^7$ - $10^8$  cfu/mL and  $10^8$  cfu/mL per 10 mg, respectively. Samples were collected periodically to analyze remaining MB concentrations by a spectrophotometer, and the specific absorbance of the dye was measured at 660 nm. The samples were centrifuged prior to measurements for 5 minutes at 10000 rpm, and the supernatant fractions were utilized for spectrophotometric measurements to avoid optical density interference from bacterial cells. Three different (10, 15, 25 mg/L) initial MB concentrations were tested for evaluation of the removal capabilities of bacteria/PVA and bacteria/PEO webs. The samples were incubated for 48 h at 125 rpm and 30 °C. Free bacteria and bacteria-free web samples were tested for their MB removal capabilities as well, as positive and negative controls, respectively. The bacterial cell viabilities of initial inocula for free viable bacterial cells were adjusted around  $10^8$  cfu/mL to compensate the initial cell

viabilities of free and encapsulated bacteria. In order to evaluate the role of dead cells in MB removal, dead cells were also tested for MB removal at the same conditions. Bacterial cell viabilities were adjusted as  $\sim 10^{10}$  cfu/mL, corresponding to the total viable bacterial number within electrospinning solutions before starting the process, before killing bacterial cells at 70 °C for 3 h. All tests were done in triplicate.

The removal capacities ( $Q_{eq}$ ) of free bacteria cells, and bacteria encapsulated webs were calculated by Eq. 1 (1):

$$Q_{eq} \text{ (mg/g)} = (C_0 - C_f) \cdot V / M \quad (1)$$

$C_0$  is the initial MB concentration (mg/L),  $C_f$  is the final MB concentration (mg/L),  $V$  is the solution volume (L) and  $M$  is the total bacterial cell biomass (g) at equilibrium [71].

## 2.6. Raman spectroscopy

Raman spectroscopy analysis was performed by using Nicolet 6700 FT-Raman Spectrometer (Thermo-Scientific, US) for confirmation of bacterial encapsulation. A near-infrared (1064 nm) laser was used for excitation and 100 scans were averaged for each measurement. The data analysis software OMNIC<sup>TM</sup> was used for Raman measurements, identification of peak locations and basic modifications such as baseline and background corrections. Background corrections for H<sub>2</sub>O and CO<sub>2</sub> were carried out for each analysis. Duplicate samples were utilized in each analysis.

## **2.7. Scanning electron microscopy (SEM)**

Millimeter-length PVA and PEO webs were prepared for SEM analysis to evaluate morphologies of bacteria-free and bacteria encapsulated webs. Samples were coated with 5 nm Au-Pd prior to SEM imaging (Quanta 200 FEG SEM, FEI Instruments, USA).

## **2.8. Adsorption isotherms and kinetics studies**

Adsorption coefficients were estimated upon three isotherm models (Langmuir, Freundlich, and Toth) using the isotherm parameter fitting software IsoFit [72]. The order of reactions for MB removal were evaluated upon the  $R^2$  values of zero, first, second and third order plots of free bacteria, bacteria/PVA and bacteria/PEO samples.

# **3. Results and discussion**

## **3.1. Encapsulation of bacteria within nanofibrous webs and evaluation of bacterial cell viability**

The electrospinning process for bacteria encapsulated nanofibrous webs is summarized in Fig. 41 schematically. Although the applied voltage for electrospinning process is highly detrimental for bacterial cells, it was needed to produce PVA and PEO nanofibers at these polymer concentrations. Therefore, in order to achieve the bacterial cell viabilities in desired amounts for the electrospun nanofibers, bacterial amounts in the electrospinning solutions were

highly condensed, so that even after electrospinning and cell viability losses, there were sufficient amounts of viable bacteria within electrospun nanofibers. The morphologies of bacteria-free and bacteria encapsulated electrospun PVA and PEO nanofibrous webs were evaluated by SEM imaging. The average diameters of pristine PVA and PEO nanofibers were measured as  $418.6 \pm 33.8$  and  $232.5 \pm 22.3$  nm, respectively (n=10). While bead-free nanofibers were obtained for pristine PVA nanofibrous web (Fig. 42a), beaded structures were obtained for pristine PEO nanofibrous web at 3.5% (w/v) polymer concentration (Fig. 42b). It was found that bacterial cells were successfully encapsulated within PVA and PEO nanofibrous webs. Encapsulation of bacterial cells caused local widening of fibers in certain regions and ball-like structures were observed in these areas (Fig. 42c and 42d). In addition, it was noticed that the ball-like structures due to bacterial encapsulation are quite different (bigger and thicker) and can be easily differentiated from the ordinary beads of pristine PEO nanofibers (Fig. 42d). Fluorescence microscopy images have shown that, the cell viabilities were preserved for the encapsulated bacteria in the PVA and PEO nanofiber matrices (Fig 42e and 42f).

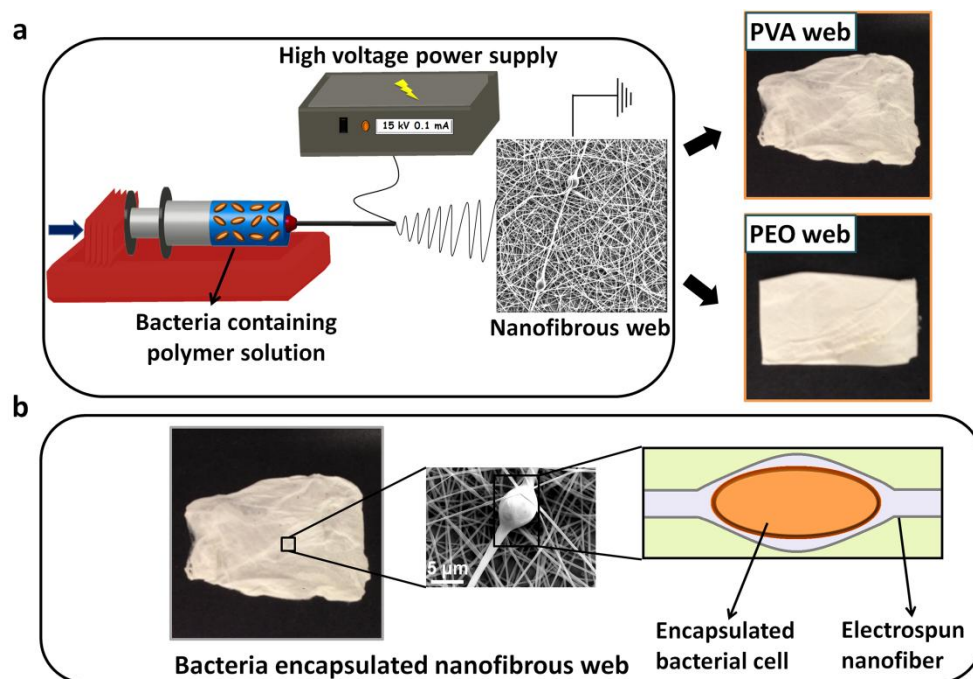


**Figure 41:** (a) Schematic representation of electrospinning process for bacteria encapsulated PVA and PEO webs, and photographs of PVA and PEO webs, (b) representative images for bacteria encapsulated webs including a SEM micrograph and a schematic representation of a bacterial cell inside PVA/PEO fibers.

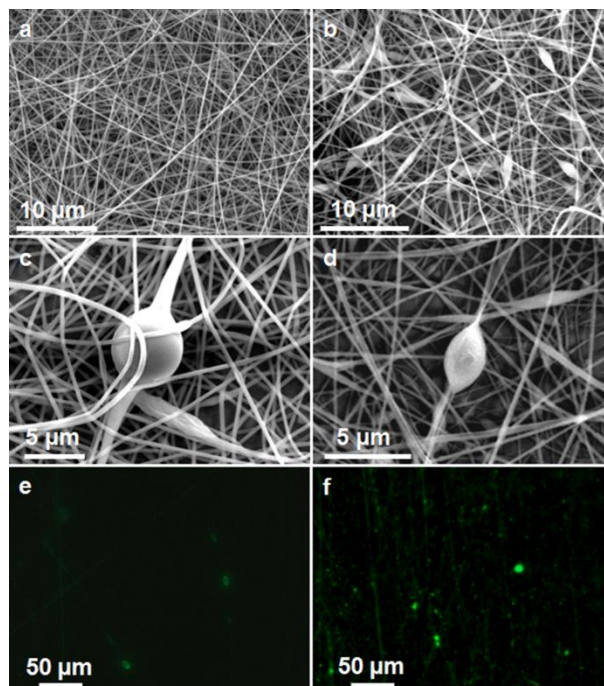


**Figure 42:** SEM micrographs of (a) pristine PVA (b) pristine PEO (c) bacteria/PVA (d) bacteria/PEO webs and fluorescence microscopy images of (e) bacteria/PVA and (f) bacteria/PEO webs.

The bacterial cell viabilities were also checked by applying VCC assay on equivalent samples of bacteria/PVA and bacteria/PEO webs. As mentioned previously, before using in MB removal experiments, the cell viabilities were determined for each 10 mg of bacteria encapsulated webs as around  $10^7$ - $10^8$  cfu/mL for bacteria/PVA and  $10^8$  cfu/mL for bacteria/PEO webs. Bacteria/PEO web samples had always higher cell viabilities, possibly due to the higher w/v ratio of bacterial cell biomass after dehydration for bacteria/PEO webs. After ensuring that the web samples have sufficient amounts of viable bacterial cells, biodegradation experiments were initiated with equivalents of those web samples.

### 3.2. Raman spectroscopy analysis of pristine and bacteria encapsulated webs

The pristine and bacteria encapsulated PVA and PEO webs were analyzed with Raman spectroscopy to track the distinct chemical signatures as a result of bacterial encapsulation. The characteristic Raman spectra of PVA and PEO webs with their bacteria encapsulated versions are shown in Fig 43.

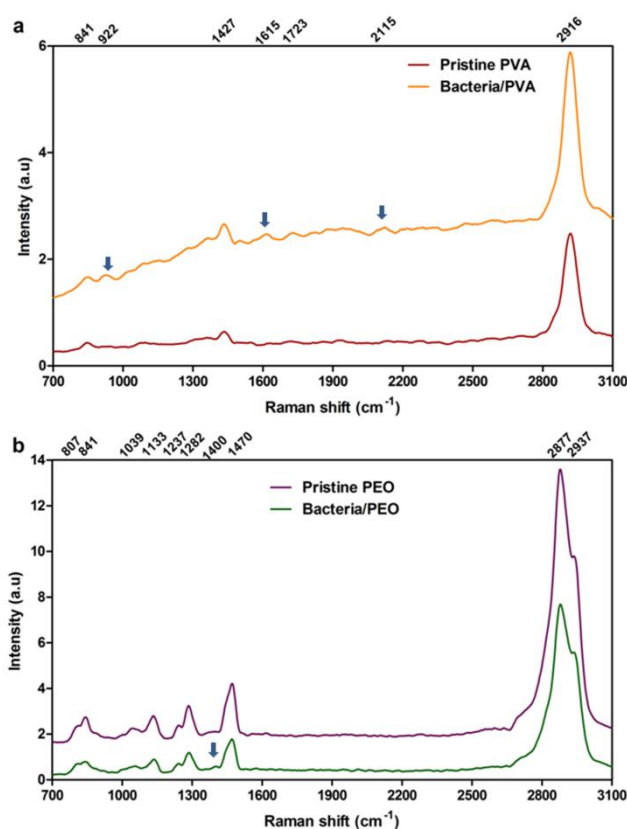


**Figure 43:** Raman spectra of (a) pristine PVA and bacteria/PVA and (b) pristine PEO and bacteria/PEO webs.

When comparing the peaks observed in pristine PVA and bacteria/PVA web samples' Raman spectra, the peaks located at 922, 1615 and 2155  $\text{cm}^{-1}$  in bacteria/PVA web sample were differentiated from pristine PVA web's Raman spectrum. The peak at 922  $\text{cm}^{-1}$  corresponds to C-C stretching [127], the peak at 1615  $\text{cm}^{-1}$  corresponds to amino acids [127], and the peak at 2115  $\text{cm}^{-1}$  corresponds to asymmetric C=C=O (ketene) stretching [128], suggesting these specific peaks might appeared as a result of bacterial presence. When comparing the peaks observed in pristine PEO and bacteria/PEO web samples' Raman spectra, the only difference was observed for the small peak located at 1400  $\text{cm}^{-1}$  in bacteria/PEO web's Raman spectrum. This peak corresponds to NH in-plane deformation [127], coming from bacterial proteins, suggesting it might appeared as a result of bacterial encapsulation.

### **3.3. MB dye removal capabilities of bacteria/PVA and bacteria/PEO webs**

Electrospun bacteria/PVA and bacteria/PEO webs are readily water-soluble biocomposites which could be handy carrier matrix for bacterial storage and can be alternative to lyophilized bacteria for environmental remediation approaches in water. The effect of PVA and PEO polymeric solutions on bacterial growth was evaluated and no apparent differences were found for bacteria which were grown in polymeric solutions (Fig. 44), hence these webs can be used safely for starting bacterial inocula.

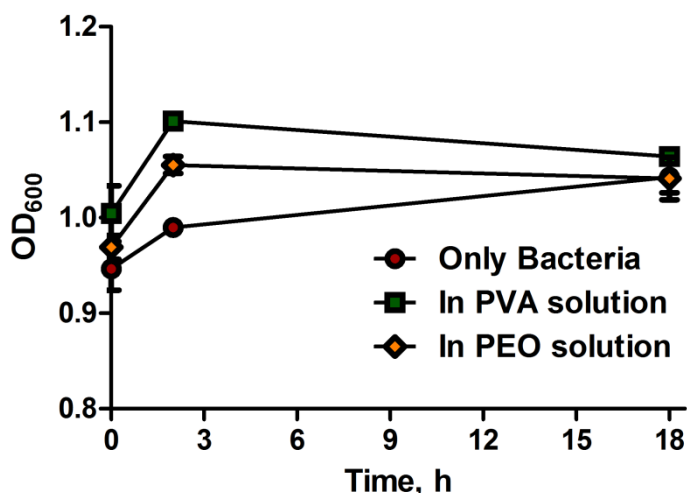


**Figure 44:** Growth profiles of bacterial cells which have grown in polymer-free LB medium, PVA containing LB medium or PEO containing LB medium within 18 h. Error bars represent mean of three independent replicates.

MB removal capabilities of bacteria/PVA and bacteria/PEO webs were tested at three different initial MB concentrations (10, 15, 25 mg/L). While both webs have shown lower removal yields at 10 mg/L of initial MB (52.5% for bacteria/PVA web and 44.4% for bacteria/PEO web), their removal yields increased at 15 mg/L (57% for bacteria/PVA web and 76% for bacteria/PEO web) and 25 mg/L (68% for bacteria/PVA web and 69% for bacteria/PEO web) of initial MB, suggesting the removal process is biological rather than adsorption based, and might be enhanced by genetic switching at a defined concentration range (Fig. 45a, Table 14). Even though PVA and PEO nanofibrous webs were quickly dissolved in MB aqueous solution, a very negligible decrease was observed in MB concentration with the addition of pristine PVA and PEO nanofibers, implying the removal performances of bacteria/PVA and bacteria/PEO webs were primarily based on the bacterial

existence (Fig. 45b). In addition, dead bacterial cells have shown a very negligible decrease in the initial MB concentration after 48 h incubation, suggesting MB dye was primarily remediated by viable bacterial cells (Fig. 46).

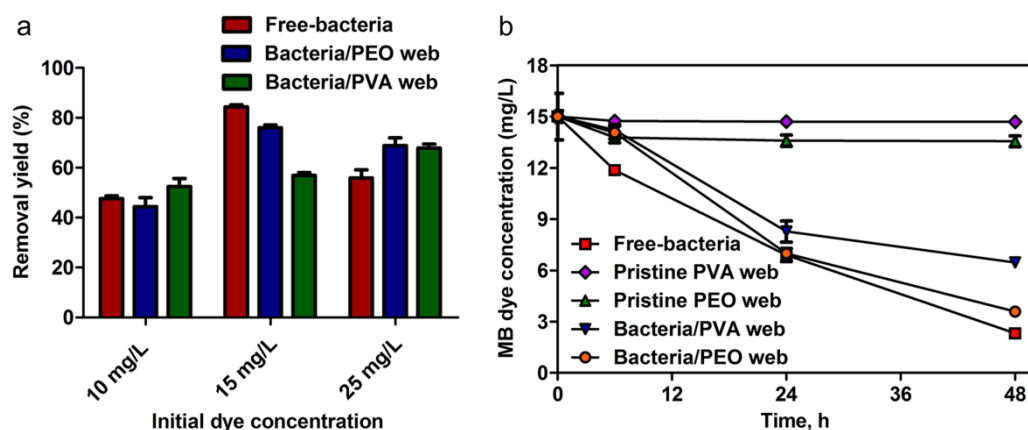


**Figure 45:** (a) MB removal profiles of free-bacteria, bacteria/PVA web and bacteria/PEO web samples at initial concentrations of 10, 15 and 25 mg/L. (b) Concentration vs. time graph of free-bacteria, bacteria/PVA web, bacteria/PEO web, pristine PVA web and pristine PEO web samples at 15 mg/L of initial MB. Error bars represent mean of three independent replicates.

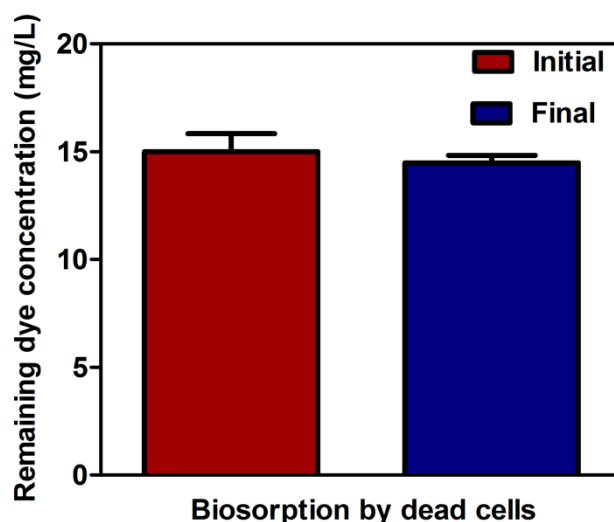


**Figure 46:** Growth profiles of bacterial cells which have grown in polymer-free LB medium, PVA containing LB medium or PEO containing LB medium within 18 h. Error bars represent mean of three independent replicates.

Degradation capacities ( $Q_{eq}$ ) of free-bacteria cells and bacteria encapsulated webs were calculated for each concentration and are presented in Table 14. The  $Q_{eq}$  values of free-bacteria, bacteria/PVA web and bacteria/PEO web samples are similar at 10 mg/L. At 15 mg/L of initial MB concentration, free-bacteria sample has a higher  $Q_{eq}$  value than bacteria encapsulated webs, and bacteria/PEO web has a higher  $Q_{eq}$  value than bacteria/PVA web. At 25 mg/L of initial MB concentration, the  $Q_{eq}$  values of bacteria/PVA and bacteria/PEO webs are very close to each other and both of them are higher than the free-bacteria sample.

**Table 14.** Removal capacities of free-bacteria, bacteria/PVA web and bacteria/PEO web samples at equilibrium at the end of the removal process. T = 30 °C, agitation rate: 125 rpm, incubation time: 48 h.

Sample name	Initial concentration ( $C_0$ )	Removal (%)	$Q_{eq}$ (mg/g)
Free-bacteria	10 mg/L	$47.6 \pm 1.09$	$25.04 \pm 0.58$
	15 mg/L	$84.4 \pm 0.8$	$66.75 \pm 6.59$
	25 mg/L	$56 \pm 3.21$	$74.02 \pm 8.61$
Bacteria/PVA web	10 mg/L	$52.5 \pm 3.24$	$27.79 \pm 3.18$
	15 mg/L	$57 \pm 1.08$	$45 \pm 1.38$
	25 mg/L	$68 \pm 1.58$	$89.22 \pm 1.17$
Bacteria/PEO web	10 mg/L	$44.4 \pm 3.63$	$23.57 \pm 3.24$
	15 mg/L	$76 \pm 1.02$	$60.04 \pm 1.46$
	25 mg/L	$69 \pm 3.13$	$89.47 \pm 3.94$

Since bacteria/PEO web samples had higher amounts of viable bacteria for the initial inoculum, their removal performances were higher than that of bacteria/PVA web samples in general, suggesting the bacteria encapsulated web samples can be improved for more efficient MB removal by increasing the encapsulated bacterial cell viabilities. In addition, by using a more capable bacterial strain, higher removal performances for MB even in shorter time periods can be obtained, as presented previously [22, 102].

Not a regular trend was observed when comparing the removal performances of free-bacterial cells and bacteria encapsulated web samples. While the highest MB removal was observed by free-bacterial cells at 15 mg/L, the highest MB removal was observed by bacteria/PEO web sample at 25 mg/L, and the highest MB removal was observed by bacteria/PVA web sample at 10 mg/L. These results might be occurred due to the differences in encapsulation efficiency in terms of cell viability preservation for different bacteria encapsulated web samples, leading differences in initial inocula and hence maximal growth of the bacterial cells for methylene blue removal. Although viable cell numbers of free-bacterial cells were equivalent in each experiment, viable cell numbers of bacteria encapsulated web samples were differentiating due to uncertainty of encapsulation efficiency. Since encapsulation efficiency can be influenced batch to batch due to slight environmental changes (e.g. humidity), some fluctuations in viable bacterial numbers were observed for equivalent samples of bacteria/PVA and bacteria/PEO webs in different experiments, which resulted in fluctuations in the methylene blue removal performances.

### **3.4. Evaluation of order of reactions and adsorption isotherm coefficients**

Adsorption isotherm coefficients and their estimated values for each tested model are listed in Table 15. While bacteria/PVA web fits well for each of the tested model, free-bacteria and bacteria/PEO web samples do not fit to any of the tested models, hence the estimated adsorption isotherm coefficients of these samples were not discussed. It was inferred that, biological removal rather than adsorption may play an important role in the remediation of MB by bacteria encapsulated web samples, as mentioned previously, since adsorption isotherm coefficients fit only in bacteria/PVA web sample. Although bacteria/PVA web has shown very similar fits in all tested isotherms, slightly higher fits in Freundlich and Toth isotherm models were observed with the  $R_y^2$  value of 0.926, suggesting the dye removal process might be heterogeneous and multilayeric through bacteria [62]. The maximum removal capacity ( $Q_{\max}$ ) of bacteria/PVA web was estimated to be 591 mg/g under the Toth model.

The  $R^2$  values of different order plots for MB removal are listed in Table 16. While bacteria/PVA web has shown the highest correlation with the zero order model ( $R^2 = 0.9797$ ), free-bacteria and bacteria/PEO web samples have shown the highest correlation with the first order model ( $R^2$  values of 0.9912 and 0.943, respectively). These results conform with the results from the literature, since enzyme-catalyzed reactions often fall under the zero order model [75] and first order reactions can fit to the enzyme-driven reactions for biological removal of water contaminants [20].

**Table 15.** Adsorption isotherm coefficients of free-bacteria, bacteria/PVA web and bacteria/PEO web samples for each isotherm model.

Samples	Isotherm	Parameters	Values	Ry <sup>2</sup> value
Free-bacteria	Freundlich	Kf	47.4	0.017
		1/n	0.09	
	Langmuir	Q <sub>max</sub>	66.6	0.001
		b	1.00	
	Toth	Q <sub>max</sub>	55.3	0.131
		b	1.00	
		n	5.00	
Bacteria/PVA web	Freundlich	Kf	8.85	0.926
		1/n	1.00	
	Langmuir	Q <sub>max</sub>	11400	0.925
		b	0.0008	
	Toth	Q <sub>max</sub>	591	0.926
		b	0.015	
		n	4.98	
Bacteria/PEO web	Freundlich	Kf	11.86	0.232
		1/n	0.92	
	Langmuir	Q <sub>max</sub>	1770	0.233
		b	0.006	
	Toth	Q <sub>max</sub>	1890	0.239
		b	0.005	
		n	3.29	

**Table 16.** The R<sup>2</sup> values of zero, first, second and third order plots for the removal of MB by free-bacteria, bacteria/PVA web and bacteria/PEO web samples.

Samples	Model	R <sup>2</sup> values
Free-bacteria	zero order	0.9717
	first order	0.9912
	second order	0.9160
	third order	0.8408
Bacteria/PVA web	zero order	0.9797
	first order	0.9398
	second order	0.8850
	third order	0.8378
Bacteria/PEO web	zero order	0.8839
	first order	0.9430
	second order	0.9399
	third order	0.8959

### **3.5. Storability and applicability of bacteria encapsulated webs**

The bacteria encapsulated web samples were tested for storability at different time periods via VCC assay, in terms of cell viability preservation. Different levels of cell viabilities were achieved in two different experiments (at 4 °C and 25 °C) and bacteria/PVA web sample had higher initial cell viability than bacteria/PEO web sample for the storage test at 25 °C, unlike from the previous experiments, probably due to an influential batch to batch variation (Fig. 47). Nevertheless, these differences did not have significant impacts on the assessment of storage test, since each sample has been evaluated individually and the comparisons were made on their initial to final cell viability ratios. In addition, although there are some variations in the cell viability measurements of bacteria encapsulated web samples for the storage test at 4 °C, these are restricted in certain levels, hence it was supposed that the partial dissimilarities in the cell viability numbers for equivalent samples might be the reason for these variations. It was found that, while bacteria encapsulated web samples can be safely stored at 4 °C for months without significant losses in the initial cell viabilities, the cell viabilities rapidly decrease at 25 °C and do not allow long-term storage at this temperature (Fig. 47, Table 17). Therefore, it was concluded that, the bacteria encapsulated web samples can be stored safely for long time periods, yet it needs cooler temperatures for cell viability preservation.

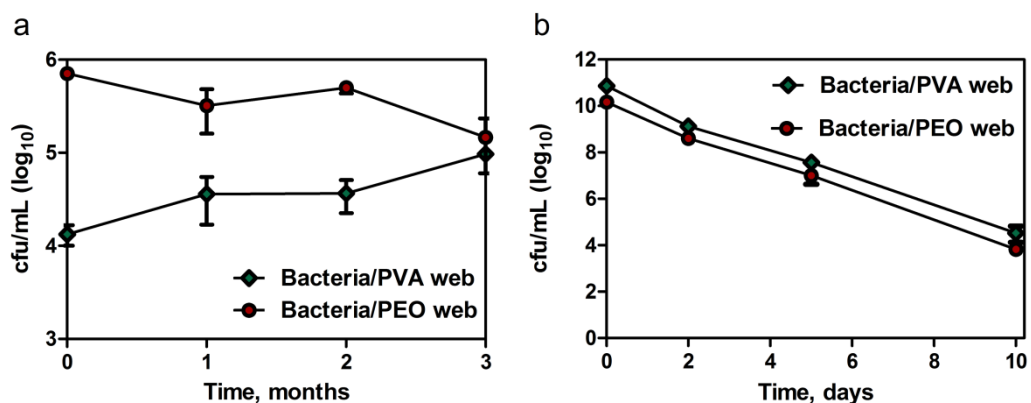


**Figure 47:** Viable cell counting (VCC) results of bacteria/PVA and bacteria/PEO web samples for storage at (a) 4 °C for 3 months and (b) 25 °C for 10 days.

**Table 17.** Viable cell counting (VCC) results of bacteria/PVA and bacteria/PEO web samples after storing at 4 °C or 25 °C for different time periods. The results are presented in cfu/mL. The w/v ratio of each web that was utilized for the VCC assay was equal (5 mg/mL).

Temperature	Time	Bacteria/PVA web	Bacteria/PEO web
4 °C	Initial	$1.3 \times 10^4 \pm 0.3$	$7.1 \times 10^5 \pm 0.5$
4 °C	After 1 month	$5.4 \times 10^4 \pm 1.1$	$4.8 \times 10^5 \pm 0.2$
4 °C	After 2 months	$3.7 \times 10^4 \pm 1.4$	$5.0 \times 10^5 \pm 0.6$
4 °C	After 3 months	$9.7 \times 10^4 \pm 1.2$	$2.2 \times 10^5 \pm 0.8$
25 °C	Initial	$7.2 \times 10^{10} \pm 2.1$	$1.5 \times 10^{10} \pm 0.3$
25 °C	After 2 days	$1.3 \times 10^9 \pm 0.3$	$4.0 \times 10^8 \pm 1.5$
25 °C	After 5 days	$3.7 \times 10^7 \pm 0.8$	$1.5 \times 10^7 \pm 0.5$
25 °C	After 10 days	$1.0 \times 10^5 \pm 0.3$	$2.0 \times 10^4 \pm 0.7$

There are many papers related with MB bioremoval in aqueous solutions and some of them present higher removal performances. Nevertheless, this study focuses on design and development of an alternative system with distinct features, rather than the removal efficiency for MB remediation. To the authors' knowledge, this is the first study which presents remediation of MB by bacteria encapsulated electrospun fibrous webs. The bacteria encapsulated webs have lower space and weight compare to free-bacteria in liquid media, which provides ease of application and lower transportation costs, as in lyophilized bacteria. In addition, these webs can be stored at cooler temperatures without significant losses in the cell viability. By optimization of environmental parameters and using a more capable bacterial strain, more efficient biocomposites can be produced for remediation of MB. In this sense, the findings here are promising for further developments in this field.

# **Chapter 9**

---

## **Conclusion and future perspectives**

In Chapter 2, the production of a novel biocomposite material by immobilization of an efficient ammonium oxidizing bacterial strain on electrospun CA nanofibrous web is presented. SEM images of STB1 immobilized CA web samples demonstrated robust attachment of bacterial cells on nanofiber surfaces, even after 5 cycles of reuse and repeated washing steps. The ammonium removal capability of STB1 immobilized CA nanofibrous web was observed to be very similar to that of suspended bacterial cells at the initial ammonium concentration of 50 mg/L, and bacteria-free CA webs displayed negligible ammonium removal capability compared to bacteria-immobilized webs. Ammonium removal was efficiently performed by STB1 immobilized webs at each experimental concentration. The production of nitrite and nitrate, the principal by-products of ammonium, were found to be at trace amounts. Reusability test results demonstrated that bacteria-immobilized nanofibrous webs can be used at least five consecutive removal experiments without significant losses in ammonium removal capacity, showing that the system can be used repeatedly for ammonium remediation with cost-effective properties compared to conventional chemical treatment methods. This biocomposite material may be easily applied by immersing into aquariums, ponds, ornamental pools and other aquatic environments, and is expected to be harmless for aquatic life during the ammonium removal process.

In Chapter 3, two novel biocomposite materials which were produced by immobilizing a Cr(VI)-removing bacterial strain on electrospun PS and PSU fibrous webs are described. SEM micrographs of STB5/PS and STB5/PSU web samples have shown robust bacterial adhesion on both fibrous surfaces after

incubation time, and no significant differences were observed for the bacterial immobilization even after five cycles of reuse. It was found that the Cr(VI) removal capability of STB5/PS and STB5/PSU biocomposites are based primarily on bacterial activity and are comparable to the Cr(VI) removal performance of free bacterial cells. Considerable amounts of Cr(VI) were removed by both STB5/PS and STB5/PSU biocomposite webs at all tested concentrations, yet the removal performances were started to decrease at higher concentrations, suggesting that the biocomposites can perform best at a defined concentration range. STB5/PS has shown higher removal performances than STB5/PSU in most experiments, implying that higher hydrophobic surfaces of PS webs allowed higher bacterial immobilization for hydrophobic STB5 cells, and thereby higher Cr(VI) removal performances. Both biocomposites were found to be reusable for several cycles and could be stored for short periods of time without exhibiting losses in attached cell numbers or Cr(VI) remediation capabilities, proposing that they may be used repeatedly for Cr(VI) remediation. Free-standing STB5/PS and STB5/PSU biocomposites may be easily utilized for continuous Cr(VI) remediation in freshwater sources by immersing them into the contaminated source.

In Chapter 4, a modified technique is presented to determine the number of bacteria that are immobilized on electrospun nanofiber surfaces as a result of natural adhesion. Initially, different kinds of bacteria were incubated with pieces of electrospun nanofibers for a defined period. During this period, bacterial cells strongly adhered on nanofiber surfaces and started to form biofilms. Bacterial population on nanofiber surfaces were monitored by SEM for different

incubation periods. The detection of the approximate number of bacteria which are pervaded within the nanofibrous web was done by applying a modified protocol for detachment of bacterial biofilms from a carrier material, and following viable cell counting (VCC) method. Before viable cell counting method, OD<sub>600</sub> values of the samples were measured by a spectrophotometer and the necessary dilutions were made upon these values. The results of detachment protocol and the further viable cell counting assay were found to be promising. Before applying this method, the optimum contact time was used to be determined via SEM analysis however, it does not give a quantity and it is not always so reliable because of the differential distribution of bacterial cells. Therefore, the aforementioned protocol to determine the optimum contact time is much more reliable and it's application in the field of bacteria immobilized electrospun nanofibers is novel for the literature.

In Chapter 5, the production and application of novel biocomposite webs which were obtained by immobilization of SDS degrading bacterial strains on electrospun cellulose acetate (CA) nanofibrous webs (non-porous (nCA) and porous (pCA) webs) are presented. The bacterial attachment has been evaluated regularly by bacterial cell counting (VCC assay) and SEM imaging, and the bacterial attachment was ended after 25 days upon these results. The results of biodegradation experiments revealed that, SDS remediation capabilities of bacteria immobilized webs were mainly based on the bacterial existence and highly similar to the unimmobilized bacterial cells. Since bacteria immobilized web samples were highly efficient for SDS remediation up to 100 mg/L of initial SDS, two most effective webs (STB3/pCA and STB4/pCA) were therefore

selected for testing their SDS remediation capability at a considerably high concentration (1 g/L). Although significant portions of SDS were degraded by STB3/pCA and STB4/pCA in this experiment, 1 g/L of SDS was found as stringent for the metabolic activity and viability of bacterial cells, therefore the test concentration of the reusability test was arranged as 100 mg/L. While the initial SDS biodegradation performances of STB3/pCA and STB4/pCA were considerably low in the reusability test (due to the harmful effects of the previous experiment on bacterial cells), they recovered in the next cycles and reached adequate levels especially for the STB3/pCA sample. It was concluded that, the bacteria immobilized webs are potentially reusable and improvable, suggesting they may be used repeatedly for SDS remediation in water systems.

In Chapter 6, morphology and fiber diameter differences of electrospun polysulfone fibers on bacterial immobilization and bioremediation performances were evaluated. Aligned and randomly oriented electrospun polysulfone (PSU) fibers were produced with thinner or thicker fiber diameters. These four different types of PSU fibers were utilized as carrier matrices for bacterial immobilization and then the sample showing highest bacterial immobilization was tested for bioremediation of ammonium and methylene blue dye in water. The results demonstrated that randomly oriented and thinner PSU fibers are favorable for bacterial immobilization among four different samples at equivalent conditions, hence further experiments were performed on this sample. Bacteria immobilized PSU fibers were found as promising for simultaneous removal of ammonium and methylene blue, though dye removal efficiency was lesser and optimization is required for higher dye removal

performances. In addition, reusability of bacteria immobilized fibers was evaluated for ammonium removal at an initial concentration of 100 mg/L and found as potentially reusable. Overall, the results suggest that randomly oriented and thinner (~1000 nm) PSU fibers are favorable for bacterial integration and bacteria immobilized PSU fibers have a potential to be used in continuous remediation of water systems.

In Chapter 7, the development of bacteria immobilized electrospun fibrous materials for textile dye bioremoval is presented. Immobilization of bacterial cells was confirmed by SEM imaging and OD<sub>600</sub> measurements of the pre-immobilized bacteria. The results of dye removal experiments demonstrated that dye removal capabilities of bacteria immobilized webs were primarily based on the bacterial cells, plus very similar and efficient removal performances were observed between bacteria immobilized webs and free-bacteria. The results of reaction kinetics studies suggest that, dye removal by bacteria immobilized webs is based on biological removal rather than adsorption. The reusability test results revealed that bacteria immobilized webs are potentially reusable for continuous remediation and their removal performances can be improved by increasing the number of immobilized bacteria. As a conclusion, bacteria immobilized electrospun nanofibrous webs are promising for remediation of textile dyes in water with reusable and improvable properties.

In Chapter 8, novel functional biocomposite materials which were produced by encapsulation of a MB remediating bacterial strain within electrospun PVA and PEO nanofibrous webs are presented. The bacterial cell viabilities were

checked by viable cell counting (VCC) assay and fluorescence microscopy imaging. Sufficient amounts of viable bacterial cells could be encapsulated within electrospun PVA and PEO nanofibrous webs, and these webs were tested for MB removal in water. The results of MB removal experiments revealed that MB removal capabilities of bacteria encapsulated webs were based on the bacterial presence, and similar removal performances were observed for free-bacteria. It was inferred that MB removal was achieved by biological removal rather than adsorption, and the removal performances can be optimized by increasing the initial cell viability numbers or using a more capable bacterial strain. In addition, storage test results showed that bacteria encapsulated webs can be stored safely for long time periods at 4 °C, while preserving the initial cell viability numbers. This type of storage can be alternative to lyophilized bacteria and bring some advantages over storage in culture media; such as the web samples do not need any minimal growth medium and it requires very small spaces for storage. In conclusion, bacteria encapsulated electrospun nanofibrous webs can be effectively used for remediation of MB in water with storable and improvable properties.

In summary, in this thesis, integration of specific bacteria with electrospun nanofibers by using immobilization/encapsulation techniques is presented and applications of these biocomposites for wastewater treatment purposes are described. Two different approaches were used for bacterial integration. In the first approach, bacterial cells were naturally adhered on CA, PS, PSU, PCL and PLA nanofibers. In order to observe the effects of morphology and diameter differences on bacterial immobilization, the

nanofibers were produced as porous or non-porous, randomly oriented or parallelly arranged, and with thicker or thinner diameters. All of them were tested for their specific remediation applications, and found as promising with potentially reusable properties. In the second approach, by using PVA and PEO polymer matrices, simultaneous encapsulation of viable bacteria within electrospun nanofibers during electrospinning was achieved. The bacteria encapsulated polymeric webs were also tested for their specific remediation applications, and found as promising with storable properties. As a future goal, our third and last approach will be bacterial integration to the polymeric structures by using core-shell encapsulation technique, to reduce the cell viability losses during electrospinning.

## LIST OF PUBLICATIONS

1. **O.F. Sarioglu**, A. Celebioglu, T. Tekinay, T. Uyar. (2016) Bacteria-immobilized electrospun fibrous polymeric webs for hexavalent chromium remediation in water. *International Journal of Environmental Science and Technology*, 13: 2057-2066.
2. E. Kalyoncu, T.T. Olmez, A.D. Ozkan, **O.F. Sarioglu**. (2016) Biosystems engineering of prokaryotes with tumor-killing capacities. *Current Pharmaceutical Design*, 22 (11): 1521-1528.
3. **O.F. Sarioglu**, A. Celebioglu, T. Tekinay, T. Uyar. (2015) Evaluation of contact time and fiber morphology on bacterial immobilization for development of novel surfactant degrading biocomposites. *RSC Advances*, 5: 102750-102758.
4. N.O. San-Keskin, A. Celebioglu, **O.F. Sarioglu**, T. Uyar, T. Tekinay. (2015) Removal of Reactive Dye and Hexavalent Chromium by Reusable *Lysinibacillus* sp. NOSK Attached Polysulfone Nanofibrous Web. *RSC Advances*, 5: 86867-86874.
5. A. Ozdemir, **O.F. Sarioglu**, T. Tekinay. (2015) Spectroscopic Evaluation of DNA–Borate Interactions. *Biological Trace Element Research*, 168 (2): 508-515.
6. **O.F. Sarioglu**, A. Ozdemir, K. Karaboduk, T. Tekinay. (2015) Comparative serum albumin interactions and antitumor effects of Au(III) and Ga(III) ions. *Journal of Trace Elements in Medicine and Biology*, 29: 111-115.
7. **O.F. Sarioglu**, R. Tekiner-Gursacli, A. Ozdemir, T. Tekinay. (2014) Comparison of Au(III) and Ga(III) ions' binding on calf thymus DNA: spectroscopic characterization and thermal analysis. *Biological Trace Element Research*, 160 (3): 445-452.
8. **O.F. Sarioglu**, O. Yasa, A. Celebioglu, T. Uyar, T. Tekinay. (2013) Efficient ammonium removal from aquatic environments by *Acinetobacter calcoaceticus* STB1 immobilized on an electrospun cellulose acetate nanofibrous web. *Green Chemistry*, 15: 2566-2572.
9. **O.F. Sarioglu**, Y.T. Tamer, A.D. Ozkan, H.I. Atabay, C. Molva, T. Tekinay. (2013) Fourier Transform Infrared spectroscopy for screening biochemical effects of surfactant biodegradation on a surfactant degrading *Arcobacter butzleri* strain. *Applied Spectroscopy*, 67: 470-475.

10. **O.F. Sarioglu**, R. Suluyayla, T. Tekinay. (2012) Heterotrophic ammonium removal by a novel hatchery isolate *Acinetobacter calcoaceticus* STB1. *International Biodeterioration and Biodegradation*, 71: 67-71.
11. **O.F. Sarioglu**, N.O. San Keskin, A. Celebioglu, T. Tekinay, T. Uyar. Bacteria encapsulated electrospun nanofibrous webs for remediation of methylene blue dye in water. *Colloids and Surfaces B: Biointerfaces* (submitted)
12. **O.F. Sarioglu**, N.O. San Keskin, A. Celebioglu, T. Tekinay, T. Uyar. Bacteria immobilized electrospun polycaprolactone and polylactic acid fibrous webs for remediation of textile dyes in water. *Chemical Engineering Journal* (submitted)

## BIBLIOGRAPHY

- [1] Berna J, Cossani G, Hager C, Rehman N, Lopez L, Schowonek D, Steber J, Taeger K, Wind T. Anaerobic biodegradation of surfactants - Scientific review. *Tenside Surfactants Detergents*, 2007; 44: 312-347.
- [2] Malik A. Metal bioremediation through growing cells. *Environment International*, 2004; 30: 261-278.
- [3] Amna T, Hassan M, Pandeya D, Khil M, Hwang I. Classy non-wovens based on animate L. gasseri-inanimate poly(vinyl alcohol): upstream application in food engineering. *Applied Microbiology and Biotechnology*, 2013; 97: 4523-4531.
- [4] Fung W, Yuen K, Liong M. Agrowaste-Based Nanofibers as a Probiotic Encapsulant: Fabrication and Characterization. *Journal of Agricultural and Food Chemistry*, 2011; 59: 8140-8147.
- [5] Gensheimer M, Becker M, Brandis-Heep A, Wendorff J, Thauer R, Greiner A. Novel biohybrid materials by electrospinning: Nanofibers of poly(ethylene oxide) and living bacteria. *Advanced Materials*, 2007; 19: 2480-2482.
- [6] Raveendran S, Dhandayuthapani B, Nagaoka Y, Yoshida Y, Maekawa T, Kumar D. Biocompatible nanofibers based on extremophilic bacterial polysaccharide, Mauran from *Halomonas maura*. *Carbohydrate Polymers*, 2013; 92: 1225-1233.
- [7] Salalha W, Kuhn J, Dror Y, Zussman E. Encapsulation of bacteria and viruses in electrospun nanofibres. *Nanotechnology*, 2006; 17: 4675-4681.
- [8] Tong H, Mutlu B, Wackett L, Aksan A. Silica/PVA biocatalytic nanofibers. *Materials Letters*, 2013; 111: 234-237.
- [9] Vajdai A, Szabo B, Suvegh K, Zeiko R, Ujhelyi G. Tracking of the viability of *Stenotrophomonas maltophilia* bacteria population in polyvinylalcohol nanofiber webs by positron annihilation lifetime spectroscopy. *International Journal of Pharmaceutics*, 2012; 429: 135-137.
- [10] Klein S, Kuhn J, Avrahami R, Tarre S, Beliavski M, Green M, Zussman E. Encapsulation of Bacterial Cells in Electrospun Microtubes. *Biomacromolecules*, 2009; 10: 1751-1756.
- [11] Klein S, Avrahami R, Zussman E, Beliavski M, Tarre S, Green M. Encapsulation of *Pseudomonas* sp ADP cells in electrospun microtubes for atrazine bioremediation. *Journal of Industrial Microbiology & Biotechnology*, 2012; 39: 1605-1613.
- [12] Korehei R, Kadla J. Encapsulation of T4 bacteriophage in electrospun poly(ethylene oxide)/cellulose diacetate fibers. *Carbohydrate Polymers*, 2014; 100: 150-157.
- [13] Lopez-Rubio A, Sanchez E, Sanz Y, Lagaron J. Encapsulation of Living *Bifidobacteria* in Ultrathin PVOH Electrospun Fibers. *Biomacromolecules*, 2009; 10: 2823-2829.

- [14] Eroglu E, Agarwal V, Bradshaw M, Chen X, Smith S, Raston C, Iyer K. Nitrate removal from liquid effluents using microalgae immobilized on chitosan nanofiber mats. *Green Chemistry*, 2012; 14: 2682-2685.
- [15] Li S, Fan Y, Hu J, Huang Y, Wu W. Immobilization of *Pseudomonas cepacia* lipase onto the electrospun PAN nanofibrous membranes for transesterification reaction. *Journal of Molecular Catalysis B-Enzymatic*, 2011; 73: 98-103.
- [16] Li S, Fan Y, Hu R, Wu W. *Pseudomonas cepacia* lipase immobilized onto the electrospun PAN nanofibrous membranes for biodiesel production from soybean oil. *Journal of Molecular Catalysis B-Enzymatic*, 2011; 72: 40-45.
- [17] Sakai S, Liu Y, Yamaguchi T, Watanabe R, Kawabe M, Kawakami K. Production of butyl-biodiesel using lipase physically-adsorbed onto electrospun polyacrylonitrile fibers. *Bioresource Technology*, 2010; 101: 7344-7349.
- [18] Sarioglu O, Yasa O, Celebioglu A, Uyar T, Tekinay T. Efficient ammonium removal from aquatic environments by *Acinetobacter calcoaceticus* STB1 immobilized on an electrospun cellulose acetate nanofibrous web. *Green Chemistry*, 2013; 15: 2566-2572.
- [19] Sarioglu O, Celebioglu A, Tekinay T, Uyar T. Evaluation of contact time and fiber morphology on bacterial immobilization for development of novel surfactant degrading nanofibrous webs. *RSC Advances*, 2015; 5: 102750-102758.
- [20] Keskin N, Celebioglu A, Sarioglu O, Ozkan A, Uyar T, Tekinay T. Removal of a reactive dye and hexavalent chromium by a reusable bacteria attached electrospun nanofibrous web. *RSC Advances*, 2015; 5: 86867-86874.
- [21] Keskin N, Celebioglu A, Uyar T, Tekinay T. Microalgae Immobilized by Nanofibrous Web for Removal of Reactive Dyes from Wastewater. *Industrial & Engineering Chemistry Research*, 2015; 54: 5802-5809.
- [22] San N, Celebioglu A, Tumbas Y, Uyar T, Tekinay T. Reusable bacteria immobilized electrospun nanofibrous webs for decolorization of methylene blue dye in wastewater treatment. *RSC Advances*, 2014; 4: 32249-32255.
- [23] Camargo J, Alonso A. Ecological and toxicological effects of inorganic nitrogen pollution in aquatic ecosystems: A global assessment. *Environment International*, 2006; 32: 831-849.
- [24] WHO, Ammonia Health and Safety Guide. World Health Organization, Geneva, 1990.
- [25] US EPA, Draft 2009 Update of Aquatic Life Ambient Water Quality Criteria for Ammonia - Freshwater. United States Environmental Protection Agency, Washington, DC, 2009.
- [26] NJDEP, Facts; Nitrate and Nitrite in Drinking Water? Department of Health and Senior Services, New Jersey, 1997.
- [27] Zhao B, He Y, Hughes J, Zhang X. Heterotrophic nitrogen removal by a newly isolated *Acinetobacter calcoaceticus* HNR. *Bioresource Technology*, 2010; 101: 5194-5200.

- [28] Taylor S, He Y, Zhao B, Huang J. Heterotrophic ammonium removal characteristics of an aerobic heterotrophic nitrifying-denitrifying bacterium, *Providencia rettgeri* YL. *Journal of Environmental Sciences*, 2009; 21: 1336-1341.
- [29] Sarioglu O, Suluyayla R, Tekinay T. Heterotrophic ammonium removal by a novel hatchery isolate *Acinetobacter calcoaceticus* STB1. *International Biodeterioration & Biodegradation*, 2012; 71: 67-71.
- [30] Ramakrishna S, Fujihara K, Teo W, Lim T, Ma Z. *An Introduction to electrospinning and Nanofibers*; World Scientific Publishing Company: Singapore, 2005.
- [31] Wendorff JH, Agarwal S, Greiner A. *Electrospinning: Materials, Processing, and Applications*; Wiley-VCH: Germany, 2012.
- [32] Greiner A, Wendorff J. Electrospinning: A fascinating method for the preparation of ultrathin fibres. *Angewandte Chemie-International Edition*, 2007; 46: 5670-5703.
- [33] Ramakrishna S, Fujihara K, Teo W, Yong T, Ma Z, Ramaseshan R. Electrospun nanofibers: solving global issues. *Materials Today*, 2006; 9: 40-50.
- [34] Yoon K, Hsiao B, Chu B. Functional nanofibers for environmental applications. *Journal of Materials Chemistry*, 2008; 18: 5326-5334.
- [35] Uyar T, Havelund R, Hacaloglu J, Besenbacher F, Kingshott P. Functional Electrospun Polystyrene Nanofibers Incorporating alpha-, beta-, and gamma-Cyclodextrins: Comparison of Molecular Filter Performance. *ACS Nano*, 2010; 4: 5121-5130.
- [36] Hall-Stoodley L, Costerton J, Stoodley P. Bacterial biofilms: From the natural environment to infectious diseases. *Nature Reviews Microbiology*, 2004; 2: 95-108.
- [37] Liu Y, Gan L, Chen Z, Megharaj M, Naidu R. Removal of nitrate using *Paracoccus* sp YF1 immobilized on bamboo carbon. *Journal of Hazardous Materials*, 2012; 229: 419-425.
- [38] Lee K, Jeong L, Kang Y, Lee S, Park W. Electrospinning of polysaccharides for regenerative medicine. *Advanced Drug Delivery Reviews*, 2009; 61: 1020-1032.
- [39] Wang Y, Hsieh Y. Enzyme immobilization to ultra-fine cellulose fibers via Amphiphilic polyethylene glycol spacers. *Journal of Polymer Science Part a-Polymer Chemistry*, 2004; 42: 4289-4299.
- [40] Tungprapa S, Jangchud I, Supaphol P. Release characteristics of four model drugs from drug-loaded electrospun cellulose acetate fiber mats. *Polymer*, 2007; 48: 5030-5041.
- [41] Stankus JJ, Freytes DO, Badylak SF, Wagner WR. Hybrid nanofibrous scaffolds from electrospinning of a synthetic biodegradable elastomer and urinary bladder matrix. *Journal of Biomaterials Science and Polymer Edition*, 2008; 19: 635-52.
- [42] Ma Z, Kotaki M, Ramakrishna S. Electrospun cellulose nanofiber as affinity membrane. *Journal of Membrane Science*, 2005; 265: 115-123.
- [43] Huang C, Tang Y, Liu X, Sutti A, Ke Q, Mo X, Wang X, Morsi Y, Lin T. Electrospinning of nanofibres with parallel line surface texture for improvement of nerve cell growth. *Soft Matter*, 2011; 7: 10812-10817.

- [44] Huang C, Niu H, Wu C, Ke Q, Mo X, Lin T. Disc-electrospun cellulose acetate butyrate nanofibers show enhanced cellular growth performances. *Journal of Biomedical Materials Research Part a*, 2013; 101: 115-122.
- [45] Bedford N, Pelaez M, Han C, Dionysiou D, Steckl A. Photocatalytic cellulosic electrospun fibers for the degradation of potent cyanobacteria toxin microcystin-LR. *Journal of Materials Chemistry*, 2012; 22: 12666-12674.
- [46] Khatri Z, Wei K, Kim B, Kim I. Effect of deacetylation on wicking behavior of co-electrospun cellulose acetate/polyvinyl alcohol nanofibers blend. *Carbohydrate Polymers*, 2012; 87: 2183-2188.
- [47] Celebioglu A, Uyar T. Electrospun porous cellulose acetate fibers from volatile solvent mixture. *Materials Letters*, 2011; 65: 2291-2294.
- [48] Greif D, Wesner D, Regtmeier J, Anselmetti D. High resolution imaging of surface patterns of single bacterial cells. *Ultramicroscopy*, 2010; 110: 1290-1296.
- [49] Liu H, Hsieh Y. Ultrafine fibrous cellulose membranes from electrospinning of cellulose acetate. *Journal of Polymer Science Part B: Polymer Physics*, 2002; 40: 2119-2129.
- [50] Brennecke J. The need for government funding for green chemistry in the USA. *Green Chemistry*, 2003; 5: G14-G15.
- [51] Keane M. Advances in greener separation processes - case study: recovery of chlorinated aromatic compounds. *Green Chemistry*, 2003; 5: 309-317.
- [52] US EPA, Process Design Manual for Nitrogen Control. United States Environmental Protection Agency, Washington, DC, 1993.
- [53] Sarioglu OF, Celebioglu A, Tekinay T, Uyar T. Bacteria-immobilized electrospun fibrous polymeric webs for hexavalent chromium remediation in water. *International Journal of Environmental Science and Technology*, 2016; 13: 2057-2066.
- [54] Quintelas C, Fonseca B, Silva B, Figueiredo H, Tavares T. Treatment of chromium(VI) solutions in a pilot-scale bioreactor through a biofilm of *Arthrobacter viscosus* supported on GAC. *Bioresource Technology*, 2009; 100: 220-226.
- [55] Bankar A, Kumar A, Zinjarde S. Removal of chromium (VI) ions from aqueous solution by adsorption onto two marine isolates of *Yarrowia lipolytica*. *Journal of Hazardous Materials*, 2009; 170: 487-494.
- [56] Kilic N, Donmez G. Environmental conditions affecting exopolysaccharide production by *Pseudomonas aeruginosa*, *Micrococcus* sp., and *Ochrobactrum* sp. *Journal of Hazardous Materials*, 2008; 154: 1019-1024.
- [57] US EPA, Chromium-6 in Drinking Water. United States Environmental Protection Agency, Washington, DC, 2010.
- [58] Zahoor A, Rehman A. Isolation of Cr(VI) reducing bacteria from industrial effluents and their potential use in bioremediation of chromium containing wastewater. *Journal of Environmental Sciences*, 2009; 21: 814-820.

- [59] Mishra S, Doble M. Novel chromium tolerant microorganisms: Isolation, characterization and their biosorption capacity. *Ecotoxicology and Environmental Safety*, 2008; 71: 874-879.
- [60] Quintelas C, Fernandes B, Castro J, Figueiredo H, Tavares T. Biosorption of Cr(VI) by three different bacterial species supported on granular activated carbon - A comparative study. *Journal of Hazardous Materials*, 2008; 153: 799-809.
- [61] Al-Gheethi A, Norli I, Lalung J, Azlan A, Farehah Z, Ab Kadir M. Biosorption of heavy metals and cephalexin from secondary effluents by tolerant bacteria. *Clean Technologies and Environmental Policy*, 2014; 16: 137-148.
- [62] Ergul-Ulger Z, Ozkan A, Tunca E, Atasagun S, Tekinay T. Chromium(VI) Biosorption and Bioaccumulation by Live and Acid-Modified Biomass of a Novel *Morganella morganii* Isolate. *Separation Science and Technology*, 2014; 49: 907-914.
- [63] Yang J, He M, Wang G. Removal of toxic chromate using free and immobilized Cr(VI)-reducing bacterial cells of *Intrasporangium* sp Q5-1. *World Journal of Microbiology & Biotechnology*, 2009; 25: 1579-1587.
- [64] Chauhan D, Dwivedi J, Sankararamakrishnan N. Novel chitosan/PVA/zerovalent iron biopolymeric nanofibers with enhanced arsenic removal applications. *Environmental Science and Pollution Research*, 2014; 21: 9430-9442.
- [65] Xu R, Si Y, Li F, Zhang B. Enzymatic removal of paracetamol from aqueous phase: horseradish peroxidase immobilized on nanofibrous membranes. *Environmental Science and Pollution Research*, 2015; 22: 3838-3846.
- [66] Pinchuk L. US Patent, 1989; 4, 882, 148.
- [67] Gopal R, Kaur S, Feng C, Chan C, Ramakrishna S, Tabe S, Matsuura T. Electrospun nanofibrous polysulfone membranes as pre-filters: Particulate removal. *Journal of Membrane Science*, 2007; 289: 210-219.
- [68] Roso M, Sundarrajan S, Pliszka D, Ramakrishna S, Modesti M. Multifunctional membranes based on spinning technologies: the synergy of nanofibers and nanoparticles. *Nanotechnology*, 2008; 19.
- [69] Uyar T, Havelund R, Nur Y, Hacaloglu J, Besenbacher F, Kingshott P. Molecular filters based on cyclodextrin functionalized electrospun fibers. *Journal of Membrane Science*, 2009; 332: 129-137.
- [70] US EPA, Chromium, Hexavalent (Colorimetric). United States Environmental Protection Agency, Washington, DC, 1992.
- [71] Buchko C, Chen L, Shen Y, Martin D. Processing and microstructural characterization of porous biocompatible protein polymer thin films. *Polymer*, 1999; 40: 7397-7407.
- [72] Wagner H, Siebert T, Ellerby D, Marsh R, Blickhan R. ISOFIT: a model-based method to measure muscle-tendon properties simultaneously. *Biomechanics and Modeling in Mechanobiology*, 2005; 4: 10-19.
- [73] Kochkodan V, Tsarenko S, Potapchenko N, Kosinova V, Goncharuk V. Adhesion of microorganisms to polymer membranes: a photobactericidal effect of surface treatment with TiO<sub>2</sub>. *Desalination*, 2008; 220: 380-385.

- [74] Giaouris E, Chapot-Chartier M, Briandet R. Surface physicochemical analysis of natural *Lactococcus lactis* strains reveals the existence of hydrophobic and low charged strains with altered adhesive properties. *International Journal of Food Microbiology*, 2009; 131: 2-9.
- [75] Tinoco I, Sauer K, Wang JC. *Physical Chemistry - Principles and Applications in Biological Sciences*; Prentice Hall: New Jersey, 1996.
- [76] Lugo-Lugo V, Barrera-Diaz C, Bilyeu B, Balderas-Hernandez P, Urena-Nunez F, Sanchez-Mendieta V. Cr(VI) reduction in wastewater using a bimetallic galvanic reactor. *Journal of Hazardous Materials*, 2010; 176: 418-425.
- [77] Flathman P, Lanza G. Phytoremediation: Current views on an emerging green technology. *Journal of Soil Contamination*, 1998; 7: 415-432.
- [78] Mulligan C, Yong R, Gibbs B. Remediation technologies for metal-contaminated soils and groundwater: an evaluation. *Engineering Geology*, 2001; 60: 193-207.
- [79] Davis T, Volesky B, Mucci A. A review of the biochemistry of heavy metal biosorption by brown algae. *Water Research*, 2003; 37: 4311-4330.
- [80] Gavrilescu M. Removal of heavy metals from the environment by biosorption. *Engineering in Life Sciences*, 2004; 4: 219-232.
- [81] Congeevaram S, Dhanarani S, Park J, Dexilin M, Thamaraivelvi K. Biosorption of chromium and nickel by heavy metal resistant fungal and bacterial isolates. *Journal of Hazardous Materials*, 2007; 146: 270-277.
- [82] Kobayashi H, Oethinger M, Tuohy M, Procop G, Bauer T. Improved Detection of Biofilm-formative Bacteria by Vortexing and Sonication: A Pilot Study. *Clinical Orthopaedics and Related Research*, 2009; 467: 1360-1364.
- [83] Goodnow, RA Harrison Jr, AP. *Applied Microbiology*, 1972; 24: 555-560.
- [84] US EPA, Fate and Transport of Nonionic Surfactants, United States Environmental Protection Agency, Washington, DC, 1999-2001.
- [85] Crawford RL, Crawford DL. *Bioremediation: Principles and Applications*; Cambridge University Press: Cambridge, 1996.
- [86] Dhouib A, Hamad N, Hassairi I, Sayadi S. Degradation of anionic surfactants by *Citrobacter braakii*. *Process Biochemistry*, 2003; 38: 1245-1250.
- [87] Otta S, Swain B, Panigrahy R, Panda K, Debata NK. *JMM Case Reports*, 2014; 1: e001065.
- [88] Ghevariya C, Bhatt J, Dave B. Enhanced chrysene degradation by halotolerant *Achromobacter xylosoxidans* using Response Surface Methodology. *Bioresource Technology*, 2011; 102: 9668-9674.
- [89] Grimont F, Grimont PAD. *The Prokaryotes*; Springer: New York, 2006.
- [90] Mahon CR, Lehman DC, Manuselis G. *Textbook of Diagnostic Microbiology*; Elsevier: Amsterdam, 2015.
- [91] Khleifat K. Biodegradation of linear alkylbenzene sulfonate by a two-member facultative anaerobic bacterial consortium. *Enzyme and Microbial Technology*, 2006; 39: 1030-1035.

- [92] Khleifat K. Biodegradation of sodium lauryl ether sulfate (SLES) by two different bacterial consortia. *Current Microbiology*, 2006; 53: 444-448.
- [93] Hayashi K. A rapid determination of sodium dodecyl sulfate with methylene blue. *Analytical Biochemistry*, 1975; 67: 503-506.
- [94] Rijpens N, Vlaemynck G, Rossau R, Herman L, Jannes G. Unidentified *Listeria*-like bacteria isolated from cheese. *Letters in Applied Microbiology*, 1998; 27: 198-202.
- [95] Hsu L, Fang J, Borca-Tasciuc D, Worobo R, Moraru C. Effect of Micro- and Nanoscale Topography on the Adhesion of Bacterial Cells to Solid Surfaces. *Applied and Environmental Microbiology*, 2013; 79: 2703-2712.
- [96] Walczak M, Donderski W. Decomposition of anionic surface active substances by bacteria from the surface microlayer of Lake Jeziorak Maly. *Polish Journal of Environmental Studies*, 2004; 13: 325-331.
- [97] Abboud M, Kheifat K, Batarseh M, Tarawneh K, Al-Mustafa A, Al-Madadhah M. Different optimization conditions required for enhancing the biodegradation of linear alkylbenzosulfonate and sodium dodecyl sulfate surfactants by novel consortium of *Acinetobacter calcoaceticus* and *Pantoea agglomerans*. *Enzyme and Microbial Technology*, 2007; 41: 432-439.
- [98] Shukor M, Husin W, Rahman M, Shamaan N, Syed M. Isolation and characterization of an SDS-degrading *Klebsiella oxytoca*. *Journal of Environmental Biology*, 2009; 30: 129-134.
- [99] Nataraj S, Hosamani K, Aminabhavi T. Distillery wastewater treatment by the membrane-based nanofiltration and reverse osmosis processes. *Water Research*, 2006; 40: 2349-2356.
- [100] Zhan Y, Li H, Chen Y. Copper hydroxyphosphate as catalyst for the wet hydrogen peroxide oxidation of azo dyes. *Journal of Hazardous Materials*, 2010; 180: 481-485.
- [101] Wang R, Guo J, Chen D, Miao Y, Pan J, Tjiu W, Liu T. "Tube brush" like ZnO/SiO<sub>2</sub> hybrid to construct a flexible membrane with enhanced photocatalytic properties and recycling ability. *Journal of Materials Chemistry*, 2011; 21: 19375-19380.
- [102] El-Sersy NA. Bioremediation of Methylene Blue by *Bacillus thuringiensis* 4 G1: Application of Statistical Designs and Surface Plots for Optimization. *Biotechnology*, 2007; 6: 34-39.
- [103] Asad S, Amoozegar M, Pourbabaee A, Sarbolouki M, Dastgheib S. Decolorization of textile azo dyes by newly isolated halophilic and halotolerant bacteria. *Bioresource Technology*, 2007; 98: 2082-2088.
- [104] Fisher K, Phillips C. The ecology, epidemiology and virulence of *Enterococcus*. *Microbiology*, 2009; 155: 1749-1757.
- [105] Lee J, Jeon C, Lim J, Lee S, Lee J, Song S, Park D, Li W, Kim C. *Halomonas taeanensis* sp nov., a novel moderately halophilic bacterium isolated from a solar saltern in Korea. *International Journal of Systematic and Evolutionary Microbiology*, 2005; 55: 2027-2032.
- [106] San N, Nazir H, Donmez G. Evaluation of microbiologically influenced corrosion inhibition on Ni-Co alloy coatings by *Aeromonas salmonicida* and *Clavibacter michiganensis*. *Corrosion Science*, 2012; 65: 113-118.

- [107] Rosales E, Pazos M, Sanroman M. Comparative efficiencies of the decolourisation of leather dyes by enzymatic and electrochemical treatments. *Desalination*, 2011; 278: 312-317.
- [108] Bhavsar M, Amiji M. Development of novel biodegradable polymeric nanoparticles-in-microsphere formulation for local plasmid DNA delivery in the gastrointestinal tract. *AAPS PharmSciTech*, 2008; 9: 288-294.
- [109] Jung Y, Kim T, Park S, Lee S. Metabolic Engineering of *Escherichia coli* for the Production of Polylactic Acid and Its Copolymers. *Biotechnology and Bioengineering*, 2010; 105: 161-171.
- [110] Hori K, Matsumoto S. Bacterial adhesion: From mechanism to control. *Biochemical Engineering Journal*, 2010; 48: 424-434.
- [111] Deniz F, Tezel-Ersanli E. Simultaneous bioremoval of two unsafe dyes from aqueous solution using a novel green composite biosorbent. *Microchemical Journal*, 2016; 128: 312-319.
- [112] Deepa K, Chandran P, Khan S. Bioremoval of Direct Red from aqueous solution by *Pseudomonas putida* and its adsorption isotherms and kinetics. *Ecological Engineering*, 2013; 58: 207-213.
- [113] Tastan B, Ertugrul S, Donmez G. Effective bioremoval of reactive dye and heavy metals by *Aspergillus versicolor*. *Bioresource Technology*, 2010; 101: 870-876.
- [114] Ertugrul S, San N, Donmez G. Treatment of dye (Remazol Blue) and heavy metals using yeast cells with the purpose of managing polluted textile wastewaters. *Ecological Engineering*, 2009; 35: 128-134.
- [115] Maurya N, Mittal A, Cornel P, Rother E. Biosorption of dyes using dead macro fungi: Effect of dye structure, ionic strength and pH. *Bioresource Technology*, 2006; 97: 512-521.
- [116] Saeed A, Iqbal M, Zafar S. Immobilization of *Trichoderma viride* for enhanced methylene blue biosorption: Batch and column studies. *Journal of Hazardous Materials*, 2009; 168: 406-415.
- [117] Vijayaraghavan K, Won S, Mao J, Yun Y. Chemical modification of *Corynebacterium glutamicum* to improve methylene blue biosorption. *Chemical Engineering Journal*, 2008; 145: 1-6.
- [118] Vilar V, Botelho C, Boaventura R. Methylene blue adsorption by algal biomass based materials: Biosorbents characterization and process behaviour. *Journal of Hazardous Materials*, 2007; 147: 120-132.
- [119] Wang X, Chen X, Yoon K, Fang D, Hsiao B, Chu B. High flux filtration medium based on nanofibrous substrate with hydrophilic nanocomposite coating. *Environmental Science & Technology*, 2005; 39: 7684-7691.
- [120] Zaghbani N, Hafiane A, Dhahbi M. Separation of methylene blue from aqueous solution by micellar enhanced ultrafiltration. *Separation and Purification Technology*, 2007; 55: 117-124.
- [121] Madigan MT, Martinko JM. *Brock Biology of Microorganisms*, Prentice Hall: New Jersey, 2006.
- [122] Karamalidis A, Evangelou A, Karabika E, Koukkou A, Drainas C, Voudrias E. Laboratory scale bioremediation of petroleum-contaminated soil by indigenous microorganisms and added *Pseudomonas aeruginosa* strain Spet. *Bioresource Technology*, 2010; 101: 6545-6552.

- [123] Wang Y, Song J, Zhao W, He X, Chen J, Xiao M. In situ degradation of phenol and promotion of plant growth in contaminated environments by a single *Pseudomonas aeruginosa* strain. *Journal of Hazardous Materials*, 2011; 192: 354-360.
- [124] Pasumarthi R, Chandrasekaran S, Mutnuri S. Biodegradation of crude oil by *Pseudomonas aeruginosa* and *Escherichia fergusonii* isolated from the Goan coast. *Marine Pollution Bulletin*, 2013; 76: 276-282.
- [125] Liu Y, Rafailovich M, Malal R, Cohn D, Chidambaram D. Engineering of bio-hybrid materials by electrospinning polymer-microbe fibers. *Proceedings of the National Academy of Sciences of the United States of America*, 2009; 106: 14201-14206.
- [126] Tong H, Mutlu B, Wackett L, Aksan A. Manufacturing of Bioreactive Nanofibers for Bioremediation. *Biotechnology and Bioengineering*, 2014; 111: 1483-1493.
- [127] Talari A, Movasaghi Z, Rehman S, Rehman I. Raman Spectroscopy of Biological Tissues. *Applied Spectroscopy Reviews*, 2007; 42: 493-541.
- [128] Socrates G. *Infrared and Raman Characteristic Group Frequencies: Tables and Charts*; Wiley: New Jersey, 2004.